UNIVERSITY OF CALIFORNIA, SAN DIEGO

The assembly and function of sensory-motor circuits in the developing spinal cord

A dissertation submitted in partial satisfaction of the requirements for the degree Doctor of Philosophy

in

Biomedical Sciences

by

Kathryn Lewallen Hilde

Committee in charge:

Professor Samuel L. Pfaff, Chair
Professor Lawrence S. Goldstein, Co-chair
Professor Yishi Jin
Professor Nicholas C. Spitzer
Professor Binhai Zheng

2015

The Dissertation of Kathryn Lewallen Hilde is approved, and it is acceptable in quality and form for publication on microfilm and electronically:

_____

_____

_____

_____

Co-Chair

_____

Chair

University of California, San Diego

2015

DEDICATION

To *Mike* and *Jackson*, for providing me with happiness in life.

To *Mom* and *Dad*, for your unconditional love and support in all of life's endeavors.

To *Eric and Carolina,* for giving me a sense of humor.

To *Laura*, the most kind hearted person I know, for helping me see the good in every situation.

EPIGRAPH

In all things of nature there is something of the marvelous

Aristotle

TABLES OF CONTENTS

LIST OF ABBREVIATIONS

AAV	Adeno-associated virus
Bhlhb5	Class B basic helix-loop-helix transcription factor
CAG	CAG promoter
CGRP	Calcitonin gene related peptide
ChAT	Choline acetyltransferase
Cherry	mCherry fluorescent protein
ChR2	Light-activated cation channel Channelrhodopsin 2
CM	Corticomotoneuronal
CNS	Central nervous system
CPG	Central pattern generator
Cre	Cre recombinase
Cre^{ERT2}	Tamoxifen-inducible Cre recombinase
Ctip2	Chicken ovalbumin upstream promoter transcription factor-interacting protein 2
DC	Descending commissurally projecting interneurons
dI	Dorsal interneuron class
e	Mouse embryonic day
ES	Embryonic stem cell
flx	Allele containing loxP site
G	Glycoprotein
GAD	Glutamate decarboxylase
GlyT2	Glycine transporter 2
GFP	Green fluorescent protein
GS	Gastrocnemius

H	Hamstring
Isl	Islet
L	Lumbar
Lbx1	Ladybird homeobox 1
Lhx3	LIM homeobox 3
Lmx1b	LIM homeobox transcription factor 1-beta
LSL	Lox-stop-lox
M1	Primary motor area
MSE	Motor synergy encoder
Neo	Neomycin
NWR	Nociceptive withdrawal reflex
Pax2	Paired box gene 2
PC1	Principle component 1
PCR	Polymerase chain reaction
polyA	Polyadenylation tail
PSD95	Postsynaptic density protein 95
Ptf1a	Pancreas transcription factor 1 subunit alpha
P	Mouse postnatal day
PV	Parvalbumin
PV:Synaptophysin-TdTomato	Synaptophysin-TdTomato fusion protein driven by PV
Rab	Rabies virus
Rosa	Rosa locus
Satb1	Special AT-rich sequence-binding protein 1
Satb2	Special AT-rich sequence-binding protein 2

$Satb2^{OFF}$	Satb2 null, also referred to as $Satb2^{Cre/Cre}$
$Satb2^{ON}$	Satb2 heterozygous, also referred to as $Satb2^{Cre/WT}$
Satb2:Synaptophysin-TdTomato	Synaptophysin-TdTomato fusion protein driven by Satb2
Satb2:TdTomato	TdTomato fluorescent protein driven by Satb2
Syp	Synaptophysin
Syn-Tom	Synaptophysin-TdTomato fusion protein
TA	Tibialis anterior
tcfAP2β	Transcription factor AP2β
TdTomato	Tandem Tomato fluorescent protein
Tlx3	T-cell leukemia homeobox 3
V	Ventral interneuron class
vGlut2	Vesicular glutamater transporter 2
WGA-HRP	Wheat germ agglutinin-horseradish peroxidase
WPRE	Woodchuck hepatitis post-transcriptional regulatory element

LIST OF FIGURES

LIST OF TEXT BOXES

LIST OF TABLES

LIST OF SUPPLEMENTARY MATERIALS

ACKNOWLEDGEMENTS

Chapter 1 is an adaptation of a review published in *Current Opinions in Neurobiology*, 2012. The full citation is: Ariel J. Levine, Kathryn A. Lewallen, and Samuel L. Pfaff. Spatial Organization of cortical and spinal neurons controlling motor behavior. *Current Opinions in Neurobiology*, 2012 Oct; 22(5):812-21. The article and publication are online at: http://www.sciencedirect.com/science/article/pii/S0959438812001110.

This manuscript was published online July 27, 2012 in advance of the print journal. This manuscript was written in collaboration with Ariel J. Levine, and with the guidance of Samuel L. Pfaff. The authors of this manuscript would like to thank Dr. Dario Bonanomi and Dr. Chris Hinckley for helpful comments on the manuscript. Ariel J. Levine was supported by George E. Hewitt Foundation for Medical Research. I was supported as a National Science Foundation Graduate Research Fellow. Samuel L. Pfaff is an HHMI investigator. Research in the laboratory was supported by NINDS.

Chapter 2 is an adaptation of a manuscript published in *Nature Neuroscience*, 2014. The full citation is: Ariel J. Levine, Christopher A. Hinckley, Kathryn L. Hilde, Shawn P. Driscoll, Tiffany H. Poon, Jessica M. Montgomery, Samuel L. Pfaff. Identification of a cellular node for motor control pathways. *Nature Neuroscience*, 2014 Apr; 17 (4): 586-93. The manuscript was received February 4, 2014, and accepted February 13, 2014. The manuscript was published online March 9, 2014 in advance of the print journal. The work presented in this chapter was done early in my graduate training in collaboration with Ariel Levine and Chris Hinckley, who designed and conducted many of the experiments in this chapter. The project was overseen by Samuel L. Pfaff. We also received tremendous help and assistance from many co-authors, whom I thank: Shawn Driscoll, Tiffany Poon, and Jessica Montgomery. The article and publication are online at: http://www.nature.com/neuro/journal/v17/n4/full/nn.3675.html. The authors of the manuscript would like to acknowledge the generosity and advice of Martyn Goulding, Reggie Edgerton,

Anne Engmann, Edward Callaway, John Young, Fumitaka Osakada and Floor Stam; Pushkar Joshi and Sue McConnell for instruction in cortical injections; and Qiufu Ma (Department of Neurobiology, Harvard Medical School; in situ probes) and Carmen Birchmeier (Max Delbruck Center for Molecular Medicine; Tlx3 antibody) for providing reagents. Matt Sternfeld, Marito Hayashi and Yoel Bogoch provided support and advice. We thank Richard Levine for his helpful reading of the manuscript. Ariel Levine was supported by George E. Hewitt Foundation for Medical Research and Christopher and Dana Reeve Foundation. Christopher Hinckley was supported by a US National Research Service Award fellowship from US National Institutes of Health NINDS. I was supported as a National Science Foundation Graduate Research Fellow. Samuel Pfaff is supported as a Howard Hughes Medical Investigator and as a Benjamin H. Lewis chair in Neuroscience. This research was supported by the National Institute of Neurological Disorders and Stroke (grant R37NS037116), the Marshall Foundation and the Christopher and Dana Reeve Foundation.

Chapter 3 is an adaptation of a paper that was submitted for publication. The working citation is: Kathryn L Hilde, Ariel J. Levine, Christopher A. Hinckley, Marito Hayashi, Jessica M. Montgomery, Rudolf Grosschedl, Yoshinori Kohwi, Terumi Kohwi-Shigematsu, Samuel L. Pfaff. Satb2 controls spinal circuit assembly and sensorimotor reflex behavior. The authors of this manuscript would like to acknowledge the generosity and advice of Martyn Goulding, Catherine Farrokhi, Steeve Bourane, and Lidia Garcia-Campmany; Shawn Driscoll for guidance in statistical analyses, Qiufu Ma, Randy Johnson, and Carmen Birchmeier for providing reagents, Yelena Dayn for help with generation of the Satb2-Cre^{ERT2} transgenic mouse line. Karen Lettieri, Miriam Gullo and Colleen Heller provided support and advice. I was supported as a National Science Foundation Graduate Research Fellow and the Chapman Foundation. Ariel Levine was supported by George E. Hewitt Foundation for Medical Research and Christopher and Dana Reeve Foundation. Chris Hinckley was supported by a US National research Service Award

Fellowship from US National Institutes of Health NINDS. Marito Hayashi was supported by the Timken-Sturgis Foundation and the Japanese Ministry of Education, Culture, Sports, Science, and Technology Long-Term Student Support Program. Samuel Pfaff is supported as a Howard Hughes Medical Institute Investigator and as a Benjamin H. Lewis chair in neuroscience. This research was supported by funding from the Howard Hughes Medical Institute, the Marshall Foundation and the Sol Goldman Charitable Trust.

In addition, I would like to further acknowledge several individuals. Wes, Tiffany, Neal, Sternfeld, and Marito, thank you for your insightful discussions during our many graduate student discussions. The long path to finishing a PhD was much more enjoyable because of the support and friendship you provided throughout my training.

Jessica, for your hard work and perseverance, as well as your friendship and sense of humor. Working with you in the lab was truly a pleasure.

Chris and Marito, thank you for being my collaborators and friends. Your discussion and insight provided great guidance for my project. Thank you for creating a workplace that never felt like work, but rather a fun and exciting environment in which to do science.

Ariel, who has been a tremendous mentor, role model, and friend during my time in the Pfaff lab. I am so grateful for your investment in my scientific development. You have provided amazing experimental training, and greatly broadened my perspective of science, as well as my career. This journey would not have been possible, or nearly as much fun, without your support and partnership.

Sam, thank you for your support and guidance throughout all stages of my scientific development. The training you provided has greatly expanded my skillset and perspective. I greatly appreciate your support of me as a scientist, but also through the many life transitions that accompanied. I cannot fully express my gratitude for all you have done for me.

VITA

2004-2008	University of Southern California Bachelor of Art, Health and Humanity - Biological Sciences *Alpha Lambda Delta Honors Society* *Phi Sigma Biological Sciences Honors Society*
2009-2015	University of California, San Diego Biomedical Sciences Graduate Program The Salk Institute for Biological Studies Graduate Research
2010-2013	National Science Foundation Graduate Research Fellow
2012-2013	H.A. and Mary K. Chapman Foundation Charitable Trust Scholarship
2015	University of California, San Diego Doctor of Philosophy, Biomedical Sciences

PUBLICATIONS

Peer Reviewed Original Research

Hilde, K.L., Levine, A.J., Hinckley, C.A., Hayashi, M., Montgomery, J.M., Grosschedl, R., Kohwi, Y., Kohwi-Shigematsu, T., Pfaff, S.L. Satb2 controls spinal circuit assembly and sensorimotor reflex behavior. (Submitted for publication, March 2015.)

Levine, A.J., Hinckley, C.A., **Hilde, K.L**., Driscoll, S.P., Poon, T.H., Montgomery, J.M., Pfaff, S.L. Identification of a cellular node for motor control pathways. *Nature Neuroscience*, 2014 Apr; 17 (4): 586-93.

Lewallen, K.A., De La Torre, A.R., Shen, Y.A., Ng, B.K., Meijer, D., Chan, J.R. Assessing the Role of the Cadherin/Catenin Complex at the Schwann Cell-Axon Interface and in the Initiation of Myelination. *Journal of Neuroscience*, 2011 Feb 23; 31(8):3032-43.

Peer Reviewed Literature Review

Levine, A.J., **Lewallen, K.A**., Pfaff, S.L. Spatial organization of cortical and spinal neurons controlling motor behavior. *Current Opinions in Neurobiology*, 2012 Oct; 22(5):812-21.

ABSTRACT OF THE DISSERTATION

The assembly and function of sensory-motor circuits

in the developing spinal cord

by

Kathryn Lewallen Hilde

Doctor of Philosophy in Biomedical Sciences

University of California, San Diego, 2015

Professor Samuel L. Pfaff, Chair

Professor Lawrence S. Goldstein, Co-Chair

A fundamental question in the study of motor control is how the nervous system accomplishes the complex task of integrating commands from multiple movement systems in order to perform a motor behavior. Even the simplest tasks, such as withdrawing the limb from a painful stimulus or taking a single step, involve multiple areas of the brain and spinal cord. Examples of movement parameters that are encoded within the nervous system include the

selection and timing of muscle contraction in order to move a body region to a desired position, and the coordination of multiple body joints and body regions. Significant progress has been made in the field to understand the contribution of individual cell types to motor control, as well as the genetic mechanisms that regulate the development of individual cell types. However, the circuit components that link multiple motor control populations, as well as the mechanisms that regulate the formation of integrative motor networks, are poorly understood.

This dissertation describes a series of original work that aims to elucidate the cellular players and developmental mechanisms that assemble circuit components into functional neural networks. The first chapter provides a framework for understanding how different motor control pathways are organized within the central nervous system. The second chapter describes a group of premotor neurons that are located in the deep dorsal horn of the spinal cord, receive input from multiple motor control pathways, and bind together the activity of multiple motor pools. Importantly, genetic markers (Satb1, Satb2, and tcfAP2β) were identified that, to date, comprise the most significant fraction of molecularly defined premotor neurons in the spinal cord.

The third chapter describes a novel population of cells that express the genetic marker Satb2, spinal interneurons that are located at the intersection of incoming sensory and outgoing motor information. This work examines the role of the *Satb2* gene in spinal interneuron development, as well as sensory-motor circuit assembly and function. This work provides an important contribution to our understanding of the organizational logic of integrative spinal networks and the types of movements they control.

Chapter 1

Spatial organization of cortical and spinal neurons controlling motor behavior

Spatial organization of cortical and spinal neurons controlling motor behavior

Abstract

A major task of the central nervous system (CNS) is to control behavioral actions, which necessitates a precise regulation of muscle activity. The final components of the circuitry controlling muscles are the motorneurons, which settle into pools in the ventral horn of the spinal cord in positions that mirror the musculature organization within the body. This 'musculotopic' motor-map then becomes the internal CNS reference for the neuronal circuits that control motor commands. This chapter describes recent progress in defining the neuroanatomical organization of the higher-order motor circuits in the cortex and spinal cord, and our current understanding of the integrative features that contribute to complex motor behaviors. We highlight emerging evidence that cortical and spinal motor command centers are loosely organized with respect to the musculotopic spatial-map, but these centers also incorporate organizational features that associate with the function of different muscle groups with commonly enacted behaviors.

Introduction

An animal's behavioral repertoire is evolved to suit its particular survival needs and originates from the nervous system circuitries that control movements. One major strategy for an animal to organize the neuronal networks for diverse behaviors is to possess ensembles of neurons that are distributed to form maps of external space or body space. These 'topographic' arrangements are a common theme in the vertebrate nervous system (Text Box 1.1). Within the motor networks that are the focus of this review, topography is a major organizing principle of many critical components, including the spinal motorneurons, the motor cortex, the spinal sensory system, and the spinal interneurons.

Text Box 1.1: Definitions and Concepts.

Topography:
The description of the locations of neurons within the central nervous system. It is often specifically used to describe an arrangement of neurons that has an orderly relationship to the space of an external input or output. Examples include the retinotopic maps of the visual cortex, the tonotopic map of the auditory cortex, the multiple somatosensory maps of the sensory cortex, and the musculotopic organization of spinal motorneurons.

Frame of reference:
The organization of the central nervous system network relative to a given external or body-based scheme. For instance, visual processing incorporates a retinotopic frame of reference with an internal reference of eye position to form a 'head-centered' frame of reference[3]. In the spinal cord, both the proprioceptive system and motorneurons are organized with respect to muscles, but the nociceptive sensory targets have a skin-based frame of reference.

Dimensionality:
The number of parameters encoded in a neural circuit. For instance, the parameters, or dimensions, of a visual image are form, color, and motion, and these can be encoded and processed separately. In cortical coding of a motor command, information may include multiple dimensions such as which muscles to contract, and the timing, force, and velocity of muscle contractions, and the final desired position of the limb.

There is a pleasing simplicity to the orderliness of topographic maps; however, we are just beginning to understand how the spatial organization of neuronal networks relates to their function. Many questions remain. For instance, how can multiple maps of the body with different frames of reference interact to produce coherent motor plans? How are non-spatial parameters of movement encoded together with spatial information in motor commands? How pervasive is topographic mapping as a scheme for organizing motor circuitry? How can topographic information be transmitted through intervening elements such as interneurons, which are not traditionally understood to have significant spatial or topographic organization? What is the purpose of topographic organization? This chapter discusses recent work related to these organizational principles and their integration within the spinal cord, as they pertain to the control of movement.

Motorneurons: The musculotopic map

As all other motor-related circuitries with their particular organizational schemes must signal to the motorneurons that control muscles, it is helpful to examine the arrangement of motorneurons first. Romanes and others have used retrograde neuronal fills from the muscles or nerves in the periphery and identified discrete clusters of motorneurons, called pools, devoted to each muscle[4-8]. These studies also identified the organizational principles of inter-pool relationships. For instance, motor pools for hip flexor muscles are located more ventrally and rostrally, while muscles of the ankle and foot are generally located more dorsally and caudally (Figure 1.1A). Thus, an orderly spatial arrangement exists between motor pools within the spinal cord and the muscles they innervate in the periphery – referred to as a musculotopic map.

A combinatorial transcription code that defines motorneuron pools for each muscle has

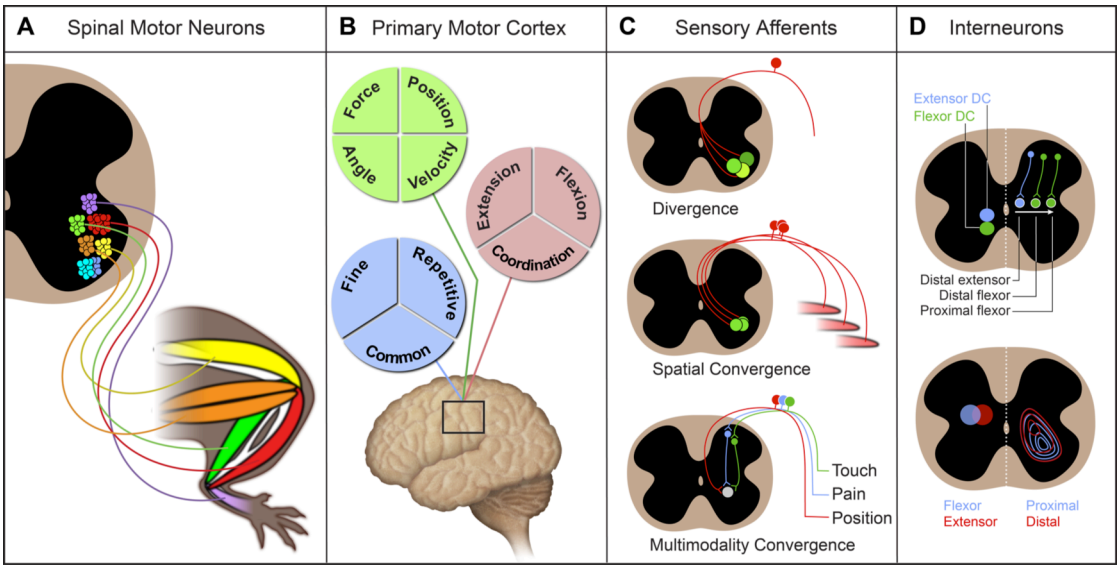

Figure 1.1: Spatial and functional relationships in the spinal cord and cortex.
(A) Spinal motorneurons display a linear organizational scheme in which they form a direct connection with their respective muscle target. This type of organization represents a low dimensional topographic scheme in which motor pools are organized with respect to a musculotopic frame of reference. Each color corresponds to muscle-specific motor pools and its corresponding target muscle. (**B)** Within small regions of the motor cortex, many parameters are compressed into a two dimensional physical space. Examples include movement characteristics (green), muscle selection (pink), and types of evoked behavior (blue) - a high-dimensional organization. (**C)** Sensory afferents transform body sensations into neural cues. Proprioceptive fibers selectively form connections with motorneurons that innervate shared muscle targets. However, proprioceptive fibers also form some connections with motorneurons controlling synergistic muscles, representing divergent input onto multiple targets. Primary afferents of sensory neurons can also converge onto shared targets. For instance, individual proprioceptive neurons share common motorneuron targets. Additionally, afferents from multiple modalities can share cellular targets (multimodality convergence) to integrate information from the periphery. Thus, sensory fibers that project into the spinal cord display an intermediate dimensional organization. (**D)** Examples of spinal interneurons with topographic distributions: Upper Panel - Left: Contralaterally projecting descending commissural (DC) interneurons that correlate with flexor (green) and extensor (blue) motorneuron activation are somewhat segregated within the ventral spinal cord. Upper Panel - Right: Reflex encoder interneurons located in the deep dorsal horn that transmit information from the nociceptive withdrawal reflex are organized with a musculotopic frame of reference, such that there is a medial to lateral arrangement of distal extensor (blue), distal flexor (green), and proximal flexor (green). Lower panel - Left: Rabies injections into flexor and extensor muscles labels pre-motor interneurons in the deep dorsal horn. Pre-flexor (blue) and pre-extensor (red) ipsilaterally projecting interneurons overlap but display a lateral and medial bias, respectively. Lower panel - Right: distal (red) and proximal (blue) pre-motor interneurons are positioned in overlapping regions within the ipsilateral spinal cord. Pre-motor interneurons contacting motor pools that control proximal muscles have a more significant ventral distribution when compared to those controlling distal muscles.

been described, and it is thought that this code directs proper motor pool and muscle connectivity[9]. Interestingly, Demireva et al have demonstrated that the positional identity of motorneuronscan be uncoupled from their transcriptional identity[10]. By removing β- and γ-catenin from motorneurons, they eliminated the stereotypical, pooled organization of motorneurons. Instead, motorneurons for a given muscle were found scattered through the motorneuron region of the spinal cord, but still found their appropriate muscular targets in the periphery. This reveals that motorneuron cell body position is dependent on β- and γ- catenin function, thereby establishing a critical role for these genes in creating the musculotopic motor-map. In addition, it suggests that soma position is not a critical determinant for axon targeting of muscles.

Overall, the relationship between motorneurons and the muscles of the body is a 'low dimensional' musculotopic scheme (Text Box 1.1), defined by a single dominant parameter, namely the control of a single target muscle by a single motor pool (Figure 1.1A). This musculotopic system provides a simple substrate for relaying neural commands for movement, but redirects the question to understanding how activity among motor pools is coordinated in order to achieve complex behaviors.

Motor cortex: Space and Function

The first observations of topographic maps within the CNS were made using electrical stimulation of the cortex[11,12]. These classic experiments revealed that the motor cortex of mammals is organized as a 'homonculus' - a map of the body represented in the brain such that contiguous parts of the body are controlled by neighboring cortical regions. In primates, the primary motor area (M1) is roughly arranged with a lateral to medial progression of head, then

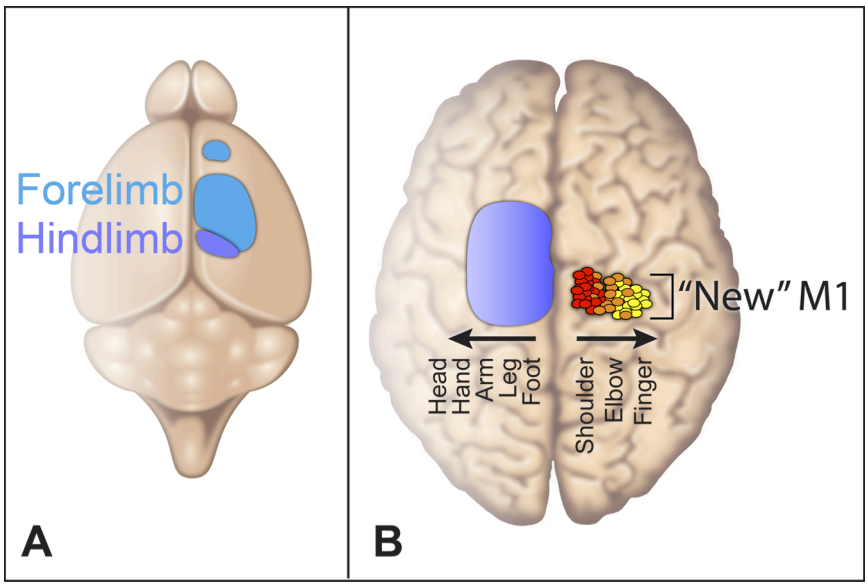

Figure 1.2: Motor cortex anatomy. (A) Rodent motor cortex is roughly segregated into rostral and caudal subdivisions. Rostral motor cortex and the lateral portion of caudal motor cortex contain cells that project to forelimb levels of the spinal cord (light blue). Caudal motor cortex also contains cells that project to hindlimb levels of the spinal cord (dark blue). **(B)** Spatial organization of primate motor cortical cells that control movement of muscle groups are located in a medial to lateral progression of foot, leg, arm, hand and head (blue). Corticomotoneuronal (CM) cells are organized in a medial to lateral progression of proximal (red) to distal (yellow) muscle targets in a region corresponding to "new M1," a subdivision of the "old M1" region (blue).

hand, then arm, then leg, then foot (Figure 1.2B)[11]. In the rodent, there are two major motor sub-divisions – a rostral forelimb area, and a caudal region that contains both forelimb and hindlimb areas (Figure 1.2A)[13,14]. Despite the appealing simplicity of this organization, from the outset Sherrington, Woolsey and others recognized that this somatotopic map exists only on a gross scale, whereas in reality the representations of body regions are overlapping, non-continuous, and flexible[15-18]. Further refinements on the idea of a topographic map of the motor cortex are based on observations that, within a cortical domain relating to one body region, many parameters are represented including the target muscles, but also force, angle, velocity, the coordination with other commonly associated muscles or parameters, and types of movement (Figure 1.1B)[19-22].

In contrast to the low-dimensional topographic arrangement of motorneurons, in which the spatial grouping of neurons correlates very well with functional output, the fine scale organization of motor cortex neurons does not have a simple relationship with either body space or behaviors. Instead, the motor cortex is a 'high-dimensional' system (Text Box 1.1) embedded within a coarse topographic spatial organization. Graziano and others have suggested that the spatial layout of the motor cortex reflects the reduction of these many different dimensions or parameters onto the two-dimensional physical space of the cortical sheet (Figure 1.1B)[23].

Recent evidence suggests that one of the main organizing principles of the motor cortex is the spatial separation of neuronal clusters that are active during complex behaviors rather than a strict mapping relationship with the motor pools and muscles. Nevertheless, behaviorally-relevant movements naturally involve muscles within the same part of the body leading to a significant local clustering of neurons that control neighboring body regions. For instance, topographic representations of the forelimb can be represented spatially in multiple, potentially overlapping, regions that each relate to a type of movement, including: (1) stereotyped repetitive behaviors such as grooming or running, (2) complex voluntary movements such as bringing the hand to the mouth in feeding, or (3) fine motor manipulation skills such as independent finger

movements (Text Box 1.2). We summarize evidence from new studies that demonstrate cortical spatial organization pertaining to these three different categories of movement.

Direct observation of neuronal activity in awake-behaving mice provides a novel and powerful approach to identify where active neurons are located as different movements are performed. To study 'stereotypical' movements (Text Box 1.2), Tank and colleagues analyzed activity with a fluorescent calcium indicator in neurons of the caudal forelimb area of the motor cortex during running and grooming, that both rely on many of the same muscles[24]. They observed networks of layer 2/3 cortical neurons that became active during these movements, but noted that the location of the sites of correlated-firing was different for each stereotypical behavior. Therefore, layer 2/3 cortical neuron position appears to be linked to particular behaviors that rely on complex patterns of muscle activation, rather than an organizational scheme that creates a one-to-one map with the motor pools.

A similar functional organization seems to characterize the motor cortex networks that direct isolated 'voluntary' movements (Text Box 1.2). Moore and colleagues first showed that long duration electrical microstimulation of primate motor cortex resulted in behaviorally relevant, also known as ethological, movements[25]. Interestingly, specific motor cortical regions reliably produced particular behaviors. For example, stimulation of an area that represents the arm and face can result in the animal bringing its hand towards its mouth in a grip posture and opening its mouth. Stimulation of a more dorsal area produced hand movements towards the trunk or hindlimb. This work was extended to the rodent by Tuszynski and colleagues, who demonstrated distinct regions of rostral and caudal forelimb areas in the rat motor cortex that directed reach, grasp, and retraction movements[26]. Recent work using light-based activation of motor cortex microdomains identified regions within the caudal motor cortex that direct

Text Box 1.2: Movement Categories. The movements of animals can be categorized along a spectrum from highly automatic to highly volitional, after Hughlings Jackson[11].

Automatic:
This category includes movements related to reflexes, autonomic control, breathing, and simple postural control. These behaviors can be highly stereotyped and repetitive, and do not require voluntary control, although they can be modulated voluntarily. The neuronal circuitries for these behaviors are generally hard-wired, evolutionarily ancient, and typically reside in the brainstem and spinal cord.

Stereotypical:
Somewhat automatic behaviors often involve the entire body, or coordination between body regions, and they are often repetitive. They include walking and grooming. These behaviors are initiated and can be modulated by voluntary cortical and brainstem control, but the core circuitry elements that mediate these behaviors often function autonomously within the spinal cord. A classic example of these features is the central pattern generator that controls locomotion.

Voluntary:
This category includes isolated, voluntary movements that involve multiple muscles, joints, and even body regions. These are generally common and behaviorally relevant, or ethological movements. For example, reaching out the forelimb, grasping an object, and retracting the forelimb as used for eating. The programs for these actions can be represented in spatially localized cortical and sub-cortical regions that are capable of activating the entire behavioral-routine when stimulated.

Fine:
These motor acts are isolated and voluntary, like those of the category above, but they involve a high degree of precision and individuated movements. This category is a relatively recent evolutionary addition to the behavioral repertoire of animals. The most refined example is the relatively independent finger movements that are a hallmark of human hand use. This reflects primate-specific neural circuitries that mediate direct cortical control over motor outputs and these command centers appear to originate from an evolutionarily-‘new’ region of the motor cortex.

abduction or adduction of the forelimb, and confirmed this type of functional organization within the motor cortex[27].

Despite the evidence for a cortical map that segregates into neuronal clusters that elicit complex behaviors, it still remains unclear to what extent the spatial organization of movement types is based on the topographic arrangements of cortical neurons. One possibility is that local clusters of topographically distributed neurons for a given body area are grouped into bigger networks that represent compound movements of that body area. A potential substrate for this type of network has been described by Capaday and colleagues, who suggest that interconnectivity within the cortex promotes spreading waves of activation[28-30]. They found that focal activation of sites within the motor cortex produced expanding waves that cover broad regions of neurons that were experimentally determined to control multiple muscles and joints. However, during a complex behavior, many neurons in the motor cortex are recruited, and distinct behaviors can involve intermingled and distributed networks of neurons. The resulting movements cannot be predicted simply from a map of muscles activated by experimental stimulation of the relevant active cortical regions. This highlights the complexity of coding multiple movement parameters overlaying a topographic spatial system, and of communicating these diverse parameters to the motor output cells of the spinal cord.

Our understanding of the relationship between function and topography has been facilitated by the study of a primate-specific population of motor cortex cells that directly target motorneurons. In most mammals, motorneurons are controlled through indirect pathways from the cortex. However, in primates, cortico-motoneuronal (CM) cells are uniquely suited to control highly precise, individuated movements[31,32]. These cells subserve ‘fine’ motor skills (Text Box 1.2), the most voluntary movements that represent another class of behavior that has a spatially distinct control region, at least in primates.

Using retrograde trans-synaptic circuit tracing with wild-type rabies virus, Strick and colleagues were able to map the location of CM cells within the primate motor cortex that contact motor pools for the shoulder, elbow, and finger muscles[33]. They observed that CM cells are mostly segregated within a caudal region of the M1 motor cortex and possessed a medial-lateral progression of shoulder to elbow to finger CM cell locations. However, a significant degree of overlap was also noted between these CM populations. Their findings suggest there is an 'old M1' and a 'new M1' that contain parallel topographic maps that exist within the primate motor cortex (Figure 1.2B).

It is important to note that cortical organization must be framed with reference to sub-cortical target organization. For instance, despite the high-dimensionality of the motor cortex (Text Box 1.1), this information must eventually be reduced to the specific patterns of spatio-temporal activation of muscle contractions. It is not known how this process occurs, but recent evidence suggests that spinal cord interneurons actively translate transient cortical commands into ongoing motorneuron activation programs during the movement. Specifically, electrical recordings from motor cortex during a movement reveal that many neurons are active and correlate with specific movement parameters, but then fail to perdure during the entire movement. Similar recordings within the interneuron regions of the spinal cord identify many cells that respond to these cortical commands but consistently code movement parameters for the duration of the movement[34].

Spinal sensory system: Mapping body space into motor commands

The sensory system functions in motor behaviors to detect the environment so that proper movements can be selected to mediate reflexes, to inform the central nervous system about the starting position of the body in preparing movements, and to provide ongoing feedback about body position during movement. This system has varied somatotopic organization that translates

body space into the spinal cord. There are three major sensory modalities, each mediated by a subpopulation of sensory neurons in the dorsal root ganglion, where their cell bodies are spatially intermingled; they are nociception (pain), mechanoreception (touch), and proprioception (position). Importantly, within a modality, there is divergence of sensory signals to multiple targets and convergence of sensory signals onto shared targets, thus blending spatially segregated inputs (Figure 1.1C). In addition, some sensory target cells within the spinal cord receive inputs from sensory neurons that mediate different modalities, thus compressing multiple types of sensory information. Accordingly, the spinal sensory system can be understood as an 'intermediate dimensional' topographic organization of inputs (Text Box 1.1).

Specifically, primary afferent fibers of the nociceptive and mechanoreceptive systems are mostly separated by modality and organized in parallel, as they enter the spinal cord and target dorsal horn cells with a well-established topographic order based on the skin body map (Figure 1.1C)[35-38]. Proprioceptive afferents innervate muscles and joints and have two major target regions in the spinal cord. These fibers enter the spinal cord from the dorsal edge and first target interneurons in the deep dorsal horn. Some of these fibers then continue to the ventral horn to synapse with motorneurons directly and with other classes of interneurons, such as 1a inhibitory interneurons (Figure 1.1C)[39-41]. Proprioceptive fibers have a tight relationship with the motorneurons of the muscles they sense, preferentially innervating "self" motor neurons, but also forming some connections with motor neurons that supply functionally synergistic muscle groups. This specificity is accomplished through the sensory-motor matching of neurotrophin-induced gene expression signatures, including the Ets transcription factors and cadherin adhesion molecules[42-44].

The simplicity of the mono-synaptic connection between proprioceptive sensory axons and motorneurons has facilitated the study of the relationship between these two topographic schemes. The mechanisms that direct assembly of muscle-specific sensory-motor connections

have recently been investigated by work from Jessell and colleagues. Surmeli et al. examined the role of motor neuron settling position in the formation of sensory-motor connections[45]. Motor neuron-specific deletion of the FoxP1 transcriptional cofactor for Hox proteins (referred to as $Foxp1^{MND}$) strips motor pools of their specific molecular identites. In $Foxp1^{MND}$ animals, motor neurons effectively innervate muscle targets in the limb, and the initial trajectory of proprioceptive fibers into the ventral horn occurs normally. However, careful analysis of sensory to motorneuron contacts using fluorescent labels revealed that when motorneuron cell body positioning is scrambled along the dorsal-ventral and medio-lateral axes in the $Foxp1^{MND}$ animals, proprioceptive fibers lose the ability to discriminate between self and non-self motor neurons. Instead, most proprioceptive fibers innervate motor neurons that are located in their "wild-type" termination zone, without regard for muscle-specific motor neuron identity. Therefore, the topographically organized terminations of the proprioceptive fibers within the ventral horn of the spinal cord is independent from the deletion of FoxP1 causing motorneurons to change their position and cell fate. These observations support the facilitation of proper connectivity as a potential function of topographic organization.

Spinal Interneurons: Integrators of motor plans

Spinal interneurons link most sensory and descending inputs to motorneuron outputs. However, they do not passively transmit this information. Rather, they translate sensory and cortical information onto the musculotopic topography of the motorneurons. A remaining question in the field is to understand how spinal interneurons are organized to fulfill the role of integrating various frames of reference of the skin, musculature, and mechanical function into coordinated motor outputs.

One of the best studies of spatial organization of interneurons is in an important series of reports by Schouenborg and colleagues on the nociceptive withdrawal reflex[35,46-48]. The response

to a noxious stimulus on the skin is to activate the muscles that withdraw that body region. For instance, a painful stimulus on the heel promotes ankle extension and knee and hip flexion. This reflex is mediated by nociceptive sensory afferents that target interneurons in the superficial dorsal horn, that relay to interneurons in the deep dorsal horn, that in turn control motorneurons. Each of these sensory and interneuronal components has a stereotypic topographic organization (Figure 1.1D). Specifically, the sensory fibers and interneurons are arranged in a medial to lateral progression to control distal extensors, then distal flexors, and then more proximal flexors. Interestingly, deprivation of the sensory cues during development perturbs this arrangement[35], suggesting neuronal activity-based mechanisms are required to establish these topographically organized connections. Ginty and colleagues have recently demonstrated that mechanoreception is also organized topographically in the superficial dorsal horn, in a pattern of longitudinal columns that is similar to the distribution of nociceptive target domains[49].

A few examples of defined locations for sub-classes of ventral interneurons have been described. However, the relevance of these spatial distributions to topography or function has yet to be determined. A rich literature has used markers and genetics to characterize a set of four cardinal lineage-related classes of ventral interneurons identifiable using well-established molecular markers: V0, V1, V2, and V3[50-53]. V1-derived Renshaw cells that mediate direct feedback inhibition to motor actions surround motorneurons, and V1-derived 1a inhibitory interneurons that are involved in proprioceptive reflexes are dorsal to motorneurons[54]. V0-derived V0c interneurons that modulate motorneuron excitability are located surrounding the central canal[55,56]. And Hb9 interneurons are only found at rostral lumbar levels, in the segments with the strongest central pattern generator drive[56,57].

Although the topographic frame of reference for molecularly-defined classes of spinal interneurons is largely unknown, there are electrophysiological experiments that suggest a function-based spatial order might exist for descending commissural-projecting interneurons (DC

neurons). Kiehn and colleagues found that activation of flexor motorneurons was correlated with ventrally-located DC neurons, whereas extension correlated with activity in a dorsally-located group of DC cells (Figure 1.1D)[58].

The characterization of interneuron topography has also been greatly facilitated by retrograde trans-neuronal labeling from the motorneurons of defined muscles. Techniques such as trans-neuronal WGA-HRP labeling and trans-synaptic wild-type rabies transmission revealed likely pre-motor interneuron distributions[59-62]. Generally, spinal pre-motor interneurons are found in the contralateral medial ventral horn, and in the ipsilateral spinal cord in the deep dorsal horn, intermediate region, and ventral horn. Recently, Callaway and Young and colleagues developed a genetically modified rabies virus that allows restricted retrograde mono-trans-synaptic spread of the virus[63]. With this technique, analysis of defined pre-motor interneurons has confirmed previously observed general distribution patterns. The comparisons of pre-motor interneuron distributions from proximal and distal muscles and from flexor and extensor muscles have revealed biases in the trends of interneuron locations (Figure 1.1D). Proximal muscles have pre-motor interneuron distributions that are more likely to have a significant ipsilateral ventral horn contribution, relative to more distal muscles that have a more intermediate region and dorsal horn bias. Within the deep dorsal horn interneuron groups, pre-extensor interneurons are more likely to be medial than pre-flexor interneurons. However, in contrast to individual motor pools that are well segregated, the pre-motor populations for multiple muscles are highly intermingled.

Very recently, a significant study by Arber and colleagues examined whether different motor pools have spatially distinct pre-motor components, using mono-synaptically restricted rabies virus[64]. They analyzed the pre-motor interneuron populations for several muscles and identified the medial extensor/lateral flexor bias in the dorsal horn interneurons. They also demonstrated that pre-motor interneurons were in turn contacted by sensory afferents. This is important because the ability to map multiple circuit elements simultaneously has yielded a much

richer understanding of network integration of multiple topographic systems. Moreover, when deprived of proprioceptive signals, the bias in pre-extensor and pre-flexor interneuron distributions is eroded[64]. This suggests that proprioceptive information can be a cue for spatial organization of interneurons, similar to the role for nociceptive/mechnoreceptive cues in refining the nociceptive withdrawal reflex.

Discussion

Topography of neural circuits is clearly a major organizational strategy of the CNS, and we have reviewed examples of topographic spatial organization within the spinal motorneurons, motor cortex, spinal sensory system, and spinal interneurons. These networks function together with the thalamus, basal ganglia, brainstem, cerebellum, and other brain regions to initiate and coordinate movements. Although the spatial organization of most of these other regions is not well characterized and not described in this review, there is evidence that motor circuits in the brainstem and cerebellum display some topographic order that relates to specific muscles or groups of muscles[61,65].

We are just beginning to understand how multiple topographic networks interact to produce coherent movements. On the one hand, it is a complicated problem to merge the high-dimensional cortical system, the intermediate-dimensional sensory system, and the diverse and poorly understood organizations of spinal interneurons. Each of these systems has its own frame of reference and parameters that it can encode. How can these be reduced to the low-dimensionality of motorneuron and muscle organization? On the other hand, the filtering and integration of multiple inputs to produce coherent outputs is a hallmark of neuronal function, and the principles that apply at the cellular scale may also be relevant to the way circuits process and transform information.

It is also important to ask what is the purpose of this complex spatial organization. Given the vast array of neurons, fibers, and connections in the CNS, perhaps topographic principles facilitate the embryonic and post-natal development of proper connectivity. Another possible purpose for topographic organization is to preserve 'wiring efficiency'. Neurons that are commonly recruited together may be physically close to minimize the time and energy that must be used for their communication[66-68]. In addition, in both the cortex and spinal cord, local neuronal ensembles may be co-recruited by traveling waves of activity. Local clustering of functionally- and topographically-related neurons provides a substrate for waves of activation to bind their related targets together into a compound output[29,69-72].

Recent work in this field has continued to provide rich descriptions of the extent of topographic organization in the spinal cord, and to provide a circuit-based framework for integrating the organization of the cortical, sensory, and interneuronal systems with the musculotopic motorneuronal system. Once we better understand the spatial and connectivity principles that govern movement at the level of the spinal cord, it will become feasible and critical to examine the role of this organization in producing coordinated behaviors. For instance, can topographic maps be re-written and if so, what are the consequences for movement? Is the alteration of topographic mapping the cellular substrate used by evolution to modify behaviors across species? These types of questions will address the importance of these schemes for function and may provide the basis for understanding motor plan integration when topographic map organization is altered in training, injury, and disease.

Acknowledgements

Chapter 1 is an adaptation of a review published in *Current Opinions in Neurobiology*, 2012. The full citation is: Ariel J. Levine, Kathryn A. Lewallen, and Samuel L. Pfaff. Spatial

Organization of cortical and spinal neurons controlling motor behavior. *Current Opinions in Neurobiology*, 2012 Oct; 22(5):812-21. The article and publication are online at: http://www.sciencedirect.com/science/article/pii/S0959438812001110.

This manuscript was published online July 27, 2012 in advance of the print journal. This manuscript was written in collaboration with Ariel J. Levine, and with the guidance of Samuel L. Pfaff. The authors of this manuscript would like to thank Dr. Dario Bonanomi and Dr. Chris Hinckley for helpful comments on the manuscript. Ariel J. Levine was supported by George E. Hewitt Foundation for Medical Research. I was supported as a National Science Foundation Graduate Research Fellow. Samuel Pfaff is an HHMI investigator. Research in the laboratory was supported by NINDS.

Chapter 2

Identification of a cellular node for motor control pathways

Identification of a cellular node for motor control pathways

Abstract

The rich behavioral repertoire of animals is encoded within the central nervous system as a set of motorneuron activation patterns, also called 'motor synergies'. However, the neurons that orchestrate these motor programs as well as their cellular properties and connectivity are poorly understood. Here we identify a population of molecularly defined motor synergy encoder (MSE) neurons in the mouse spinal cord that may represent a central node in neural pathways for voluntary and reflexive movement. This population receives direct inputs from the motor cortex and sensory pathways and, in turn, has monosynaptic outputs to spinal motorneurons. Optical stimulation of MSE neurons drove reliable patterns of activity in multiple motor groups, and we found that the evoked motor patterns varied based on the rostrocaudal location of the stimulated MSE. We speculate that these neurons comprise a cellular network for encoding coordinated motor output programs.

Introduction

Common movements, such as reaching and grasping an object or stepping, involve complex neural calculations to select the appropriate muscles and precisely control the timing of their contractions to achieve the desired outcome. This motor coordination involves many regions in the central nervous system (CNS), including the motor cortex, red nucleus, basal ganglia, brainstem, cerebellum, peripheral sensory system and spinal neurons. These neural pathways ultimately converge onto motorneuron pools that are each dedicated to controlling a single muscle of the body. Given the number of muscles and possible joint positions of the body that can vary at each moment, the efficiency and reliability of common movements are remarkable.

To simplify the motor-control tasks of the CNS, neural plans for compound movements that invoke multiple joints or body regions are thought to be fractionated into a series of subroutines or 'synergies' that bind together useful combinations of motorneuron activation[73-75]. These synergies may then be flexibly recruited into multiple types of movement, such as voluntary and reflexive behaviors. It has long been recognized that voluntary movements and those evoked by direct stimulation of the motor cortex have similarities with movements activated by sensory reflexes[25,76-78]. Because the cortex and peripheral nervous system have direct connections into the spinal cord, we tested whether these inputs converge onto a shared spinal motor circuitry for coordinating motor actions. We identified a spatially and molecularly defined population of neurons in the deep dorsal horn of the spinal cord that are candidates to encode the programs for motor synergies; this population comprises a network of neurons at the point of intersection between the corticospinal and sensory pathways. Because activation of these neurons is sufficient to elicit reliable and coordinated motorneuron activity, we designated these cells "motor synergy encoder" (MSE) neurons. Functional studies of MSE neurons revealed an orderly circuit organization, which we speculate helps to simplify the selection of the appropriate programs that underlie complex motor actions for purposeful movements.

Results

A premotor neuron column in lamina V

Motor synergies that involve multiple hindlimb joints typically employ motor pools that are present in different lumbar (L) segments. For example, the stance phase of locomotion involves coextension by quadriceps motor pools in L2–3 and gastrocnemius motorneurons in L4–5[4,5,79]. To identify spinal neurons that may mediate coordination of motorneuron activity, we searched for intersegmentally projecting neurons with strong direct connections to motorneurons. We used a monosynaptic circuit–tracing strategy that limits the spread of trans-synaptic rabies

virus to only first-order premotor neurons. This approach is based on co-infecting motorneurons with genetically modified rabies virus (RabΔG) and adeno-associated virus (AAV) encoding glycoprotein (AAV:G)[2,80]. Experiments were performed on mice between postnatal days 0–15 (P0–P15) because this time window provides the most efficient trans-synaptic labeling, with a minimum of neuronal toxicity, and because the distribution of premotor neurons is similar between pups and adults[61,81].

RabΔG and AAV:G were co-injected into a range of muscles that control joint movements of the hindlimb and forelimb. We studied the medial and lateral gastrocnemius muscles (ankle extensors), the tibialis anterior (ankle flexor), the quadriceps (knee extensor), the hamstrings (knee flexor), the wrist extensors, the wrist flexors, the triceps (elbow extensor) and the biceps (elbow flexor). We observed a dense column of ipsilateral neurons in the deep dorsal horn extending the length of the lumbar spinal cord for hindlimb muscles or the cervical spinal cord for forelimb muscles (n = 89 spinal cords; Figure 2.1A-C, Figure 2.2A, Figure 2.3, and data not shown). The cell bodies of this column were predominantly concentrated in medial lamina V, but we also observed sparse cell labeling in lateral lamina V and medial laminae IV and VI (Figure 2.1B-E, Figure 2.2A, and Figure 2.3. To determine whether the premotor neurons in laminae IV–VI were a unique subset of cells or representative of typical neurons in this region of the spinal cord, we examined their morphology in spinal cords with sparse premotor trans-synaptic RabΔG labeling to better identify individual cells. The laminae IV–VI premotor neurons had large cell bodies (10–30 μm) and dendritic morphologies typical of Golgi-labeled laminae IV–VI neurons[82], which suggested that the premotor neurons were representative of the general population of neurons in the deep dorsal horn rather than a unique morphological cell type (Figure 2.2A, B).

Trans-synaptic labeling revealed the processes of these deep dorsal horn premotor cells to be within a dense cluster centered in medial lamina V. Axons of these cells entered the

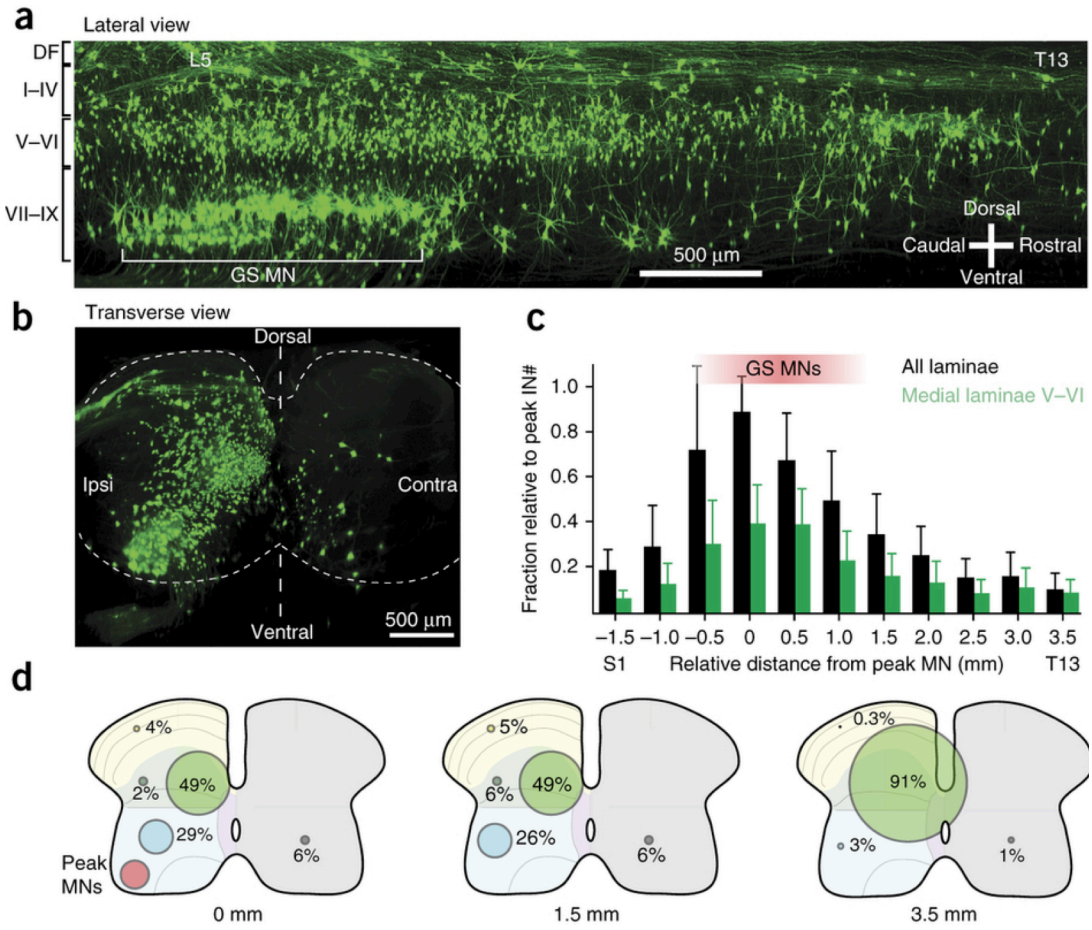

Figure 2.1: Labeling of first-order spinal neurons targeting gastrocnemius motorneurons. (A,B) Images of a RabDG:GFP-labeled spinal cord following injection into the medial gastrocnemius (GS) muscle. **(A)** Lateral projection of an optically cleared lumbar spinal cord, shows motorneurons (GS MN) in the ventral horn of L4 and L5 spinal segments. Premotor cells and fibers can be seen in the dorsal funiculus (DF), laminae I–IV, laminae V–VI and laminae VII–IX. **(B)** Collapsed transverse view of the lumbar spinal cord in A, shows ipsilateral (ipsi) and contralateral (contra) premotor cells. **(C)** Quantification of total pregastrocnemius spinal neurons (all laminae) and of the subset of pregastrocnemius neurons in medial laminae V–VI along the rostral-caudal axis of the lumbar spinal cord. Neuron counts (IN#) were normalized to the maximum number of neurons in a single section for each spinal cord to control for the variability in labeling. Means and s.d. are shown. Values are listed in Figure 1.4. Location "0" indicates the section with the peak number of motorneurons, and is usually in caudal L4. **(D)** Premotor cell distributions depicted on transverse spinal cord images representing the spinal level with peak motorneurons (0 mm), at a level 1.5 mm rostral (mid-lumbar) and at a level 3.5 mm rostral (upper lumbar/lower thoracic). Laminae were divided into functional regions, and the percentage of total premotor cells at each level are shown for each region, represented by the diameter of the colored circles. These regions are superficial dorsal horn (laminae I–IV, yellow), medial deep dorsal horn (medial laminae V–VI, green), lateral deep dorsal horn (lateral laminae V–VI, gray), ventral horn (laminae VII–IX, blue) and contralateral (gray).

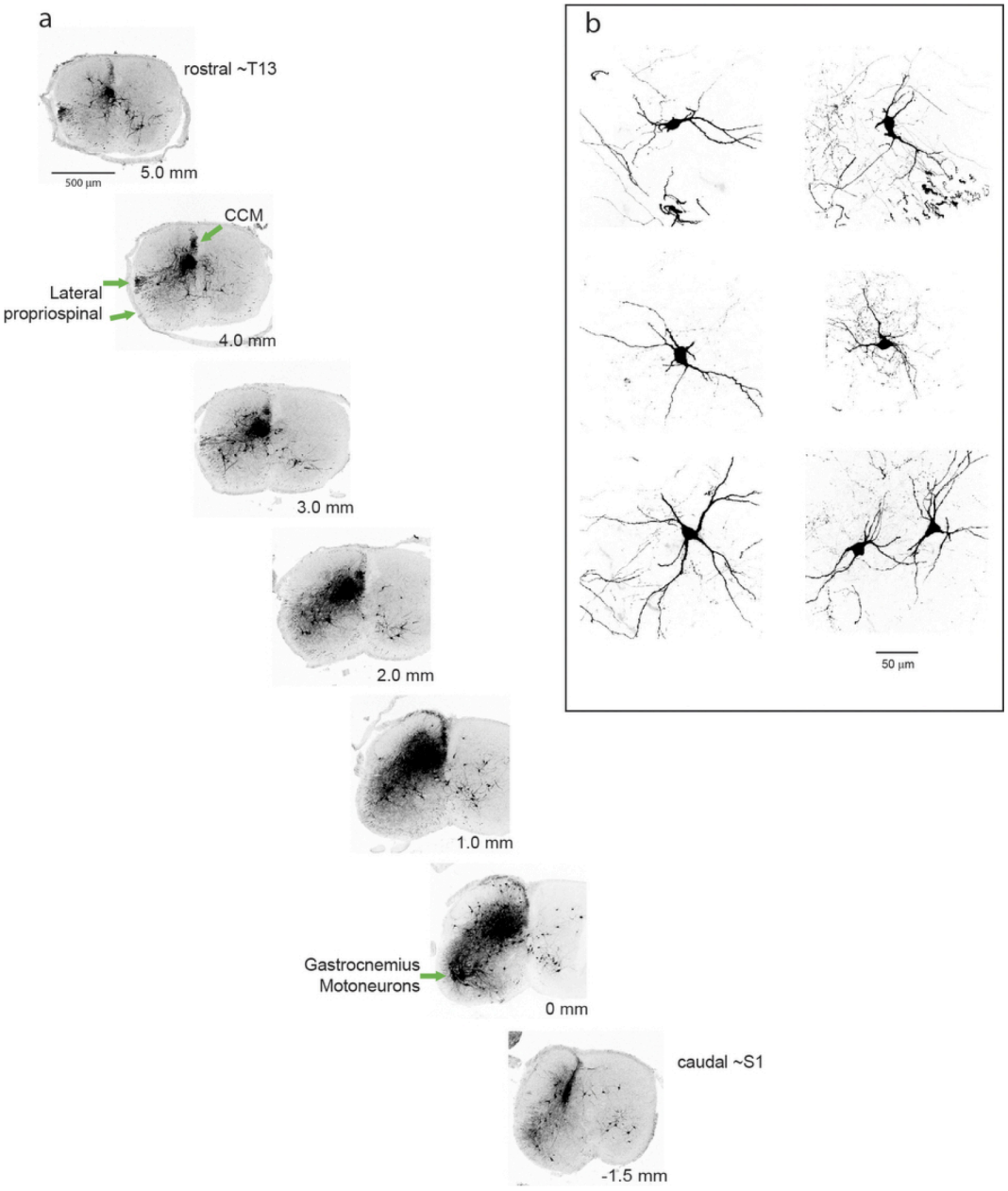

Figure 2.2: Characterization of cellular morphology of MSE column neurons. (A) Transverse 50 µm sections of a spinal cord labeled with RabΔG from the gastrocnemius muscle, showing gastrocnemius motorneurons and pre-gastrocnemius neurons from different rostral (top) to caudal (bottom) levels. The lateral propriospinal white matter tracts and the cornu-commisuralis of Marie (CCM) white matter in the dorsal funiculus are indicated. These white matter tracts are known to contain axons of intersegmentally projecting propriospinal interneurons. MSE column neurons can be seen projecting axons into both white matter tracts. **(B)** Examples of typical cellular morphology of MSE column neurons.

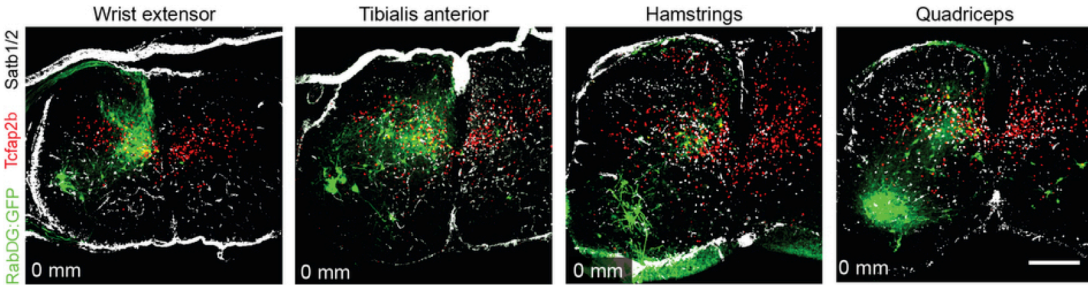

Figure 2.3: Medial deep dorsal horn premotor distribution for diverse muscles. Distribution of spinal neurons pre-synaptic to the wrist extensor, tibialis anterior, hamstrings, and quadriceps motorneurons, each shown at the level of peak motorneurons for that muscle, together with immunolabeling of Tcfap2β (red) and Satb1/2 (white). Images are projected confocal stacks. Scale bar is 250 μm.

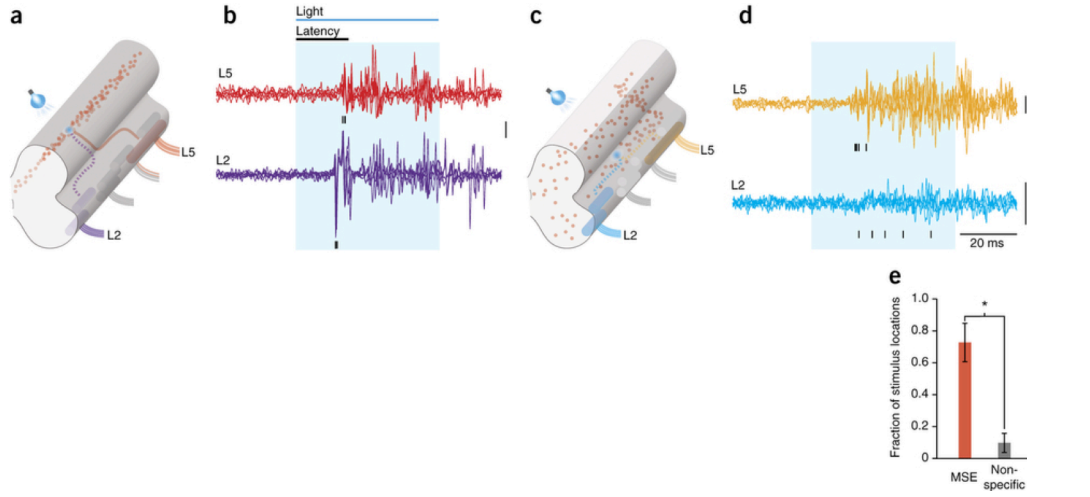

Figure 2.4: Motorneuron responses to optical stimulation of medial deep dorsal horn premotor neurons or of nonspecific ventral interneurons. (A,C) Experimental setups for optical stimulation of transynaptic MSE neurons (A) or non-specific ventral interneuron (C). Following transynaptic RabΔG:ChR2 labeling (A) or spinal injection of non-transynaptic RabΔG:ChR2 (C), focal blue light was used to optically excite spinal neurons in the deep dorsal horn (A) or ventral horn (C). Electrical recordings were performed on the L5 ventral root that contains gastrocnemius motorneuron axons (red) and the L2 ventral root that contains ileo-psoas and quadriceps motorneuron axons (purple). **(B,D)** Ventral root recordings after stimulation of L3 MSE neurons (B) and L3 non-specific ventral interneurons (D). Black ticks indicate latency from the onset of light stimulation (blue box) to the first motorneuron action potentials. Five consecutive traces are shown for each example. **(E)** Mean (±s.e.m.) fraction of stimulus locations with reliable L2 and L5 ventral root activity analyzed in each spinal cord (see methods). Reliable dual root responses were significantly enriched for MSE neuron stimulations (72.7%) compared to nonspecific ventral neuron stimulations (8.3%), $*P = 0.0034$, two-sided t-test. Vertical scale bars, 20 μV.

ventrolateral white matter and cornu-commissuralis of Marie in the dorsal funiculus (Figure 2.2), which are known tracts for intersegmentally projecting axons[82,83]. Consistent with this intersegmental axonal labeling pattern, we detected premotor neurons up to eight spinal cord segments from their motorneuron targets (Figure 2.1A, C, D, and data not shown).

To quantify distributions of premotor neurons, we selected a single muscle, the ankle extensor gastrocnemius, and analyzed its premotor circuitry by regional and laminar distribution[84]. 52% of all rabies virus–labeled pregastrocnemius spinal neurons were located in the medial deep dorsal horn (laminae V–VI), compared with 28% in the ipsilateral ventral horn (laminae VII–IX), 7% in the contralateral spinal cord, 4% in the superficial dorsal horn (laminae I–IV) and 3% in the lateral deep dorsal horn (laminae V–VI) (n = 4,594 cells in 20 spinal cords; Figure 2.1B-D). The fraction of total premotor spinal neurons that were located in the medial deep dorsal horn increased at progressively rostral levels, reaching over 90% in upper lumbar and lower thoracic levels (Figure 2.1C, D, and Figure 2.2A).

These viral tracing studies revealed a column of premotor spinal neurons for a variety of motor pools located in the medial area of the deep dorsal horn, consistent with previous studies that identified premotor and putative premotor spinal neurons using a wide range of techniques[2,59,61,81,85-88]. Medial deep dorsal horn premotor neurons are notable because they quantitatively represent the most prominent source of rabies virus-identified monosynaptic input onto motorneurons, extend axons across multiple spinal cord segments and are in the deep dorsal horn of the spinal cord, a region that is sufficient to drive motor synergies after electrical stimulation[89].

Premotor lamina V neurons bind the activity of multiple motor pools

We hypothesized that rabies-labeled premotor neurons concentrated in medial lamina V

were cellular candidates to mediate motor synergies for multijoint movements. To explore this possibility, we tested whether direct activation of these neurons was sufficient to evoke reliable and coordinated motorneuron activity in the functionally related motor groups of the L2 and L5 spinal segments. This provides a simple model of a motor synergy. We used monosynaptic rabies-virus tracing to deliver the light-activated cation channel, channelrhodopsin 2 (RabΔG:ChR2)[90] to pregastrocnemius neurons, exposed the medial surface of the spinal cord and delivered focal, short-duration pulses of light to directly excite the pregastrocnemius medial deep dorsal horn neurons (Figure 2.4A). To analyze motor activity, we performed electrical recordings of the L5 ventral root, which includes gastrocnemius motorneuron axons, and the L2 ventral root, which contains the motorneuron axons of the functionally related muscles: the quadriceps and ileo-psoas hip flexors. Quadriceps activity is coordinated with gastrocnemius activity during the stance phase of locomotion[79] and the ileo-psoas has been reported to be activated with the gastrocnemius in specific cases of the pain-withdrawal reflex[91-93]. We considered that optical stimulation of gastrocnemius premotor neurons would drive only L5 electrical activity if these neurons control only the gastrocnemius motor pool or would drive dual L2 and L5 activity if these neurons control coordinated activity of motor groups for multiple joints.

We found that optical stimulation of medial deep dorsal horn pregastrocnemius neurons evoked detectable motorneuron responses in both the L5 ventral root (10/10 spinal cords) and the L2 ventral root (9/10 spinal cords; Figure 2.4B). We analyzed spinal cords that met our minimum criteria for efficiency of labeling with rabies virus (see methods) by performing optical stimulations in sets of ten trials over a range of stimulation locations from L1 to L6. Among this set, we found that all stimulation locations produced some motor response, but 72.7 ± 0.2% (mean ± s.d.) of premotor medial deep dorsal horn stimulation locations produced dual L2 and L5 motorneuron activity without any trial failures (n = 78 locations in four spinal cords, with ten

trials at each location; Figure 2.4E). These data show that first-order premotor medial deep dorsal horn neurons have reliable and functional outputs capable of activating multiple motor groups.

Taken together, these findings reveal a population of spinal neurons that have four key features related to motor synergies. (i) These neurons represent a major source of the direct synaptic input to motorneurons. (ii) They extend axons intersegmentally and therefore are well-suited to bind spatially segregated but functionally related motor pools. (iii) These cells are located in the deep dorsal horn, the region from which electrical stimulation of the spinal cord can best evoke motor synergies[89]. (iv) Direct stimulation of these cells is a sufficient and reliable means to activate multiple motor groups. Accordingly, we considered that these cells are candidates to be motor synergy encoders, and we designated them MSE neurons.

Features of MSE neuron–evoked motor responses

We sought to determine the specific features of motorneuron activity evoked by candidate MSE neurons by comparison with motor responses driven by other classes of spinal neurons. To provide a control group of spinal interneurons with which to compare MSE cell function, it was necessary to achieve comparable levels of ChR2 expression in a comparable number of cells but in an unbiased set of spinal interneurons. We performed intraspinal injections of replication-defective RabΔG:ChR2 to infect spinal neurons at L4 or L5 as well as the intersegmental neurons that project to these levels and take up the RabΔG:ChR2 at their terminals (n = 7 spinal cords; Figure 2.4C). We performed these experiments without complementing glycoprotein, to restrict RabΔG:ChR2 expression to initially infected neurons following intraspinal injection. We then performed optical excitation experiments over the ventral spinal cord, to probe the effects of nonspecific ventral interneurons on L2 and L5 motor activity. We found that optical stimulation of nonspecific ventral interneurons evoked some detectable motor response from all stimulation locations, which is consistent with the known motor function

of the ventral spinal cord (n = 54 locations in seven spinal cords; for example, Figure 2.4D). However, only 8.3 ± 1.4% of stimulation locations evoked reliable dual L2 and L5 motor responses (mean and s.d.). This is in marked contrast with the 72.7% of MSE stimulation trials (two-sided t-test; P = 0.0034; Figure 2.4E). Thus, although multiple classes of spinal neurons contribute to motor control in behavior, direct optical excitation of a broad and unbiased set of ventral spinal interneurons does not consistently evoke dual L2 and L5 motor group responses.

We next considered that the reliability of the dual motor responses may be explained by individual MSE neurons that contact multiple motorneuron pools through monosynaptic connections. To probe whether MSE neurons directly contact multiple motor pools, we performed two-color RabΔG-Cherry and RabΔG-GFP labeling experiments to visualize cells in the premotor circuitries of two muscles simultaneously. Although we observed doubly labeled (yellow) premotor cells for pairs of muscles that are commonly co-recruited during behavior, their infrequency suggests that they represent a minor portion of the paths by which MSE neurons access motorneurons (13/389 premedial gastrocnemius neurons, n = 6 spinal cords; Figure 2.5). The very low fraction that we observed may be an experimental underestimate owing to additive inefficiencies of two RabΔG viruses, but independent studies confirm that dual-labeled premotor cells represent a small fraction of the total premotor population[2,85].

These labeling studies suggested that MSE neurons likely use indirect connections to coordinately regulate multiple motor groups via polysynaptic pathways. This is supported by our measurements of the relatively long latencies to the first motorneuron spikes after optical stimulation of MSE neurons (for example, Figure 2.4B). This polysynaptic transmission could be mediated by other neuron classes, but the relative unreliability of ventral interneuron-evoked dual L2 and L5 responses (Figure 2.4D, E, and data not shown) suggests that this possibility is not sufficient to explain the reliable MSE neuron–evoked responses that we observed (Figure 2.4B, E, and data not shown). Alternatively, MSE neurons may contact multiple groups of

motorneurons through an interconnected MSE neuron network that enhances the robustness and reliability of motor responses, despite its polysynaptic path.

To determine whether candidate MSE neurons synaptically contact each other, we analyzed spinal cords in which medial gastrocnemius MSE neurons were labeled with RabΔG:Cherry and lateral gastrocnemius MSE neurons were labeled with RabΔG:GFP. In the medial deep dorsal horn, we observed dense Cherry$^+$ processes and GFP$^+$ processes surrounding MSE neurons labeled with both fluorescent proteins (Figure 2.6). We performed immunofluorescence assays to identify excitatory (vGlut2$^+$) and inhibitory (Gad67$^+$ or GlyT2$^+$) MSE GFP$^+$ synaptic terminals that overlapped with the Cherry$^+$ cell bodies (and vice versa). We found examples of both excitatory and inhibitory MSE-to-MSE neuron connectivity (Figure 2.6), which provides a potential pathway for MSE neurons to indirectly coordinate motorneuron responses via other MSE neurons. Thus, MSE neurons likely target multiple motorneuron groups through a combination of direct monosynaptic connections to multiple motorneuron pools and indirect connections through a polysynaptic MSE neuron network.

A molecular description of MSE cells

Having studied the connectivity and functional features of MSE neurons, we next began to characterize their cellular identity. To identify markers of the MSE cell population, we systematically screened the Gensat expression database[94] and cross-referenced these results with the Allen Brain Institute expression database[95]. We identified three candidate genes that are expressed in the medial deep dorsal horn at embryonic and postnatal stages, the transcription factor *Tfap2b* (also known as *Tcfap2β*) and the nuclear and chromatin organization factors *Satb1* and *Satb2*[96,97]. Tcfap2β is expressed at late embryonic and early postnatal stages across lamina V (with overlap into laminae IV and VI) and in a few scattered cells in the ventral horn (Figure 2.7A). We studied Satb1 and Satb2 together (Satb1/2), using an antibody that recognizes both

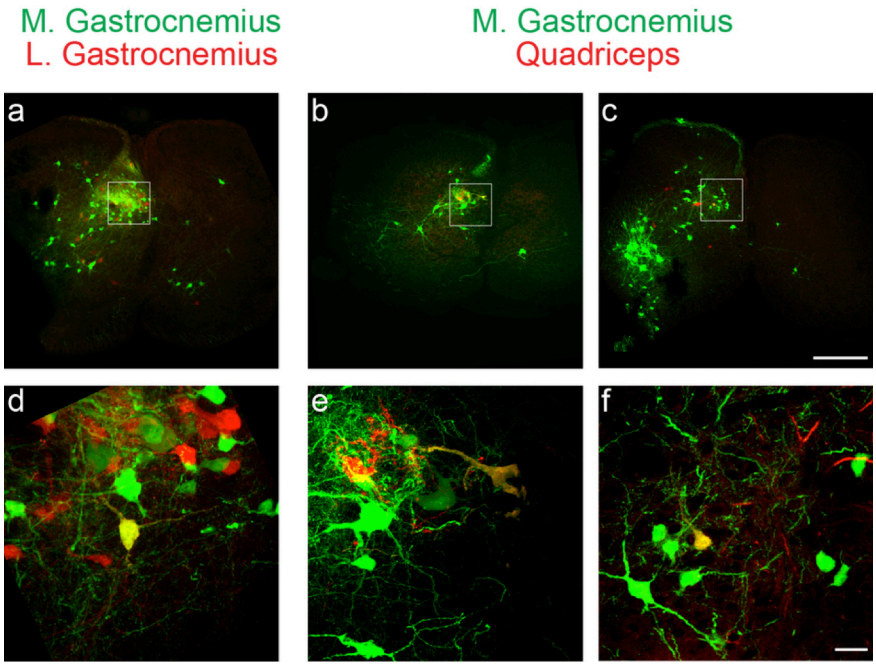

Figure 2.5: MSE neurons target functionally related motor pools. Individual MSE neurons that directly contact two motor pools were identified using RabΔG:GFP that was injected into the medial gastrocnemius and RabΔG:Cherry was injected into the lateral gastrocnemius or quadriceps at P0. Spinal cords were analyzed at P8. The locations **(A-C)** and high magnification views **(D-F)** of individual cells that were directly pre-synaptic to the medial gastrocnemius muscle (green) and either the lateral gastrocnemius (red) (A, D) or the quadriceps (red) (B, C, E, F) are shown, as projected confocal images. Double pre-motor MSE are yellow. We found that 13/389 (n=6 cords) pre-medial gastrocnemius neurons were yellow following lateral gastrocnemius or quadriceps injections. We did not observe any yellow cells following injections of the antagonistic pair of medial gastrocnemius and tibialis anterior (0/278), suggesting that yellow double premotor neurons are specifically associated with functionally co-recruited muscles. Scale bars are 250 μm in A-C and 25 μm in D-F.

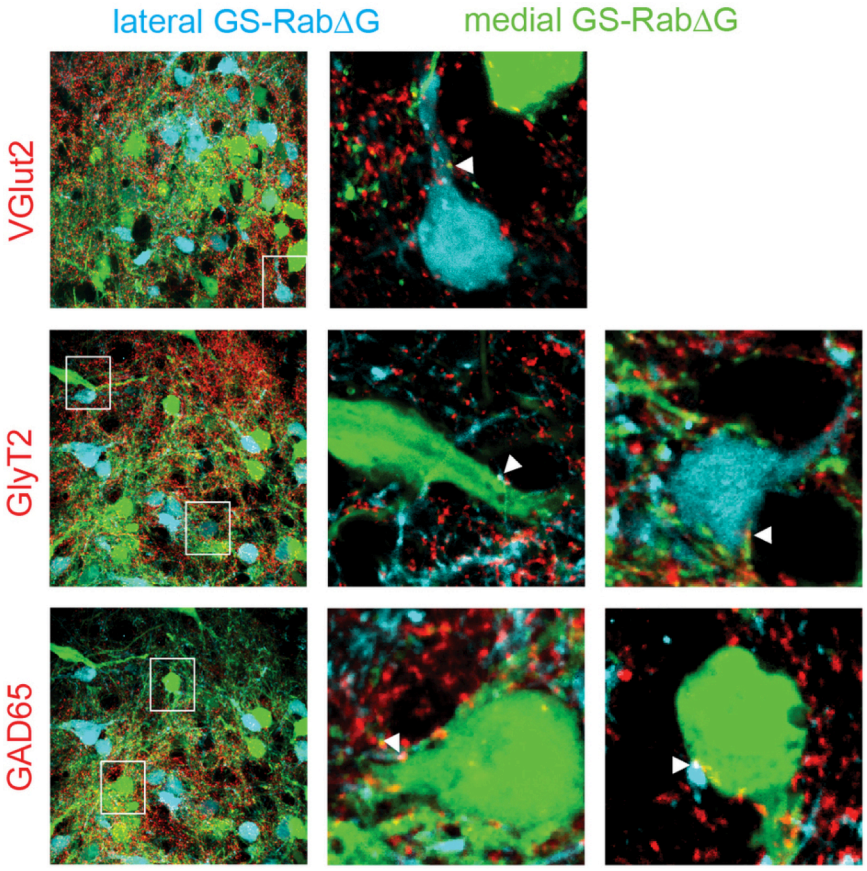

Figure 2.6: Interconnectivity among MSE cells. Projected confocal images of sections from P8 spinal cords with pre-medial gastrocnemius (medial GS-RabΔG, green) and pre-lateral gastrocnemius (lateral GS-RabΔG, cyan) labeling. Excitatory (vGlut2, red) and inhibitory (Gad65 or GlyT2, red) synaptic contacts between medial GS MSE and lateral GS MSE neurons are highlighted with arrowheads. Middle and right panels are single optical sections.

proteins. Satb1/2 were expressed at mid-late embryonic stages in a cluster of cells in medial lamina V/VI (data not shown), and through postnatal stages in medial lamina V/VI and lamina III (Figure 2.7B). Next, we examined whether Tcfap2β and Satb1/2 are expressed by MSE cells using immunofluorescence analysis of spinal cords with RabΔG-labeled MSE neurons. Tcfap2β was expressed in 23 ± 12% and Satb1/2 were expressed in 13 ± 11% of all pregastrocnemius spinal neurons (mean and standard deviation, *n* = 4,594 cells in 20 spinal cords; Figure 2.7). This is in comparison with other previously reported markers of premotor neurons that account for 2.1% ($V0_c$ $ChAT^+$), 2.5% (dI3 $Isl1^+$), 3% (V2 $Lhx3^+$) and 3.4% (Renshaw calbindin$^+$) of premotor spinal neurons[1,2]. In the medial deep dorsal horn, Tcfap2β antibody labeling identified 41 ± 17% and Satb1/2 labeling identified 20 ± 13% of pregastrocnemius neurons (mean and standard deviation, *n* = 2,402 cells in 20 spinal cords; Figure 2.7I, L). A small percentage of cells were positive for both Tcfap2β and Satb1/2 antibodies. We observed similar results in pre-tibialis anterior, pre-hamstrings, pre-quadriceps and pre-wrist extensor studies (Figure 2.7I-K and data not shown).

We determined the neurotransmitter status of Tcfap2β^+ and Satb1/2^+ cells. We found that the Tcfap2β^+ sub-population of MSE neurons comprises a minor excitatory subtype and a major inhibitory subtype (Figure 2.7C-H). Among the Satb1/2^+ MSE neuron population, we found these cells could be subdivided into distinct dorsal and ventral subgroups based on their gene expression profiles. Most of the Satb1/2^+ neurons in the ventral region of medial lamina V–VI expressed the inhibitory marker Pax2, whereas most of the Satb1/2^+ neurons in the dorsal area of medial lamina V–VI expressed the excitatory marker Tlx3 (Figure 2.7C-H).

These data provide the first assignment of molecular markers to this population of premotor cells, reveal that MSE neurons are a heterogeneous population and suggest that the combination of medial deep dorsal horn cell location, together with Tcfap2β or Satb1/2

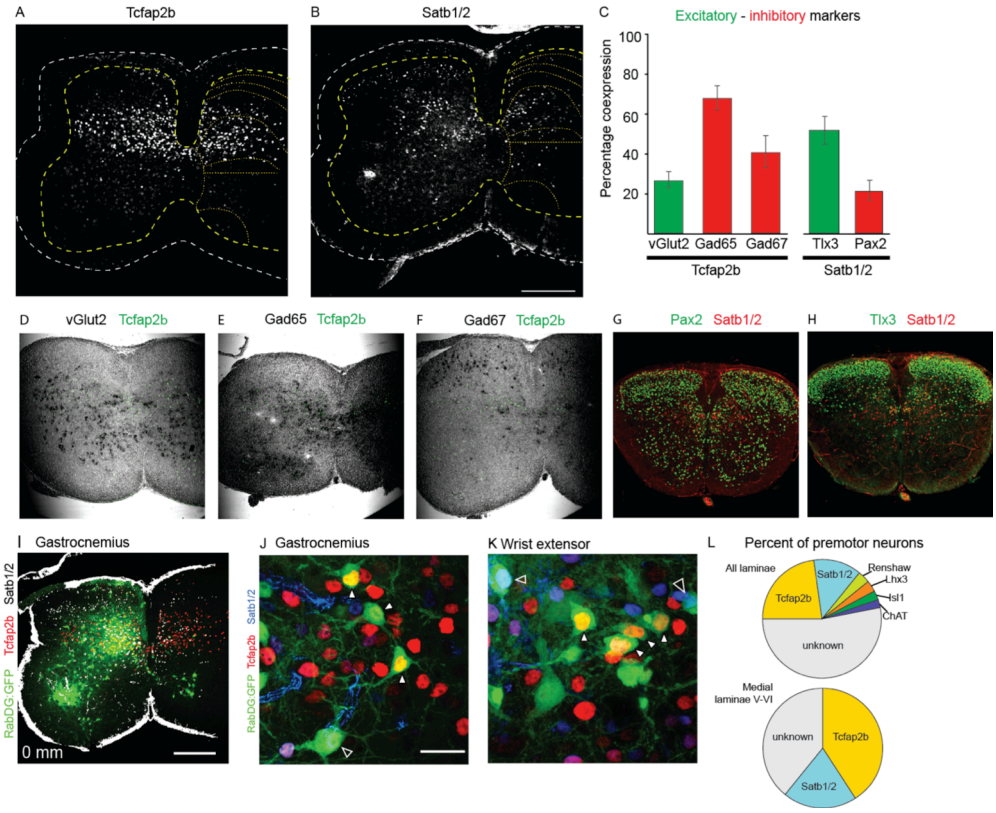

Figure 2.7: **Molecular markers Tcfap2β and Satb1/2 identify medial deep dorsal horn premotor neurons. (A,B)** Projected confocal stacks showing immunolabeling of Tcfap2β (A) and Satb1/2 (B) in transverse sections of P8 lumbar spinal cord. **(C)** Neurotransmitter status of Tcfap2β and Satb1/2 cells determined using *in situ* hybridization at P10 against vGlut2 (excitatory), Gad65 (inhibitory), and Gad67 (inhibitory), or with antibodies at P2 to identify Tlx3 (excitatory) and Pax2 (inhibitory). Mean percentages ± s.d. are: 26 ± 4% of Tcfap2β^{+} neurons expressed vGlut2 (n = 570 neurons in 5 P10 spinal cords), 67 ± 6% of Tcfap2β^{+} neurons expressed Gad65 (n = 344 neurons in 4 P10 spinal cords) and 40 ± 8% expressed Gad67 (n = 201 neurons in 3 P10 spinal cords). Among the Satb1/2^{+} population, 22 ± 5% of all Satb1/2^{+} expressed Pax2 (n = 1,056 neurons in 4 P2 spinal cords), and 52 ± 7% of all Satb1/2^{+} expressed Tlx3 (n = 956 neurons in 4 P2 spinal cords). **(D-F)** In situ hybridization in P10 spinal cords against excitatory vGlut2 (D), inhibitory Gad65 (E), and inhibitory Gad67 (F) in black, with immunolabeling against Tcfap2β (green). **(G-H)** Immunolabeling in P2 spinal cords against Satb1/2 (red), and inhibitory Pax2 (green) or excitatory Tlx3 (green). (**I**) Projected confocal stacks showing immunolabeling and RabΔG labeling in transverse sections of P8 lumbar spinal cords. Distribution of gastrocnemius motorneurons and pregastrocnemius spinal neurons (RabΔG:GFP) at peak of motorneuron labeling, together with immunolabeling of Tcfap2β and Satb1/2 (white) **(J, K)** High-magnification images of RabΔG-labeled premotor spinal neurons in the medial deep dorsal horn (green), positive for Tcfap2β (yellow, filled arrowheads) and Satb1/2 (light blue, unfilled arrowheads), that are directly presynaptic to the gastrocnemius (J) or wrist extensors (K). **(L)** Fraction of total pregastrocnemius neurons (top) and medial laminae V–VI premotor spinal neurons (bottom) identified by Tcfap2β, Satb1/2 and other previously described premotor spinal neuron classes[1,2]. Scale bars, 250 mm (A, B, G-H, I) and 25 mm (J,K).

expression status can serve as a surrogate for identification of MSE neurons. Further studies will be needed to probe the functions of MSE neuron subpopulations.

MSE neurons receive sensory and corticospinal inputs

It has been shown that motor synergies can be activated by different neural pathways, including sensory reflexes and motor cortex stimulation[25-27,76]. This creates specific expectations for the types of inputs that MSE neurons should receive, namely, inputs from sensory pathways and from pyramidal cells in the motor cortex.

Proprioceptive sensory inputs may modulate motor synergies, cooperate with them to engage multiple motor pools or inform MSE cells about the position of the limb before initiation of movement. It is known that primary proprioceptive afferents have dense terminations in the medial deep dorsal horn[98,99], and we found that 98 ± 2% of MSE cells were contacted by proprioceptive parvalbumin$^+$ and vGlut1$^+$ terminals or parvalbumin-synaptophysin-tdTomato$^+$ terminals (n = 84 cells in three spinal cords; Figure 2.8A, D). We then analyzed a set of premotor medial deep dorsal horn neurons that expressed Tcfap2β or Satb1/2 and found that 93.8% of these cells received proprioceptive synaptic contacts that we validated by co-localization of a genetic label of presynaptic terminals (parvalbumin-synaptophysin-tdTomato) and the post-synaptic marker PSD95 (n = 30 cells in eight spinal cords; data not shown). The proprioceptive inputs onto premotor, marker-positive, medial deep dorsal horn cells were numerous, with 36 ± 7 contacts per cell (n = 8 cells in three spinal cords), and we observed these over the cell body and processes (26 ± 16% on cell bodies and 74 ± 16% on processes; means and standard deviations; Figure 2.8D and data not shown).

To determine whether motor cortex projections via the corticospinal tract may direct motor commands using MSE neurons as intermediaries, we analyzed spinal cords at P14–15 when the corticospinal tract is relatively mature[100,101]. We used a new genetic strategy

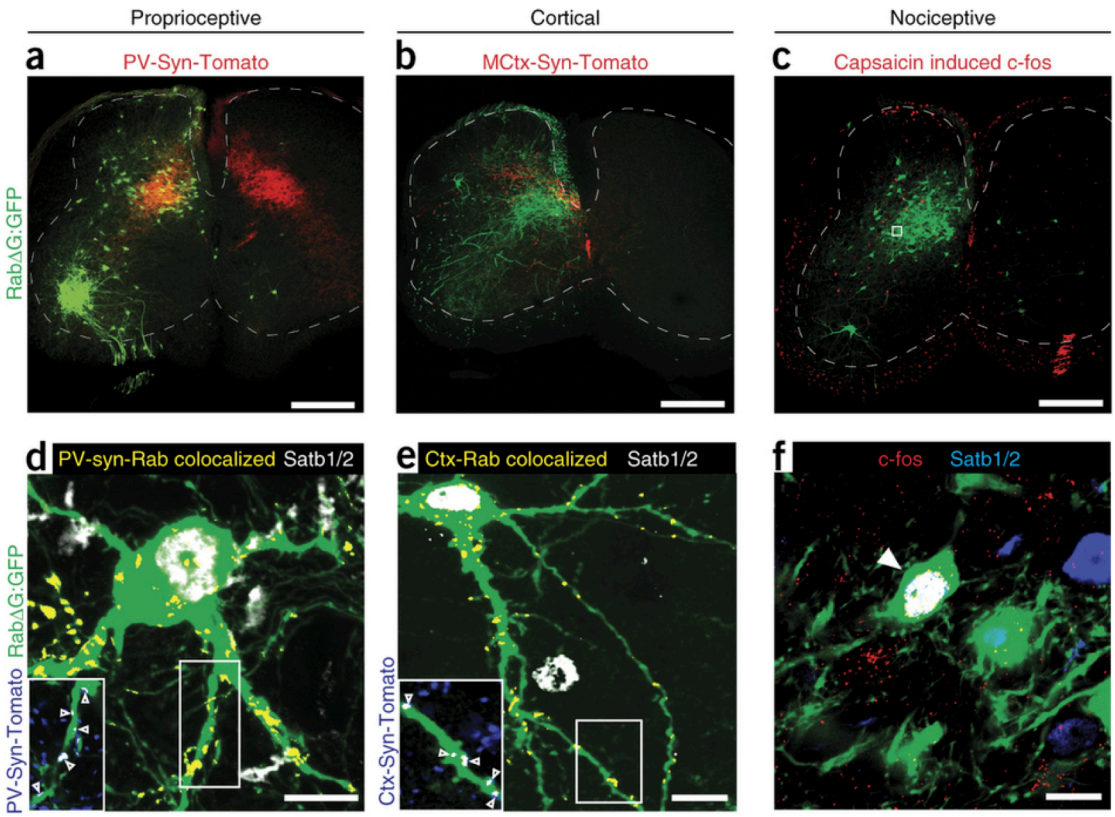

Figure 2.8: MSE neurons receive sensory and corticospinal inputs. (A) RabΔG labeling of pregastrocnemius MSE (green) and genetic labeling of proprioceptive afferent synaptic terminals (*Parvalbumin::synaptophysin-tdTomato* (PV-Syn-Tomato), red). **(B)** RabΔG labeling of pre-tibialis anterior (TA), MSE (green) and genetic labeling of corticospinal terminations from the caudal motor cortex, following focal unilateral injection of AAV:Cre into the caudal motor cortex of cre-dependent *synaptophysin-tdTomato* (MCtx-Syn-Tomato, red) pups. **(C)** RabΔG labeling of MSE and immunolabeled capsaicin induced c-fos expression. **(D,E)** To stringently identify synaptic inputs onto RabΔG:GFP^{+} (green) and Satb1/2^{+} (white) MSE neurons from *Parvalbumin::synaptophysin-tdTomato* (D) or *Emx1::synaptophysin-tdTomato* (Ctx-Syn-Tomato) (E) neurons, colocalized GFP^{+} and Tomato^{+} pixels were identified, pseudocolored yellow and projected onto the GFP^{+} neuron. As a result of this analysis, Syn-Tomato that was not colocalized with the GFP^{+} neuron is not shown. Insets show single optical slices and also depict the total Syn-Tomato (blue) so that sites of synaptic contacts appear white. **(F)** High-magnification projected confocal image of a RabΔG-pre-TA(green)/Satb1/2^{+}(blue) MSE neuron boxed in C activated by a painful heel stimulus (c-fos, red), arrowhead. Scale bars, 250 μm (A–C) and 10 μm (D–F).

(*Emx1::synaptophysin-tdTomato*) to identify total corticospinal presynaptic terminals. We found that 93% of Tcfap2β^{+} or Satb1/2^{+} MSE cells received corticospinal synaptic contacts (n = 14 cells in seven spinal cords; Figure 2.8E). We found multiple synaptic contacts on each positive cell (22.5 ± 18 contacts per cell; mean and standard deviation), with up to 65 contacts on a single cell. We found these synapses on both the cell bodies and the processes of MSE cells (22.7% of contacts on cell bodies and 77.3% of contacts on processes, n = 292 contacts on 13 cells in seven spinal cords), and on dendritic spines (Figure 2.8E and data not shown). It has previously been shown that the medial deep dorsal horn is the major target of the caudal motor cortex[102]. To determine specifically whether the caudal motor cortex has direct input onto candidate MSE cells, we performed focal injections of AAV:Cre into the caudal motor cortex of lox-stop-lox-synaptophysin-tdTomato mice and examined the spinal targets of labeled synapses. We observed synaptic terminals of the caudal motor cortex in the deep dorsal horn, overlapping with the region of MSE neurons (Figure 2.8B) and directly contacting MSE cells (n = 16 contacts on nine cells in four spinal cords; data not shown).

We next characterized whether candidate MSE neurons are functionally recruited by nociceptive pathways. Although most primary nociceptive fibers terminate in the superficial dorsal horn, these neural signals are then relayed to the deep dorsal horn. Here they target multimodal neurons, including pain-withdrawal 'reflex encoder' neurons that translate noxious cutaneous signals into the appropriate single muscle reflex movements[47]. We found that a painful stimulus to the heel activated neurons in the superficial dorsal horn laminae I and II, and in the deep dorsal horn, where these neurons overlapped with Satb1/2^{+} cells (Figure 2.8C). In the deep dorsal horn, 71 ± 14% of c-fos^{+} activated neurons expressed Satb1/2 (n = 247 cells in 11 spinal cords). In addition, we observed cells that were c-fos^{+}, Satb1/2^{+} and directly premotor (Figure 2.8F). Thus, MSE neurons are likely interposed in pain-withdrawal pathways and may encompass previously described 'reflex-encoder' neurons, serving to bind together smaller reflex modules.

Our findings demonstrate that putative MSE neurons receive inputs from sensory and cortical pathways, which places these cells in the networks that command multiple types of motor synergy–based movement. Thus, it is possible that MSE cells that receive both sensory and cortical inputs may represent the underlying cellular network for controlling motor programs common to reflex and voluntary motor behaviors.

Discussion

We provide a circuit-based, spatial, molecular and functional characterization of a population of spinal neurons that are sufficient to trigger complex patterns of motor activity. We found that these cells uniquely combine the key features to mediate motor synergy programs as building blocks for both volitional and reflex motor behaviors (Figure 2.9). They are a major source of monosynaptic input to motorneurons. They can cross multiple spinal segments to reach target motorneurons, potentially linking spatially segregated but functionally related motorneuron pools. They are located in the medial deep dorsal horn, the region from which motor synergies are most efficiently evoked by electrical stimulation[89,103]. They drive reliable patterns of action potentials in multiple motorneuron pools in a reduced model of a motor synergy. They receive direct inputs from neural sources known to recruit motor synergies, such as sensory pathways and the corticospinal tract. Accordingly, we propose that these spinal neurons encode the motorneuron activation patterns for motor synergies, and we designate them MSE neurons.

In addition to MSE neurons, multiple interneuron classes in the spinal cord have important motor coordination function, particularly those ventral interneurons that make up the ‘central pattern generator’ (CPG) network that supports rhythmic locomotion and the embryonic lineage–defined classes that make up this network[1,50]. Direct activation of the CPG network drives patterns of motorneuron activation, and in this respect, the ventral CPG interneurons and MSE neurons are similar. However, we describe here that MSE neurons in the medial deep dorsal

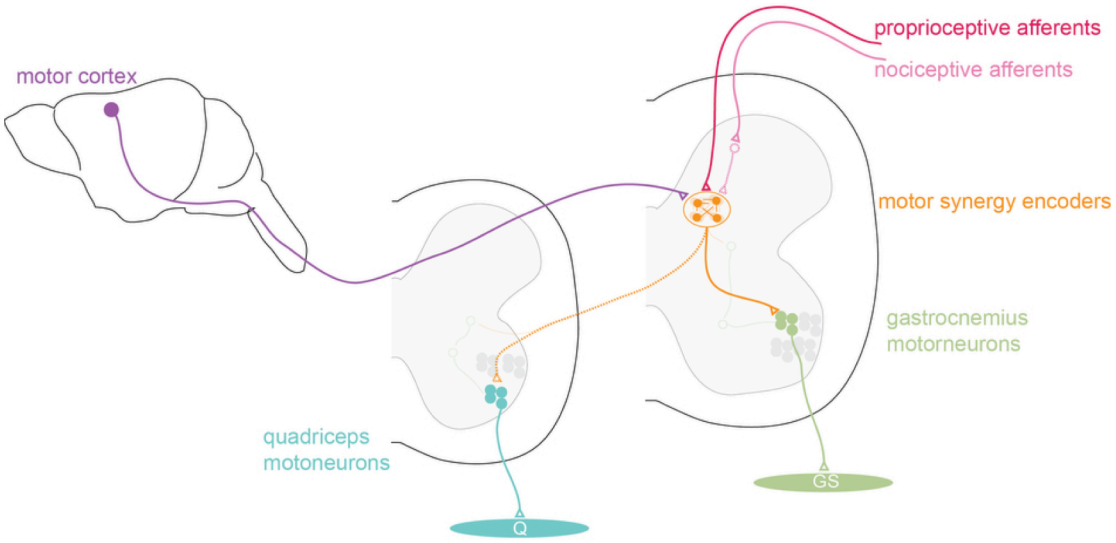

Figure 2.9: MSE cells are a central node in motor control networks. L2 (left) and L5 (right) lumbar spinal cord segments are depicted with the L5 MSE network (orange). This population receives direct corticospinal (purple) and proprioceptive information (red), and indirect inputs from nociceptive sensory pathways (pink). Outputs include motor pools in multiple segments, such as quadriceps (blue, Q) and gastrocnemius (green, GS).

horn have the ability to coordinate motor activity and are major synaptic targets of the cortical and sensory pathways that can recruit motor synergies. Having identified MSE neurons as a key node in neural pathways for motor control, it is an important future direction to study the relationship between MSE neurons and the ventral locomotor circuitry.

Previous anatomical and physiological experiments provide strong support for the medial deep dorsal horn being an important site for motor control. This region is the major point of intersection of several important circuitry elements: the densest region of corticospinal fibers[85,100,102,104] and rubrospinal fibers[105-107], substantial multimodal sensory input including 'reflex-encoder' sensory relay neurons[47,108,109], and a major fraction of premotor neurons[2,59,61,81,85-88]. Functional experiments have demonstrated that spinal motor synergies are best evoked with electrical stimulation of the spinal cord from deep dorsal horn locations, even in spinal cords in which descending and sensory inputs have been removed[89,103]. Our data provide a medial deep dorsal horn cellular substrate for the neurons that control complex motor actions by forming a columnar network in which descending and sensory inputs can converge, and selected motor commands can be sent to multiple motor pools.

It has been noted that grasping of an object resembles the palmar grasp reflex and that the swing phase of locomotion is related to the flexor withdrawal reflex. If the MSE neuron network first arose in simple animals lacking a motor cortex, perhaps the earliest functions of this network were related to mediating motor synergies of multijoint reflexes. The similarity of movements activated by volitional and reflex pathways suggests that as the cortex evolved, the corticospinal pathway may have coopted the existing MSE cell circuitry to likewise simplify the task of controlling complex multijoint movements. In spinal cord injury, spinal neuronal networks are effectively isolated from descending input, and volitional movement of the body is lost below the injury level. If motor synergies are autonomously encoded in spinal MSE neuron networks, perhaps in the same way evolution may have coopted this circuitry, it may be useful to target

MSE cells for therapeutic intervention in order to facilitate purposeful movements in patients with spinal cord injury.

Acknowledgements

Chapter 2 is an adaptation of a manuscript published in *Nature Neuroscience*, 2014. The full citation is: Ariel J. Levine, Christopher A. Hinckley, Kathryn L. Hilde, Shawn P. Driscoll, Tiffany H. Poon, Jessica M. Montgomery, Samuel L. Pfaff. Identification of a cellular node for motor control pathways. *Nature Neuroscience*, 2014 Apr; 17 (4): 586-93. The manuscript was received February 4, 2014, and accepted February 13, 2014. The manuscript was published online March 9, 2014 in advance of the print journal. The work presented in this chapter was done early in my graduate training in collaboration with Ariel Levine and Chris Hinckley, who designed and conducted many of the experiments in this chapter. The project was overseen by Samuel L. Pfaff. We also received tremendous help and assistance from many co-authors, whom I thank: Shawn Driscoll, Tiffany Poon, and Jessica Montgomery. The article and publication are online at: http://www.nature.com/neuro/journal/v17/n4/full/nn.3675.html. The authors of the manuscript would like to acknowledge the generosity and advice of Martyn Goulding, Reggie Edgerton, Anne Engmann, Edward Callaway, John Young, Fumitaka Osakada and Floor Stam; Pushkar Joshi and Sue McConnell for instruction in cortical injections; and Qiufu Ma (Department of Neurobiology, Harvard Medical School; in situ probes) and Carmen Birchmeier (Max Delbruck Center for Molecular Medicine; Tlx3 antibody) for providing reagents. Matt Sternfeld, Marito Hayashi and Yoel Bogoch provided support and advice. We thank Richard Levine for his helpful reading of the manuscript. Ariel Levine was supported by George E. Hewitt Foundation for Medical Research and Christopher and Dana Reeve Foundation. Christopher Hinckley was supported by a US National Research Service Award fellowship from US National Institutes of Health NINDS. I was supported as a National Science Foundation Graduate Research Fellow.

Samuel Pfaff is supported as a Howard Hughes Medical Investigator and as a Benjamin H. Lewis chair in Neuroscience. This research was supported by the National Institute of Neurological Disorders and Stroke (grant R37NS037116), the Marshall Foundation and the Christopher and Dana Reeve Foundation.

Chapter 3

Satb2 controls spinal circuit assembly and sensorimotor reflex behavior

Satb2 controls spinal circuit assembly and sensorimotor reflex behavior

Abstract

Basic motor behaviors, such as walking or withdrawing the limb from a painful stimulus, require integrative circuitry within the spinal cord that can translate diverse sensory cues into an appropriate motor response. However, both the cellular components, and the molecular mechanisms that instruct the assembly of these sensory-motor circuits, are poorly understood. Here we describe a population of Satb2+ spinal interneurons that form a cellular node at the intersection of sensory and motor circuitry within the spinal cord. Loss of the *Satb2* gene perturbs interneuron cell body position, molecular profile and proper integration into sensory-motor circuitry. Further, specific loss of Satb2 in spinal interneurons alters the behavioral response of mice to painful stimuli. These findings establish Satb2 as a critical regulator of developmental events that link peripheral sensory encounters to motor action.

Introduction

The movements of animals are controlled by a highly integrative circuitry within the spinal cord that not only translates volitional commands from higher brain centers into actions, but also adapts movements to a variety of sensory cues that are being monitored in the periphery. Sensory information continuously streams into the central nervous system as an animal moves and includes detection of limb position, mechanical touch and in the case of environmental threats, noxious pain. The ability to revise motor plans based on peripheral sensory information helps to adapt motor actions and produce rapid responses to potentially harmful encounters. Although there is an increasing understanding of the sensory neuron types that detect each sensory modality, the cellular and molecular features of the sensory-motor circuit hub within the spinal cord that integrates and processes multiple streams of information is not known.

A critical example of a behavior that dynamically integrates proprioceptive (limb position) and nociceptive (painful) sensations is the nociceptive withdrawal reflex (NWR), an adaptive response that protects animals by triggering a rapid combination of muscle flexions to retract the limb from painful stimuli such as heat or sharp objects. The NWR is mediated by circuitry that is state dependent, controlling the selection of muscles and the order and timing of contractions depending on where the limb is located at the moment of sensed pain [110-116]. Thus responses to painful stimuli are protective and appropriate regardless of whether the animal is resting or moving the limb through different positions in the stepping or reaching cycle. Sensory pathways that relay information about limb position and pain share a target domain within the spinal cord: the deep dorsal horn (Figure 3.1A). This region is the primary target region of proprioceptive fibers, and it has long been recognized that cells in the deep dorsal spinal laminae are recruited following a painful stimulus in the periphery, via first order neurons in the superficial dorsal horn [117-119]. Recently, circuit tracing has revealed that a significant fraction of neurons that are directly premotor are located in the medial deep dorsal horn [64,120].

Physiology and tracing studies suggest that sensory-motor circuit components have a topographic organization along the mediolateral axis of the spinal cord [121]. This organizing feature of interneurons is mirrored by the orderly alignment of sensory afferent fibers arrayed along the mediolateral axis of the dorsal horn according to body region representation [36,37]. Studies to map the relative position of spinal interneurons that mediate motor responses to painful stimuli have found that NWR "reflex encoders" are organized along the mediolateral axis of the spinal cord based on the body region for the painful stimulus [35,46,47]. Similarly, mapping of premotor interneurons for flexor and extensor muscle groups revealed a medial-extensor and lateral-flexor bias in this same deep dorsal horn region of the spinal cord [64]. Together these studies raise the possibility that sensory information converges on motor circuitry within the deep dorsal horn (Figure 3.1A), which translates somatotopic and modality-specific sensory

information into the musculotopic outputs observed at the level of the motor neuron. We focused our studies on interneurons at the convergence point of sensory-motor commands to identify molecularly-distinct cells that comprise subcomponents of this integrative motor network.

A subset of premotor cells in the deep dorsal horn can be identified by the expression of the chromatin remodeling factor Satb2 [120]. Case studies of human mutations in the *Satb2* gene have reported developmental delays in motor skill acquisition, coordination, and sensorimotor behavior [122-124]. Although Satb2 is known to regulate neural development in the cortex of mice [125,126], a link between *Satb2* gene function and motor control is unknown.

Here we describe the connectivity patterns and developmental mechanisms that assemble Satb2+ interneurons into spinal circuitry, and test a role for the *Satb2* gene in sensorimotor behavior. We found that Satb2+ inhibitory neurons receive direct inputs from proprioceptive neurons and indirect information from nociceptive cells, and therefore are well suited to integrate these two types of sensory modalities. Cell bodies of Satb2+ interneurons are arrayed across the mediolateral axis of the deep dorsal horn suggesting they monitor sensory information from a variety of somatotopic positions. When the *Satb2* gene is mutated we found that the cell position, molecular profile, synaptic inputs and synaptic outputs were markedly altered. These changes reconfigure the cellular components of sensory-motor circuits in the spinal cord deep dorsal horn. Animals with targeted deletion of *Satb2* within spinal interneurons display abnormal limb responses to noxious stimuli. Our findings establish that the *Satb2* gene is an essential regulator of the instrinsic program that establishes a critical hub for sensory-motor processing within the spinal cord.

Results

Satb2 is expressed in a restricted population of deep dorsal horn inhibitory neurons

To provide a comprehensive description of spinal neurons that selectively express Satb2, we performed immunohistochemistry using a Satb2-specific antibody. In contrast to other molecular markers that have been described in the deep dorsal horn [120,127], Satb2 is expressed in a very restricted population of spinal interneurons, beginning at embryonic day e12 and continuing through the first postnatal week (Figure 3.1B, Figure 3.2). Satb2+ interneurons span the mediolateral extent of laminae V (Figure 3.1B), corresponding to a region where cells that are activated during the NWR have been described electrophysiologically [46]. We also observed transient expression of Satb2 in motor neurons of the medial and lateral motor columns, as early as e10.5 and continuing in a subset of medial motor neurons into the first postnatal week (Figure 3.2). Satb2 expression is also detectable in the developing neocortex and specific regions of the musculoskeletal system (data not shown). Therefore, Satb2 is expressed in numerous cell and tissue types associated with motor function.

These findings are consistent with reports of Satb2 expression in the nervous system and other tissues [96,128,129]. To extend previous studies and to determine whether Satb2 marks interneurons of known lineage, we performed colocalization experiments with antibodies for dorsal interneuron subtypes [1,127]. Satb2 is expressed in the Lbx1+ lineage of dorsal interneurons [96], a marker that is expressed broadly in the dorsal spinal cord including interneuron subtypes dI4-6 and dIL_A and dIL_B [127,130,131]. Satb2+ interneurons also co-express the LIM homeodomain markers Lim1/2 [96], and a subset of Satb2+ interneurons coexpress Ptf1a, a marker of dI4 and dIL lineages. However, when we performed double labeling experiments with markers that subdivide these broad lineage classes (Pax2, Tlx3, Brn3a, Lmx1b, Bhlhb5, or Isl1/2), we found that the Satb2+ interneuron population did not express additional markers of dI4, dI5, dIL, or dI6 lineages (Figure 3.3A-P).

To gain genetic access to Satb2+ interneurons and define their circuit properties, we

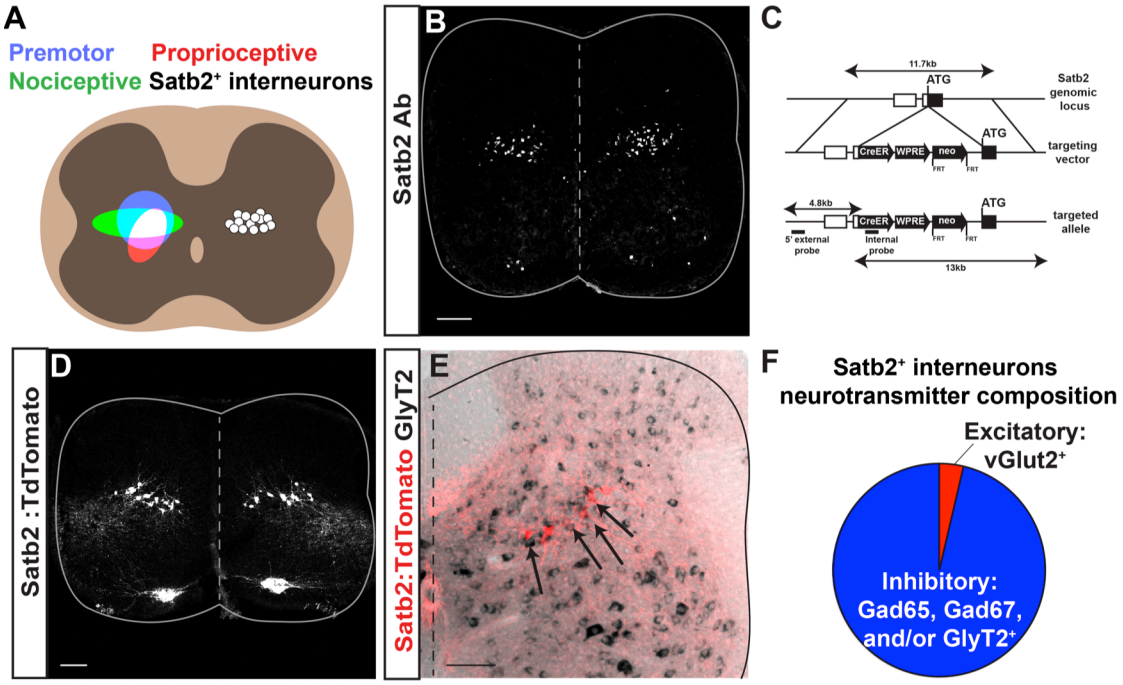

Figure 3.1: Expression of Satb2 in inhibitory neurons in the spinal cord deep dorsal horn
(A) Schematic illustrating the alignment of Satb2+ interneurons with the termination domains of multiple motor control pathways. Left, Premotor neurons (blue), proprioceptive fiber termination (red), and neurons that are recruited in the nociceptive withdrawal reflex (green) are located in the deep dorsal horn of the spinal cord. The overlap between these pathways is shown in white. Right, Location of Satb2+ interneurons aligns with the overlap in left panel. (**B)** Immunohistochemistry using a Satb2-specific antibody (Satb2 Ab) reveals Satb2 expression in a subset of motor neurons in the medial motor column (MMC) and a band of spinal interneurons at embryonic day 15.5. (**C)** Schematic for generation of Satb2-Cre^{ERT2} mouse line. Targeted insertion of Cre^{ERT2}-WPRE-pA-FRT-neo-FRT cassette into the ATG of the *Satb2* locus. (**D)** Crossing Satb2-Cre^{ERT2} with the reporter line Rosa-CAG-LSL-TdTomato (Satb2:TdTomato) recapitulates the pattern of expression seen in B. Lumbar, e18.5. (**E)** Dorsal spinal cord following in situ hybridization for the inhibitory neurotransmitter marker GlyT2 (black) in Satb2:Tomato animals (red). Double positive neurons are indicated with arrows throughout the Satb2+ interneuron population. (**F)** Quantification of in situ hybridization experiments in Figure 3.1E and Figure 3.3Q-S for neurotransmitter markers in which composition of inhibitory (blue) and excitatory (red) of Satb2+ interneurons are shown. Percentages correspond to mean values. Spinal cords were analyzed at P13 for in situ hybridization. Scale bars in B, D and E, 100um.

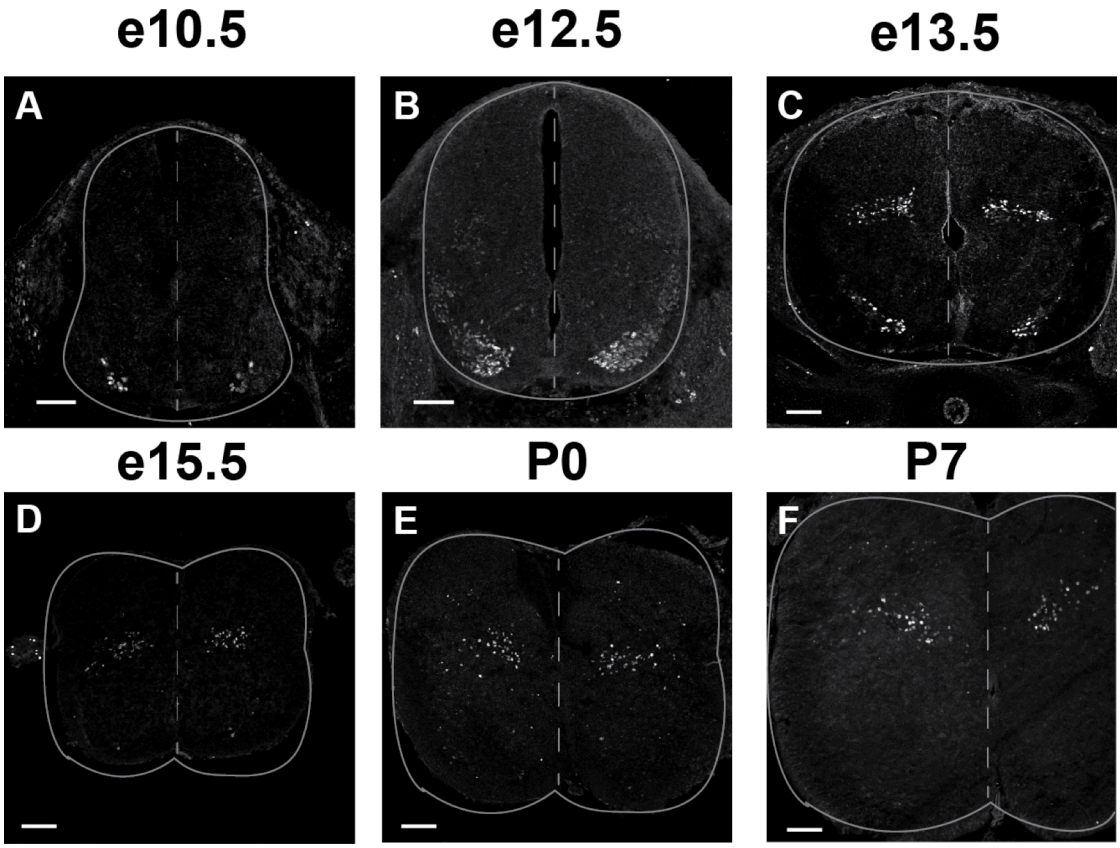

Figure 3.2: Timeline of Satb2 expression in the developing spinal cord
Immunohistochemistry using a Satb2-directed antibody at e10.5 **(A)**, e12.5 **(B)**, e15.5 **(C)**, e15.5 **(D)**, P0 **(E)**, and P7 **(F)**. Expression of Satb2 was first identified in spinal interneurons at low levels at e12.5, continuing until P7. Expression in motor neurons was first identified at e10.5 with expression in the medial motor column (MMC). Satb2 was observed throughout the medial and lateral motor columns (LMC) at e12.5, then continued in a subset of MMC motor neurons through embryonic stages. After e15.5, Satb2 expression was rarely observed, but when present, was observed in MMC motor neurons. Scale bars, 100um.

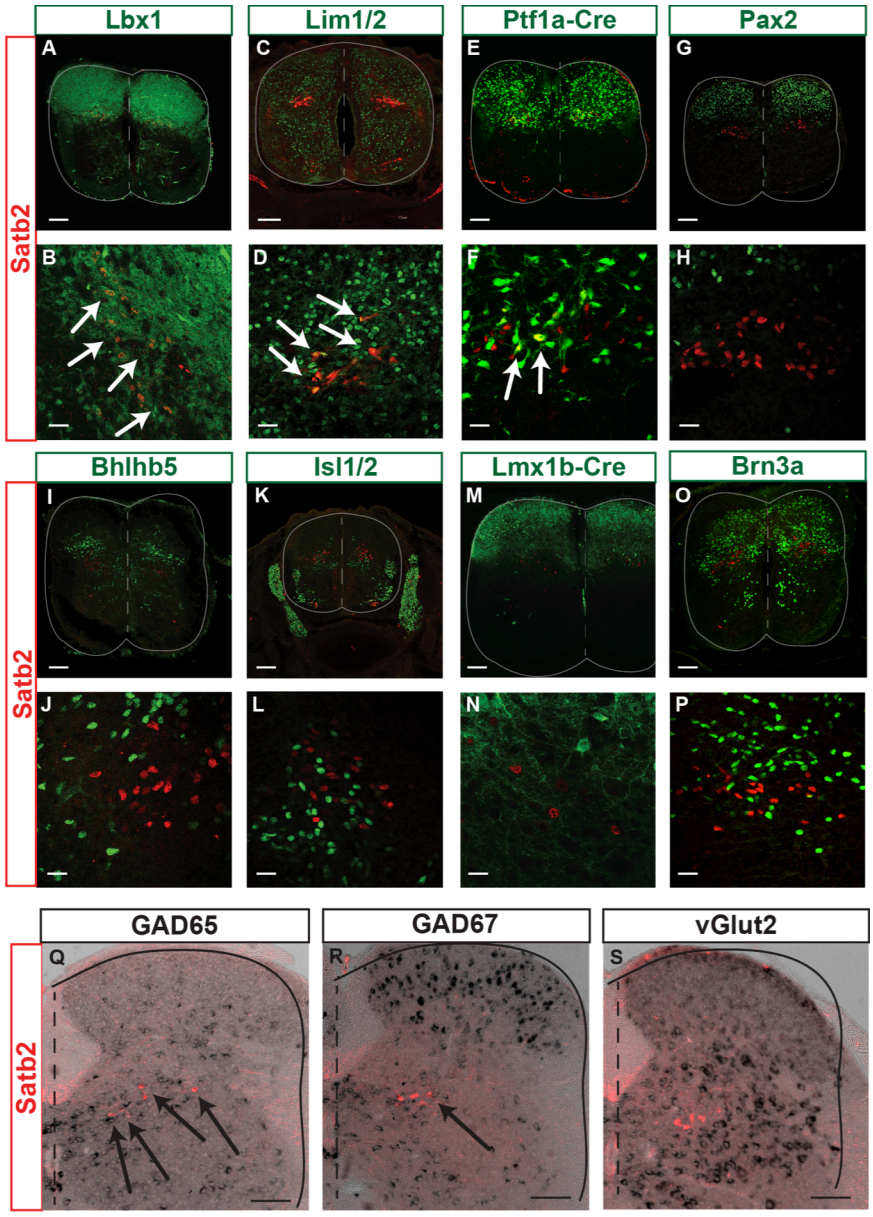

Figure 3.3: Satb2+ interneurons represent novel class of inhibitory dorsal interneurons. Co-labeling experiments for Satb2 and lineage markers for dorsal interneuron populations. High and low magnification images are shown for each marker. **(A, B)** Satb2 antibody and Lbx1:TdTomato, e15.5. **(C, D)** Satb2:TdTomato and Lim1/2 antibody, e13.5. **(E, F)** Satb2 antibody and Ptf1a:TdTomato, e15.5. **(G, H)** Satb2 antibody and Lbx1:TdTomato, e15.5. **(I, J)** Satb2 antibody and Pax2 antibody, e18.5. **(K, L)** Satb2 antibody and Bhlhb5 antibody, e18.5. **(M, N)** Satb2 antibody and Isl1/2 antibody, e13.5. **(O, P)** Satb2 antibody and Lmx1b:TdTomato, e18.5. **(Q, R)** Satb2 antibody and Brn3a antibody, e13.5. **(S-U)** Satb2 antibody and in situ hybridization for Gad65 (S), Gad67 (T), and vGlut2 (U) at P13. Arrows indicate Satb2+ interneurons that co-express lineage marker or in situ hybridization probes. Scale bars in A, C, E, G, I, K, M, O, 100um. Scale bars in B, D, F, H, J, N, P, 20um. Scale bars in in situ hybridization images, 100um. See also Figure 3.9 for quantification in Satb2^{ON}:TdTomato.

devised a temporally inducible Cre labeling strategy. To generate a Satb2:Cre^{ERT2} knock-in mouse line, Cre^{ERT2} was inserted into the ATG of the *Satb2* locus, and ES clones were selected with neomycin and screened using PCR and Southern strategies (Figure 3.1C, and data not shown). Though Satb2 is downregulated during the first postnatal week, crossing our transgenic line with the Cre-dependent reporter Rosa-CAG-LSL-TdTomato (Satb2:TdTomato) provides indelible labeling of Satb2+ interneurons. Embryonic induction of Satb2:Cre^{ERT2} with tamoxifen at e12 labels a restricted population of motor neurons in the medial motor column and spinal interneurons (Figure 3.1D). Thus, TdTomato expression driven by our transgenic line accurately recapitulates Satb2 protein expression (compare Figure 3.1B to 3.1D).

Genetic labeling of Satb2+ interneurons facilitated further descriptive analyses of this population. To determine the neurotransmitter status of Satb2+ interneurons we performed double labeling experiments in which we examined the overlap of TdTomato expression with in situ hybridization probes for excitatory or inhibitory neurotransmitter markers. 3.8% of Satb2+ interneurons express the excitatory marker vGlut2, with the remainder of the population expressing Gad65, Gad67, and/or GlyT2 (Figure 3.1E, F, Figure 3.3Q-S), indicating that Satb2+ interneurons are predominantly inhibitory.

Taken together, these experiments reveal that Satb2+ neurons represent a population of inhibitory dorsal interneurons derived from the Lbx1+ lineage that does not align with previously described classes of dorsal interneurons. Satb2+ interneurons are a spatially restricted population located within the convergence domain of sensory and motor pathways in the spinal cord.

Satb2+ interneurons are located at the intersection of multiple sensory pathways

Tracing experiments have revealed that peripheral sensory commands converge on spinal neurons in the deep dorsal horn of the spinal cord, providing the first point of intersection

between the nociceptive and proprioceptive systems [120]. Primary fibers of proprioceptive sensory neurons and second order neurons that are recruited during the hindlimb nociceptive withdrawal reflex reside in overlapping domains within the deep dorsal horn. Although the site of convergence for these two pathways aligns with Satb2+ interneuron position (Figure 3.1A), the connectivity pattern of Satb2+ interneurons has not been described.

To test whether Satb2+ interneurons receive proprioceptive input, we used a genetic labeling strategy (Parvalbumin-Cre x Rosa-CAG-LSL-Syp-TdTomato-deltaNeo; abbreviated PV:Synaptophysin-TdTomato) in which the presynaptic terminals of proprioceptive fibers are labeled with TdTomato fluorescent protein [120]. We identified proprioceptive contacts on the cell bodies of Satb2+ interneurons (Figure 3.4A, B). We next used a second strategy to visualize the full cell morphology of Satb2+ interneurons. Immunohistochemistry for parvalbumin and vGlut1 revealed proprioceptive contacts along the soma and processes of Satb2:TdTomato+ spinal interneurons (data not shown). Although there were quantitative differences along the mediolateral axis (see below), we found that all Satb2+ interneurons received contacts from proprioceptive fibers.

Nociceptive sensory fibers predominantly target superficial spinal laminae, but relay information through the deep dorsal horn via spinal interneurons. To explore whether Satb2+ interneurons relay nociceptive sensory information we injected formalin, a reactive chemical that induces tissue damage and pain [132], into the footpads of Satb2:TdTomato animals and performed immunohistochemistry for cfos to identify cells that are recruited in response to a painful stimulus. Following formalin injection, cfos+ neurons were predominantly located in superficial laminae ipsilateral to the injection site, as well as in the deep dorsal horn. At spinal levels of peak cfos labeling, 37% of Satb2+ interneurons coexpress cfos in response to formalin injection into the footpad (Figure 3.4C; 17 of 50 TdTomato+ cells), indicating that a significant fraction of Satb2+ interneurons are active even in response to focal stimulation of nociceptive pathways.

Because all Satb2+ interneurons receive proprioceptive input (Figure 3.4B and data not shown), cfos labeling experiments demonstrate that Satb2+ interneurons are a site of convergence of multimodal sensory inputs. These findings establish Satb2+ interneurons as spinal circuit components that integrate information from sensory pathways that relay limb position and those that relay noxious stimuli.

Satb2+ interneuron diversity along the mediolateral axis

Sensory-motor circuit components have a functional organization along the mediolateral axis of the spinal cord [121,133]. To test whether interneuron cell body location is a determinant of the amount of proprioceptive input, we quantified the number of PV:Synaptophysin-TdTomato+ contacts on neurotrace+ cell bodies of Satb2+ interneurons, and mapped the number of contacts per cell along the mediolateral axis. These experiments revealed an inverse relationship between cell body distance from the midline and the amount of proprioceptive input: cells positioned closer to the midline had a greater number of proprioceptive contacts, while lateral cells had fewer contacts (Figure 3.4D). These findings indicate that mediolateral position of spinal neurons is an organizational feature that dictates proprioceptive sensory connectivity.

Although interneurons are topographically organized along the mediolateral axis of the deep dorsal horn, genetic markers that subdivide these groups have not been described. In the cortex, *Satb2* participates in an antagonistic genetic interaction with another cortical gene *Ctip2* to subdivide cortical progenitors into functionally distinct pools[125,126]. To test whether Satb2 and Ctip2 also have mutually exclusive expression in the spinal cord, we performed immunohistochemistry for both markers. Surprisingly, in the spinal cord Satb2 and Ctip2 are only partially segregated; medial neurons are Satb2+/Ctip2+, while lateral neurons are Satb2+/Ctip2- (Figure 3.4E, F), a molecular organization that is detectable as early as e13.5 and is maintained

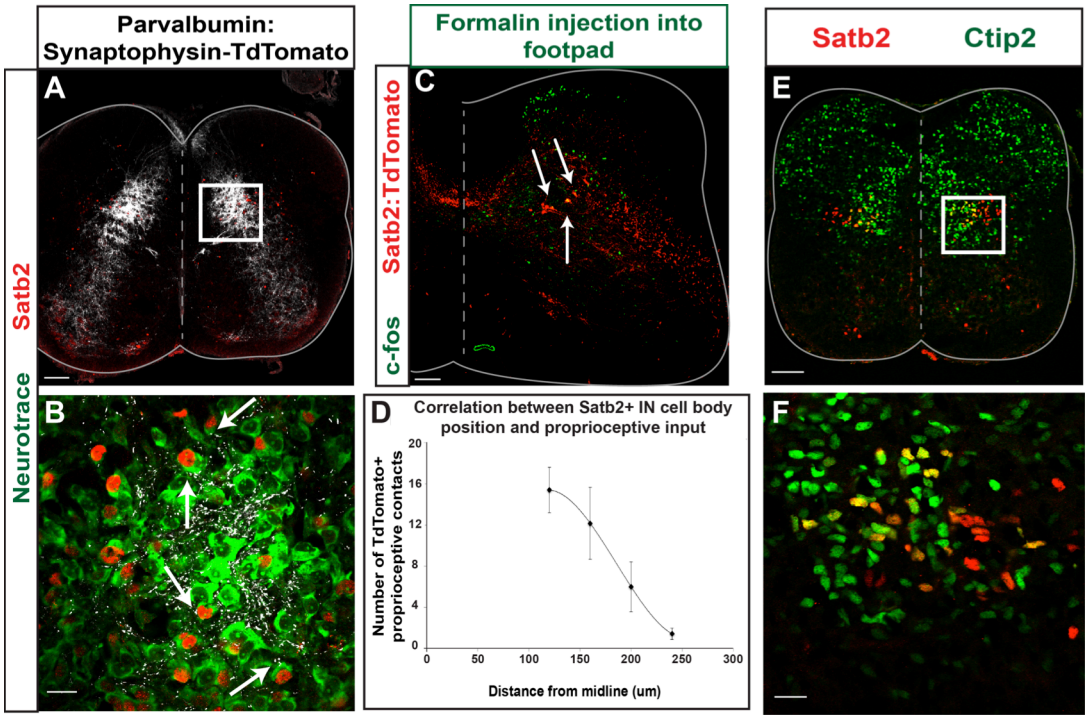

Figure 3.4: Satb2+ interneurons receive diverse sensory inputs and display heterogeneity along the mediolateral axis. (A, B) Proprioceptive fibers have a dense termination in the deep dorsal horn. Presynaptic terminals of proprioceptive fibers (white) were identified by crossing Parvalbumin-Cre to Rosa-LSL-Syp-TdTomato-deltaNeo (PV:Synaptophysin-TdTomato). Proprioceptive contacts (white) were identified on neurotrace+ cell bodies (green) of Satb2+ interneurons (red), highlighted by arrows. White box in a refers to high magnification image in B. P1 spinal cords in A, B. **(C)** C-fos immunoreactivity (green) was used to identify cells in the spinal cord that are recruited following painful stimulation. Formalin was injected into the footpad of adult Satb2:TdTomato animals. Yellow cells that are co-positive for Satb2+ (red) and cfos (green) are indicated by arrows. n=4 spinal cords. **(D)** Mediolateral position of Satb2+ interneurons is a determinant of the number of contacts from proprioceptive fibers. Medial cells positioned closer to the midline had a greater number of contacts and lateral cells had fewer contacts. Quantified cells were binned by mediolateral position and the number of synaptic contacts is represented as mean +/- SEM. n=34 cells in 3 spinal cords. **(E, F)** Ctip2 expression subdivides Satb2+ interneurons along the mediolateral axis. Medial Satb2+ interneurons (red) co-express Ctip2, as indicated by yellow labeling in E, F. e15.5 spinal cords used for E, F. Scale bars in A, C, E, 100um. Scale bars in B, F, 20um.

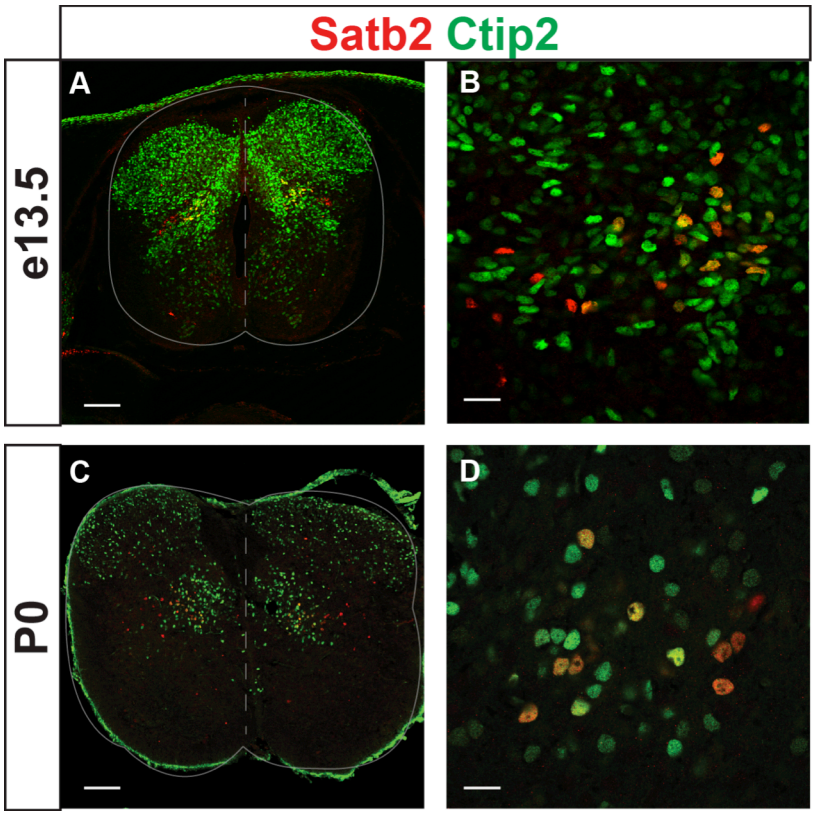

Figure 3.5: Timeline of Satb2 and Ctip2 expression in the developing spinal cord. (A-D) Immunohistochemistry for Satb2 and Ctip2 at e13.5 (A, B) and P0 (C, D). Low magnification in (A, C), high magnification in (B, D). Satb2 and Ctip2 are partially segregated beginning at early developmental stages (e13.5) such that there is a medial Satb2+/Ctip2+ population and a lateral Satb2+/Ctip2- population. This organization is maintained into postnatal stages (P0). See also Figure 2E, F for e15.5. Scale bars in A, C, 100um. Scale bars in B, D, 20um.

into postnatal stages (Figure 3.5). These experiments reveal that in addition to sensory connectivity, molecular profile can be used to subdivide Satb2+ interneurons along the mediolateral axis of the spinal cord. Importantly, our characterization of Satb2 and Ctip2 expression in the developing spinal cord is the first to identify molecular heterogeneity along the mediolateral axis of the deep dorsal horn.

Satb2+ interneurons target ventral circuitry associated with motor function

To test whether Satb2+ interneurons may serve as a cellular substrate for transmitting sensory cues to motor circuitry, we used an unbiased approach to identify synaptic targets of Satb2+ interneurons. Satb2:Cre^{ERT2} x Rosa-CAG-LSL-Syp-TdTomato-deltaNeo (Satb2:Synaptophysin-TdTomato) labeling allowed us to visualize the overall distribution of presynaptic terminals of Satb2+ interneurons, revealing a specific pattern of connectivity in the ventral spinal cord. Synaptophysin:TdTomato+ terminals were located throughout the ventral spinal cord, but enriched in a diagonal region covering lamina V-VII and IX (Figure 3.6A, left panel).

We compared the location of Satb2:Synaptophysin-TdTomato labeling with the presynaptic terminals of other dorsal interneuron classes. In contrast to the specific pattern of labeling in ventral lamina that we observed in Satb2:Synaptophysin-TdTomato spinal cords, both Ptf1a- and Lmx1b- expressing interneurons broadly target dorsal spinal laminae in which their cell bodies reside (Figure 3.7A, B). The location and distribution of synaptic terminals from Satb2+ interneurons suggests they are integrated into a feedforward network that receives diverse sensory cues and transmits them to specific recipients in the ventral spinal cord..

Given the distribution of Satb2 presynaptic terminals in the ventral spinal cord, we hypothesized that Satb2+ interneurons contact diverse cellular targets that occupy this region and

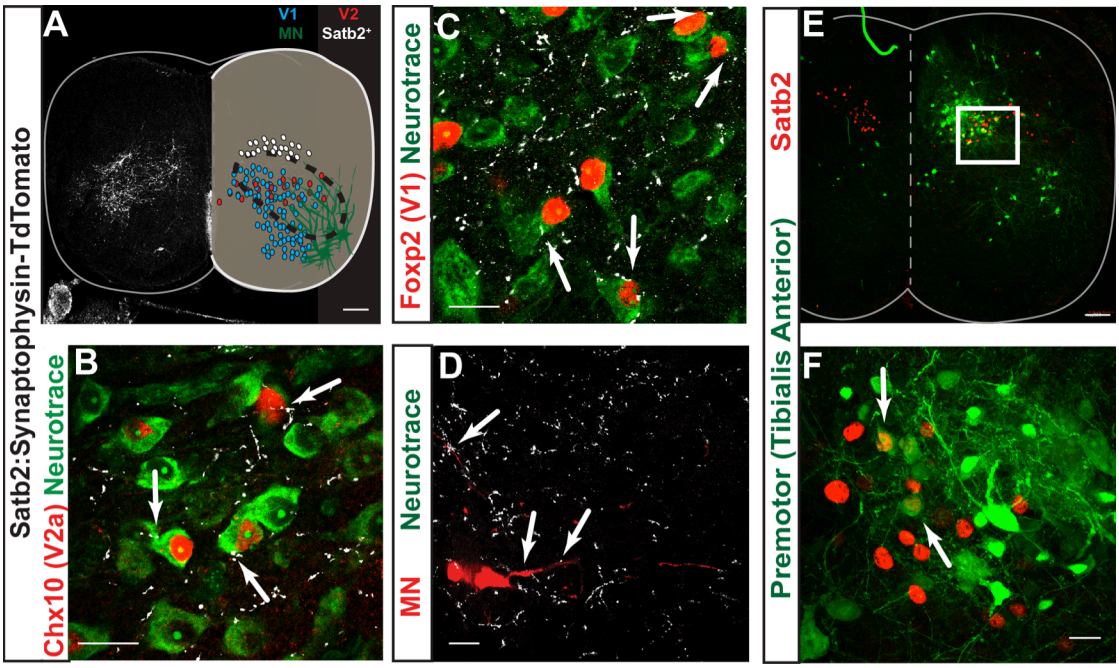

Figure 3.6: Satb2+ interneurons target multiple components of ventral motor circuitry. **(A)** Presynaptic terminals of Satb2+ interneurons (white) broadly target the ventral spinal cord, overlapping with a region where components of ventral motor circuitry reside (right panel). Distribution of presynaptic terminals of Satb2+ interneurons was identified by genetic labeling (Satb2:Synaptophysin-TdTomato, left panel). V1 (blue), V2 (red) interneurons, motor neurons (MN, green) and Satb2+ interneuron (white) position shown in schematic in right panel. Dotted lines encompass the area of dense labeling of presynaptic terminals of Satb2+ interneurons and the position of ventral neuron populations. (**B-D)** Satb2+ interneurons target cellular components of ventral motor circuitry. High magnification images from the ventral spinal cord showing contacts from presynaptic terminals of Satb2+ interneurons (white) on neurotrace+ cell bodies (green) of (B) Chx10+ V2a interneurons (red), (C) Foxp2+ V1 interneurons (red), (D) motor neurons from hindlimb muscles (red). **(E, F)** Satb2+ interneurons represent a fraction (<5%) of premotor neurons in the deep dorsal horn. Monosynaptically restricted rabies labeling identifies premotor neurons from tibialis anterior muscles (green) that co-express Satb2 (red). White box in E corresponds to high magnification image shown in F. Arrows in F identify yellow cells that are positive for rabies to identify premotor neurons (green) and Satb2 (red). P7 spinal cords used in A-F. See also Figure 3.7. Scale bars in A, E, 100um. Scale bars in B-D, F, 20um.

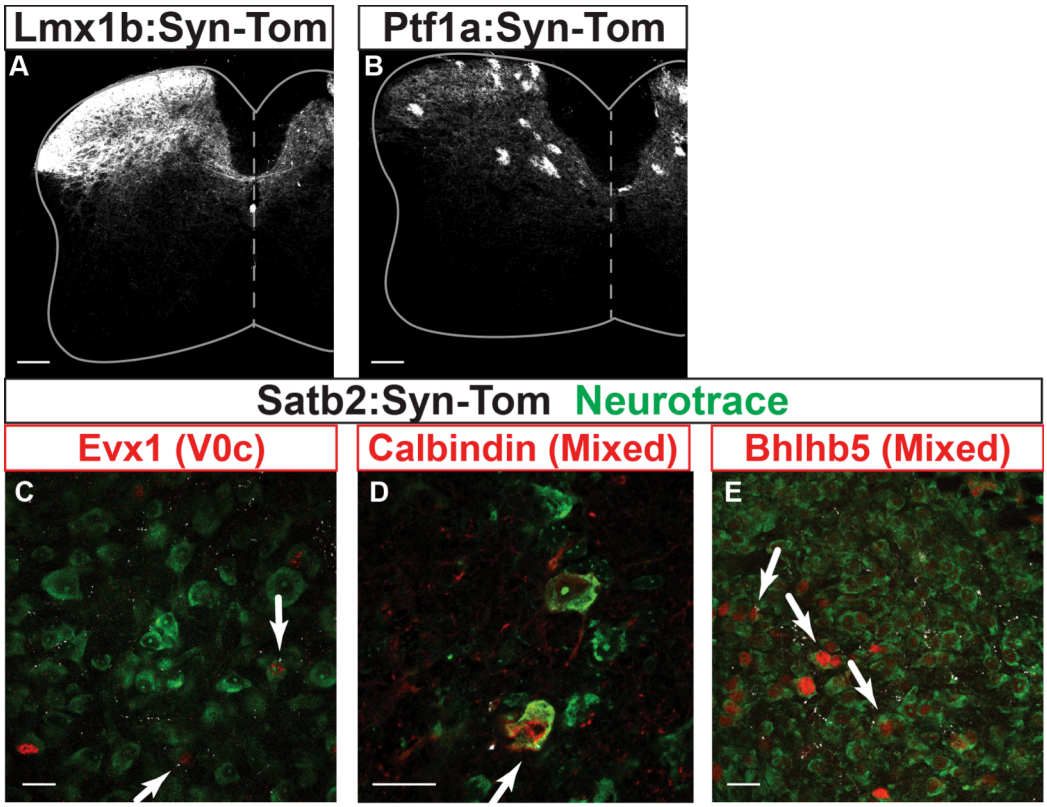

Figure 3.7: Distribution of presynaptic terminals in dorsal interneuron subtypes in contrast to specificity of Satb2+ interneuron targeting of ventral motor circuitry. (A, B) In contrast to the specific, ventral distribution of presynaptic terminals of Satb2+ interneurons (see Figure 3A), Lmx1b- (A) and Ptf1a-expressing (B) dorsal interneurons target dorsal laminae broadly. We also noted glial expression of the fluorescent reporter in B. P29 spinal cords in A, B. **(C-E)** Immunohistochemistry of Satb2:Syn-Tom spinal cords for Evx1 (C), Calbindin (D), and Bhlhb5 (E). Presynaptic terminals of Satb2+ interneurons (white) were identified on cell bodies (marked with neurotrace, green) of ventral interneurons (red), as indicated by arrows. Scale bars in A, B, 100um. Scale bars in C-E, 20um.

are known to control motor function (Figure 3.6A, right panel)[50]. To test whether Satb2+ interneurons target ventral cell types indiscriminately or with absolute specificity for synaptic partners, we performed immunohistochemistry for transcription factor markers of ventral interneuron populations. We identified Synaptophysin:TdTomato+ labeling on neurotrace+ cell bodies of multiple ventral interneuron populations implicated in motor control. Chx10+ V2a interneurons receive numerous contacts on their soma (Figure 3.6B). We also identified contacts onto Foxp2+ V1 interneurons, Evx1+ V0 interneurons, Calbindin+ ventral interneurons of mixed identity, and Bhlhb5+ ventral interneurons of mixed identity (Figure 3.6C and Figure 3.7C-E). Viral labeling of motor neurons for tibialis anterior (TA), gastrocnemius (GS), and hamstring (H) muscles provided a complete visualization of motor neuron soma and processes (see Methods) and revealed contacts from Satb2+ interneurons onto hindlimb motor pools (Figure 3.6D). We next used an independent strategy to confirm synaptic contacts onto motor neurons in which monosynaptic connections between spinal interneurons and motor neurons were identified by rabies labeling [2,80]. These experiments confirmed that Satb2+ interneurons target motor neurons in the ventral spinal cord, but revealed that Satb2+ interneurons represent a small fraction (<5%) of premotor cells for hindlimb motor pools (Figure 3.6E, F).

These findings reveal that Satb2+ interneurons target a network of ventral interneurons and motor neurons that are known to coordinate motor activity [50]. Taken together, our data suggests that Satb2+ interneurons are excellent candidates for converting diverse sensory cues into meaningful motor outputs.

Loss of Satb2 perturbs spinal interneuron position and molecular profile

Identification of Satb2 as a marker provides access to this population of cells, allowing us to genetically manipulate a key circuit link in sensory-motor pathways, and probe the function of both the gene and the neuron in circuit assembly and behavior.

Satb2 and its downstream targets are known to regulate cell fate specification and migration of cortical neurons [125,126], developmental events that are critical for establishing a functional neural circuit. We therefore sought to disrupt *Satb2* gene function and probe the requirement of the *Satb2* gene in cell position and identity within the spinal cord.

Insertion of Cre^{ERT2} into the ATG of *Satb2* generates a null allele (Figure 3.8A, B), providing the opportunity to track the lineage and circuit integration of Satb2 null interneurons in $Satb2^{Cre/Cre}$:TdTomato animals ($Satb2^{OFF}$:TdTomato). Consistent with previous reports using Satb2 null animals, $Satb2^{OFF}$ animals have defects in mandibular development, and die several hours after birth [128].

$Satb2^{OFF}$ interneurons are generated in normal numbers (Figure 3.9A, B, and data not shown), however there are marked changes in cellular position along the mediolateral axis. $Satb2^{Cre/WT}$: TdTomato ($Satb2^{ON}$:TdTomato) interneurons are normally organized in a tight band in the deep dorsal horn, spanning the mediolateral axis. In contrast, $Satb2^{OFF}$:TdTomato interneurons were shifted to a lateral position, and were more loosely organized with cells scattered dorsally (Figure 3.9A, B).

To measure the shift from medial to lateral deep dorsal horn, we analyzed cell body position in $Satb2^{ON}$ and $Satb2^{OFF}$ animals. Comparison of $Satb2^{ON}$:TdTomato+ and $Satb2^{OFF}$:TdTomato+ neurons revealed a significant shift in the mean cell body position along the mediolateral axis. The mean distance of $Satb2^{ON}$:TdTomato+ neurons from the midline at lumbar levels was 201.6 +/- 4.7um, while $Satb2^{OFF}$:TdTomato+ neurons were located 301.5+/-

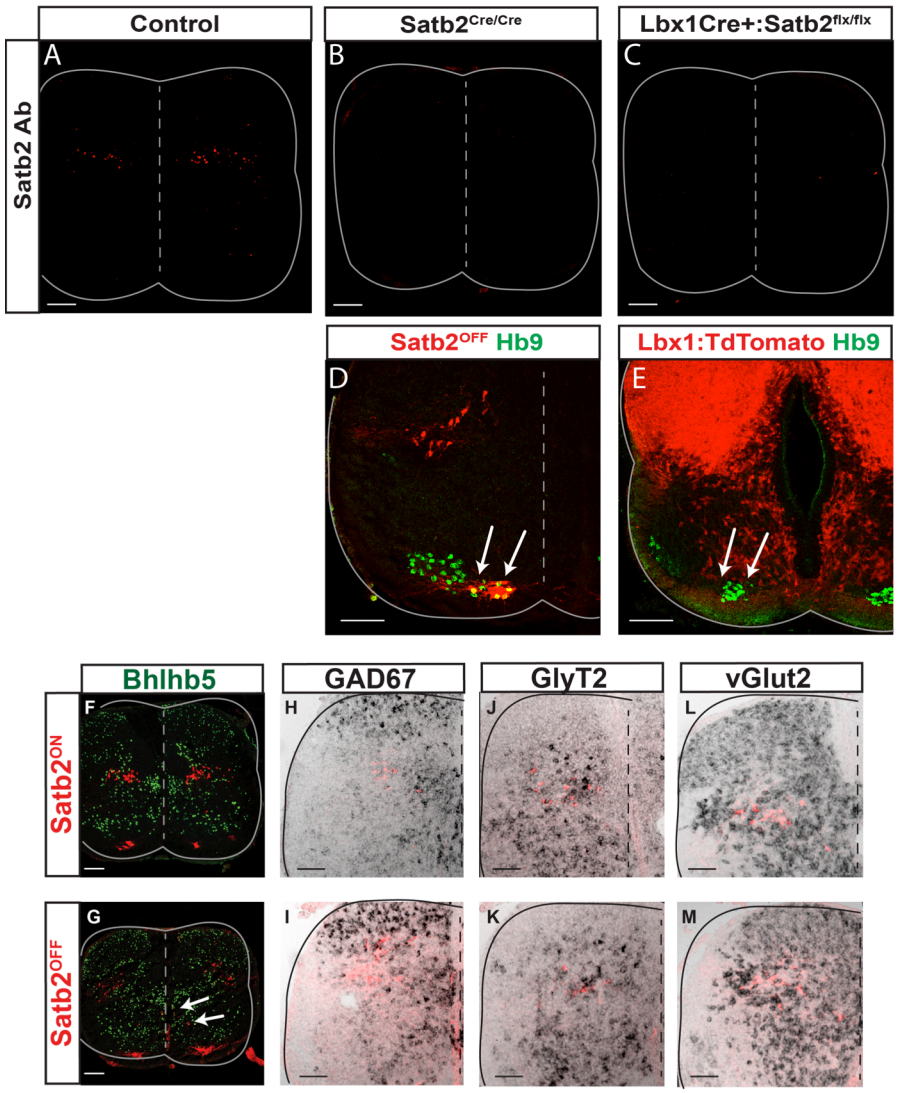

Figure 3.8: Strategy for eliminating Satb2 in the developing spinal cord and changes in molecular profile. (A-C) Immunohistochemistry for Satb2 antibody in control (A), Satb2^{OFF} (B), and Lbx1Cre+/Satb2$^{flx/flx}$ (C) spinal cords. **(D)** In Satb2^{OFF}:TdTomato spinal cords, motor neurons in the medial motor column (MMC) maintain the expression of Hb9. Arrowheads indicate expression of Hb9 in TdTomato+ MMC motor neurons. MMC motor neurons also express additional markers Lhx3, Isl1/2 and have a normal axon trajectory (data not shown). **(E)** Immunohistochemistry for Hb9 antibody in Lbx1:TdTomato spinal cords, e14.5. Lbx1:TdTomato labeling revealed a broad expression pattern inclusive of the dorsal spinal cord where Satb2+ interneurons reside. Lbx1:TdTomato expression was not detected in Hb9-expressing motor neurons, the cortex, or limb and facial skeletal structures (data not shown), indicating that use of Lbx1-Cre for behavioral testing is a genetic strategy that excludes other tissue types that normally express Satb2. **(F-G)** Immunohistochemistry for Bhlhb5 in Satb2^{ON}:TdTomato (F) or Satb2^{OFF}:TdTomato (G). In Satb2^{OFF}:TdTomato spinal cords, TdTomato+ neurons along the dorsal midline upregulate the expression of Bhlhb5 (arrows). **(H-M)** In situ hybridization for neurotransmitter markers in Satb2^{ON}:TdTomato (H, J, L) or Satb2^{OFF}:TdTomato (I, K, M). See Figure 3.9 and Table 3.1 for quantification for F-M. Scale bars, 100um.

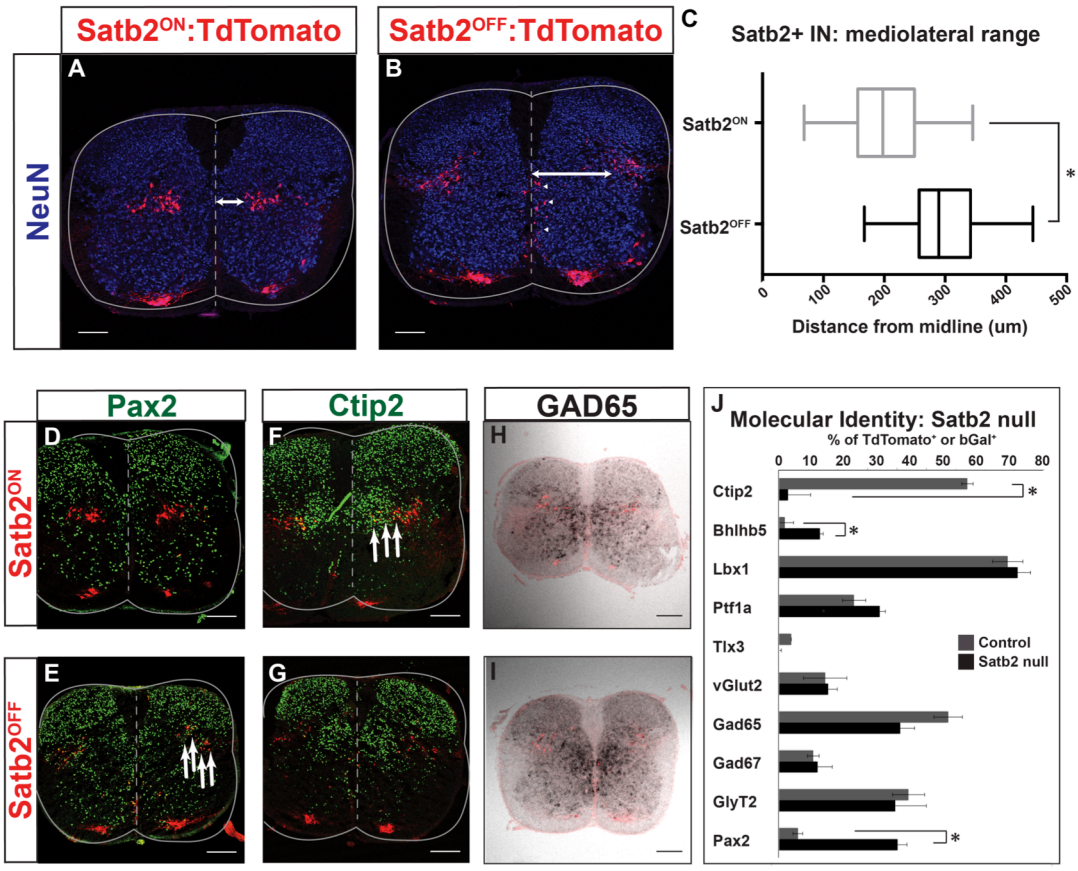

Figure 3.9: Alterations in cell body position and molecular profile in Satb2 null spinal cords. (A-C) Cell body position is shifted to the lateral margin of the spinal cord in Satb2 null interneurons. (A) Examination of Satb2^{ON}:TdTomato control spinal cords reveals that Satb2+ interneurons (red) are positioned throughout the mediolateral extent of lamina V in the deep dorsal horn. **(B)** Satb2 null interneurons (red) in Satb2^{OFF}:TdTomato animals reveals a lateral shift in cell body position in response to loss of Satb2. Arrows in A,B represent the distance from the midline to the medial edge of the TdTomato+ population. Arrowheads in B emphasize the position of a subset of Satb2 null interneurons that are positioned along the ventral midline. NeuN, blue. **(C)** Quantification of cell body position from A, B. Control (Satb2^{ON}) and Satb2 null (Satb2^{OFF}) data are presented as box and whisker plots indicating the median and middle 50% of the range of cell body position. The middle 50% of cell body position encompassed a range of 156.6-249.8um for Satb2^{ON} interneurons and 257.4-342.0um for Satb2^{OFF} interneurons. * indicates significant difference in the median ($p<0.05$; Mann-Whitney). **(D-J) Changes in molecular profile in response to loss of Satb2.** Comparison of control Satb2+ (Satb2^{ON}:TdTomato) and Satb2 null (Satb2^{OFF}:TdTomato) interneurons. **(D, E)** Pax2 expression (green) is upregulated in Satb2 null (red in E) compared with control (red in D). Arrows in E highlight the presence of clusters of yellow double labeled cells in Satb2^{OFF} interneurons. **(F, G)** Loss of Ctip2 expression (green) in Satb2 null (red in G) neurons compared with control (red in F). Arrows in F highlight the presence of yellow double labeled cells in control Satb2^{ON} interneurons. **(H, I)** Colabeling of GAD65 (black) and TdTomato labeling is comparable in control (red in H) and Satb2 null (red in I). **(J)** Quantification of colabeling of Tomato+ neurons in control Satb2^{ON} and Satb2^{OFF} spinal cords. Data is represented as mean +/- S.E.M. * indicates significant difference ($p<0.05$; Mann Whitney). See also Figure 3.8, Table 3.1. Scale bars in A, B, D-G, 100um. Scale bars in H, I, 200um.

Table 3.1: Changes in molecular profile in response to loss of Satb2. Quantification of co-labeling experiments for various lineage and transcription factor markers in $Satb2^{ON}$ and $Satb2^{OFF}$ spinal cord. $Satb2^{ON}$ and $Satb2^{OFF}$ columns report the percentage of TdTomato+ neurons colabeled with marker, and corresponding p-value. Significant changes in gene expression are shown in bold for Ctip2, Bhlhb5, and Pax2. P-value < 0.05, Mann-Whitney. See also Figure 3.8, 3.9J.

	$Satb2^{ON}$	$Satb2^{OFF}$	p-value
Ctip2	**63.97**	**2.9**	**0.016**
Bhlhb5	**1.9**	**13.8**	**0.016**
Lbx1	77.7	81.04	0.5714
Ptf1a	25.4	34	0.1429
Tlx3	4.105	0.655	0.3333
vGlut2	15.6	18.45	0.99
Gad65	55	40	0.2
Gad67	12.5	13.94	0.9428
GlyT2	44	41.25	0.8
Pax2	**6.3**	**40.2**	**0.016**

4.4um from the midline (Figure 3.9C; p-value: <0.0001, Mann-Whitney). These experiments reveal that loss of Satb2 drastically alters the final settling position of TdTomato+ interneurons along the mediolateral axis such that they are positioned at the lateral margin of the spinal cord. In addition to the main cluster of interneurons in the deep dorsal horn, we also observed a scattered population along the ventral midline in Satb2^{OFF} spinal cords. This population may represent a subset of neurons that were unable to exit the ventricular zone or that have an altered migration pattern (Figure 3.9B, arrowheads).

Satb2 is a DNA-binding protein that is known to regulate the expression of a number of genes during bone and cortical development. Loss of Satb2 leads to widespread gene misregulation [125,126,128], and in the cortex this ultimately leads to a cell fate conversion of cortical progenitors and alterations in migration pattern and projection identity [125,126].

To test whether Satb2 regulates gene expression in the spinal cord and to compare the molecular profile of Satb2^{ON}:TdTomato+ and Satb2^{OFF}:TdTomato+ spinal neurons, we performed double labeling experiments with immunohistochemistry or in situ hybridization.

Transcription factor markers for dorsal and ventral spinal interneuron populations were evaluated with immunohistochemistry, revealing a number of gene expression changes (Figure 3.8F, G Figure, 3.9D-G, J, Table 3.1, and data not shown). Genes that are known regulators of broad lineage classification, Ptf1a and Lbx1, were unchanged in response to loss of Satb2. In contrast, there were significant changes in the expression of Pax2 (Figure 3.9D, E, J; p-value: 0.016, Mann Whitney) and Bhlhb5 (Figure 3.8F, G, Figure 3.9J; p-value:0.016, Mann Whitney), genes that regulate neuronal circuit assembly and inhibitory neurotransmitter identity, respectively [134,135]. In addition, Ctip2 expression is almost completely lost in the absence of Satb2 expression. (Figure 3.9F, G, J; p-value: 0.016, Mann Whitney). Interestingly, TdTomato+ spinal neurons in Satb2^{OFF} animals that express Bhlhb5 were located in a small number of cells near the

ventral midline, whereas Ctip2 reduction and Pax2 upregulation in Satb2^{OFF} animals was observed predominantly in interneurons in the deep dorsal horn.

The changes we observed in the molecular profile of Satb2^{OFF}:TdTomato+ neurons prompted us to test whether there are corresponding alterations in neurotransmitter identity, as this would likely alter the function of these cells within a circuit. To test this we performed in situ hybridization for neurotransmitter markers in Satb2^{ON} or Satb2^{OFF} animals. Importantly, the ratio of inhibitory/excitatory status of Satb2+ interneurons is unchanged in the absence of *Satb2* gene function (Figure 3.8H-M, Figure 3.9H-J, and Table 3.1).

Consistent with the role of Satb2 in the regulation of gene expression and migration in the cortex, these results demonstrate that in response to loss of *Satb2* gene function, Satb2^{OFF}:TdTomato+ spinal neurons display an altered molecular profile and a dramatic shift in cell body position.

Loss of Satb2 disrupts interneuron circuit integration

Cell body positioning within the spinal cord is an important regulator of synaptic connectivity [133]. In particular, Satb2+ interneuron cell body position along the mediolateral axis is a determinant of proprioceptive sensory input (Figure 3.4). We therefore hypothesized that changes in Satb2 expression and consequently, changes in cell body position and gene expression, would alter spinal circuit assembly.

To identify changes in sensory input, we performed immunohistochemistry for parvalbumin and vGlut1 to visualize synaptic contacts from proprioceptive fibers. In Satb2^{ON} animals, a significant majority of Satb2+ interneurons were located within the proprioceptive target domain. In contrast, the percentage of TdTomato+ interneurons receiving proprioceptive input was greatly reduced in response to loss of Satb2 (Figure 3.10A-E, p-value=0.0043). This effect was also noted at cervical levels.

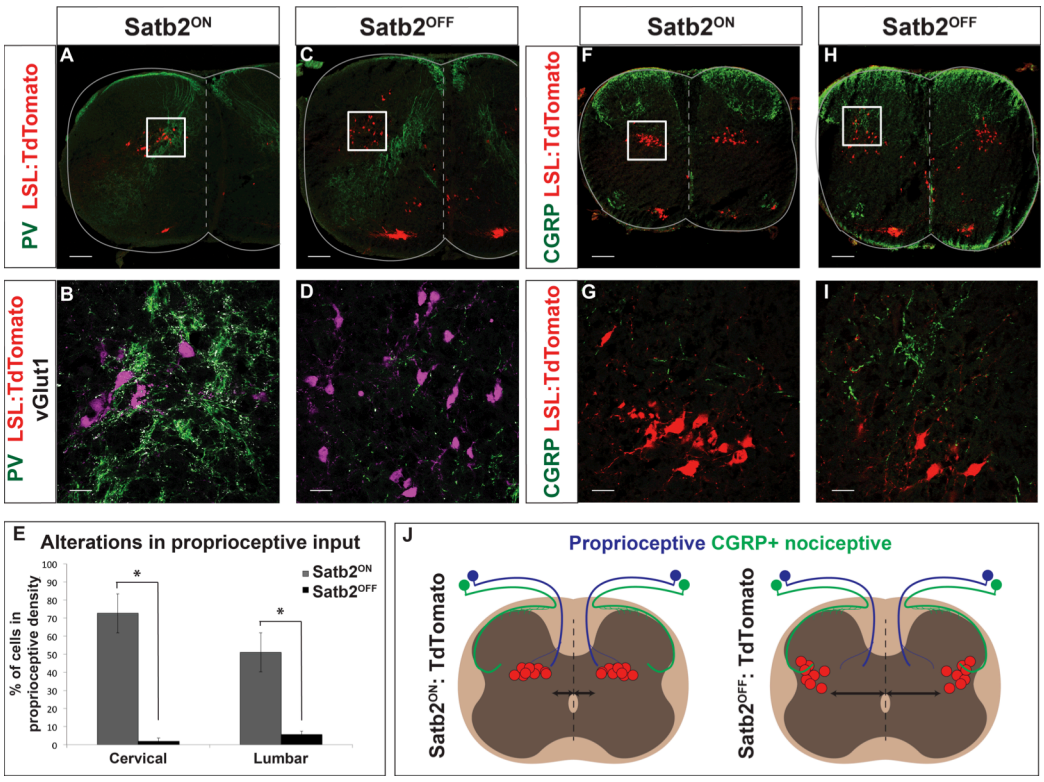

Figure 3.10: Alterations in sensory connectivity in Satb2 null spinal cords. (A-E) Loss of proprioceptive input in Satb2 null interneurons. (A, B) Wild type Satb2+ interneurons (Satb2^{ON}) are located in the dense termination zone of proprioceptive afferents. Proprioceptive contacts, identified by coexpression of parvalbumin (green) and vGlut1 (white), were identified on TdTomato+ neurons (red) in control Satb2^{ON} (in A, B) or Satb2^{OFF} (in C, D) spinal cords. **(C, D)** Satb2 null interneurons (Satb2^{OFF}) located at the lateral margin of the spinal cord are no longer positioned in the proprioceptive targeting domain. **(E)** Significant loss of Satb2 null interneurons (black) in the proprioceptive density, compared with control Satb2+ interneurons (grey). Number of cells in the main density of proprioceptive fibers were quantified. At cervical levels, 72.6 +/- 2.5% of Satb2^{ON} interneurons were located in the proprioceptive density (n=4 spinal cords). 1.8 +/- 1.8% of Satb2^{OFF} interneurons were located in the proprioceptive density (n=4 spinal cords). At lumbar levels, 51.0 +/- 3.4% of Satb2^{ON} interneurons were located in the proprioceptive density (n=5 spinal cords). 5.6 +/- 2.6% of Satb2^{OFF} interneurons were located in the proprioceptive density (n=6 spinal cords). Data is represented as mean +/- S.E.M. * indicates significant difference ($p<0.05$; Mann Whitney). **(F-I) Satb2 null interneurons occupy targeting domain of CGRP+ nociceptors. F, G.** Wild type Satb2+ interneurons (red) in Satb2^{ON} animals do not overlap with the CGRP+ nociceptor (green) targeting domain. **H, I.** Satb2 null interneurons (red) in Satb2^{OFF} animals located in the lateral deep dorsal horn are positioned in an area overlapping with CGRP+ nociceptors (green). White box in A, C, E, H corresponds to high magnification image shown in B, D, G, I, respectively. **J.** Left panel, Satb2+ interneurons (red) in Satb2^{ON}:TdTomato animals are located in the dense termination zone of proprioceptive fibers, but do not normally overlap with the fibers in lateral lamina V that originate from a subset of nociceptors expressing CGRP+. Right panel, Satb2 null interneurons (red) in Satb2^{OFF}:TdTomato animals are shifted to a lateral position, losing their position in the proprioceptive targeting domain. Instead, Satb2 null interneurons are overlapping with the termination zone of CGRP+ nociceptors. Scale bars in A, C, F, H, 100um. Scale bars in B, D, G, I, 20um.

Interestingly, the trajectory and density of proprioceptive fibers in the spinal cord is largely unchanged in response to loss of Satb2, and monosynaptic connections from proprioceptive fibers onto motor neurons are normal in their overall distribution and electrophysiological properties (Figure 3.10A, C, and data not shown).

To determine whether laterally shifted Satb2^{OFF} interneurons receive a new pattern of synaptic inputs, we examined primary afferents of a subset of peptidergic nociceptors expressing CGRP that are known to target spinal neurons in lateral lamina V [136]. To test whether Satb2+ interneurons are positioned in the target zone of peptidergic nociceptors, we performed immunohistochemistry for CGRP. Under normal conditions Satb2^{ON} interneurons are located medial to the CGRP+ fiber density in the lateral deep dorsal horn (Figure 3.10F, G). The overall projection of CGRP+ fibers was unchanged in Satb2^{OFF} animals, however examination of lateral Satb2^{OFF}:TdTomato+ interneurons revealed that the ectopic position of these cells overlaps with the termination domain of CGRP+ fibers (Figure 3.10H, I), an alteration that may reflect ectopic direct nociceptive connectivity.

In summary, these experiments reveal that in Satb2^{OFF}:TdTomato+ spinal cords, sensory-interneuron wiring is transformed such that TdTomato+ interneurons reposition to an overlapping domain with CGRP+ peptidergic nociceptive fibers at the expense of proprioceptive connections (Figure 3.10J). These findings suggest that although the pattern of proprioceptive and nociceptive fibers is unchanged, the redistribution of spinal interneurons may lead to a new pattern of synaptic inputs.

Loss of Satb2 disrupts synaptic targeting of the ventral motor network

Satb2+ interneurons normally link multimodal sensory input broadly to motor circuitry in the ventral spinal cord (Figure 3.4, Figure 3.6). However, in response to loss of Satb2, we

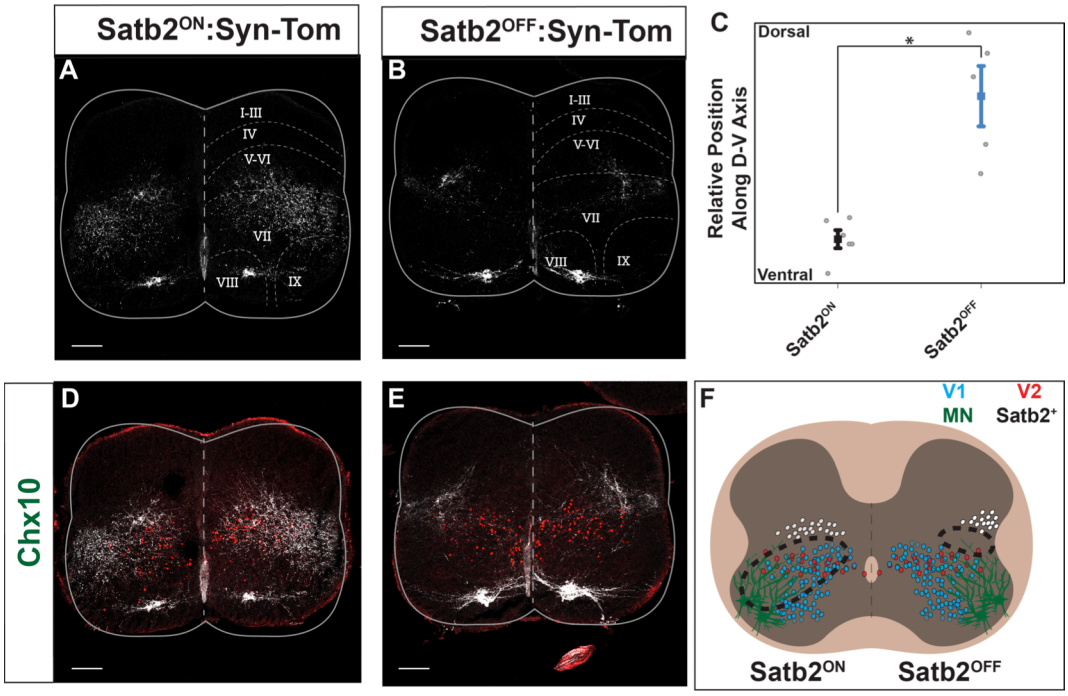

Figure 3.11: Loss of Satb2 reduces synaptic input to ventral motor circuitry.
A. Synaptic target domain of Satb2+ interneurons (red), identifiable by genetic labeling with Satb2:Synaptophysin-TdTomato (Satb2:Syn-Tomato). Synaptophysin-TdTomato labeling (white) was observed throughout lamina V-VII and IX in Satb2^{ON}:Syn-Tom animals. **B.** In Satb2 null spinal cords, Synaptophysin-TdTomato labeling (white) was instead restricted to lamina V and dorsal lamina VI in Satb2^{OFF}:Syn-Tom animals **C.** Quantification of fluorescent pixel intensity for control (Satb2^{ON}) and Satb2 null (Satb2^{OFF}) animals reveals a significant shift in the relative position of presynaptic terminals along the dorsal-ventral axis. Data is represented as mean +/- S.E.M. * indicates significant difference ($p<0.05$; Student's t-test). **D.** In control animals (Satb2^{ON}), the presynaptic terminals of Satb2+ interneurons (red) are intermingled with Chx10+ V2a interneurons (green), one of the known target populations of Satb2+ interneurons. See also Figure 3B. **E.** In Satb2 null animals (Satb2^{OFF}), the density of presynaptic terminals (red) is instead shifted dorsal to the Chx10+ V2a interneurons (green). **F**. Schematic showing the wild type distribution of presynaptic terminals of Satb2+ interneurons (left panel, dotted line) overlapping with ventral interneurons (blue, red) and motor neurons (green). In contrast, the density of presynaptic terminals of Satb2 null interneurons (right panel, dotted line) is shifted dorsally to a position that no longer encompasses cellular components of ventral motor circuitry. Scale bars in A, B, D, E, 100um.

hypothesized that the drastic alteration in cell position would correspond with changes in synaptic targeting of ventral motor circuitry.

To test whether postsynaptic connectivity is altered in response to loss of Satb2, we compared the distribution of Satb2+ interneuron presynaptic terminals in Satb2^{ON}:Synaptophysin-TdTomato (Satb2^{ON}:Syn-Tom) and Satb2^{OFF}:Synaptophysin-TdTomato (Satb2^{OFF}:Syn-Tom) animals. In Satb2^{ON}:Syn-Tom animals, synaptic contacts were distributed broadly throughout the ventral spinal cord (Figure 3.11A), overlapping with cellular components of the central pattern generator (CPG) circuitry. In contrast, the overall distribution of presynaptic terminals was shifted to a dorsal position in Satb2^{OFF} spinal cords at the lateral margin of the spinal grey matter, aligning to spinal lamina where Satb2^{ON} cell bodies are normally located (Figure 3.11A, B). To map the redistribution of Satb2 connections onto the ventral spinal cord, we quantified this effect by plotting fluorescent pixel intensity along the dorsoventral axis and generating an average dorsoventral location of peak labeling (see methods). This analysis revealed that Synaptophysin-TdTomato+ labeling in Satb2^{OFF}:Syn-Tom animals is significantly shifted to a dorsal position when compared to Satb2^{ON}:Syn-Tom animals (Figure 3.11C; $p=0.00073$, Student's t-test).

To determine whether this change in distribution of presynaptic terminals altered connections onto postsynaptic targets, we compared Synaptophysin-TdTomato labeling to Chx10+ V2a interneurons that receive synaptic input from wild type Satb2+ interneurons. In Satb2^{ON}:Syn-Tom spinal cords, dense labeling was identified throughout the V2a domain. However in Satb2^{OFF}:Syn-Tom spinal cords, fluorescent labeling was instead positioned dorsal to the V2a population, indicating that Satb2 null interneurons no longer form synaptic connections across their normal target zone within the ventral spinal cord (Figure 3.11D, E). These findings reveal a significant loss of synaptic input to the ventral spinal cord, an area in which components of locomotor circuitry reside (Figure 3.11F).

Basic motor function is intact in response to loss of Satb2

We next considered how loss of synaptic input to the ventral spinal cord may alter motor function. One possibility is that the intrinsic properties of CPG networks are altered such that they can no longer generate a normal motor output. To test for changes in ventral interneuron and motor neuron function, we performed fictive locomotion experiments in Satb2 null ($Satb2^{lacZ/lacZ}$) and control ($Satb2^{+/lacZ}$ or $Satb2^{+/+}$) animals [128].

Ventral root activity was normally coordinated in the absence in Satb2: comparison of motor activity for left-right (left and right L2) and flexor-extensor pairs (ipsilateral L2 and L5) revealed that CPG activity was normal in Satb2 null spinal cords. Satb2 null animals also displayed normal cycle period length, cycle period variation, and burst duration (Figure 3.12 and data not shown), parameters that are altered when ventral interneuron function is perturbed [55,137-141].

These experiments reveal that although connectivity to the ventral spinal cord is altered in Satb2 null animals, ventral motor networks remain intrinsically capable of producing a functional motor output. These findings are consistent with the autonomy of CPG circuitry from the dorsal spinal cord that has been reported in this experimental context [142], but reveal that Satb2 is not required for normal function of the CPG.

To test whether loss of Satb2 impacts the behaving animal, we specifically eliminated Satb2 in spinal interneurons using a conditional allele. Lbx1-Cre was selected based on its coexpression with Satb2 in the spinal cord, and its exclusion from other cell and tissues types that express Satb2 (Figure 3.3A, B, Figure 3.8D, E, and data not shown). Use of $Lbx1Cre+/Satb2^{flx/flx}$ animals allows for behavioral analysis of motor and sensory function following specific excision of the *Satb2* gene in spinal interneurons.

By crossing $Satb2^{flx/flx}$ animals with Lbx1-Cre, we observed a loss of Satb2 protein expression within spinal interneurons (Figure 3.8C). $Lbx1Cre^{+}/Satb2^{flx/flx}$ animals are

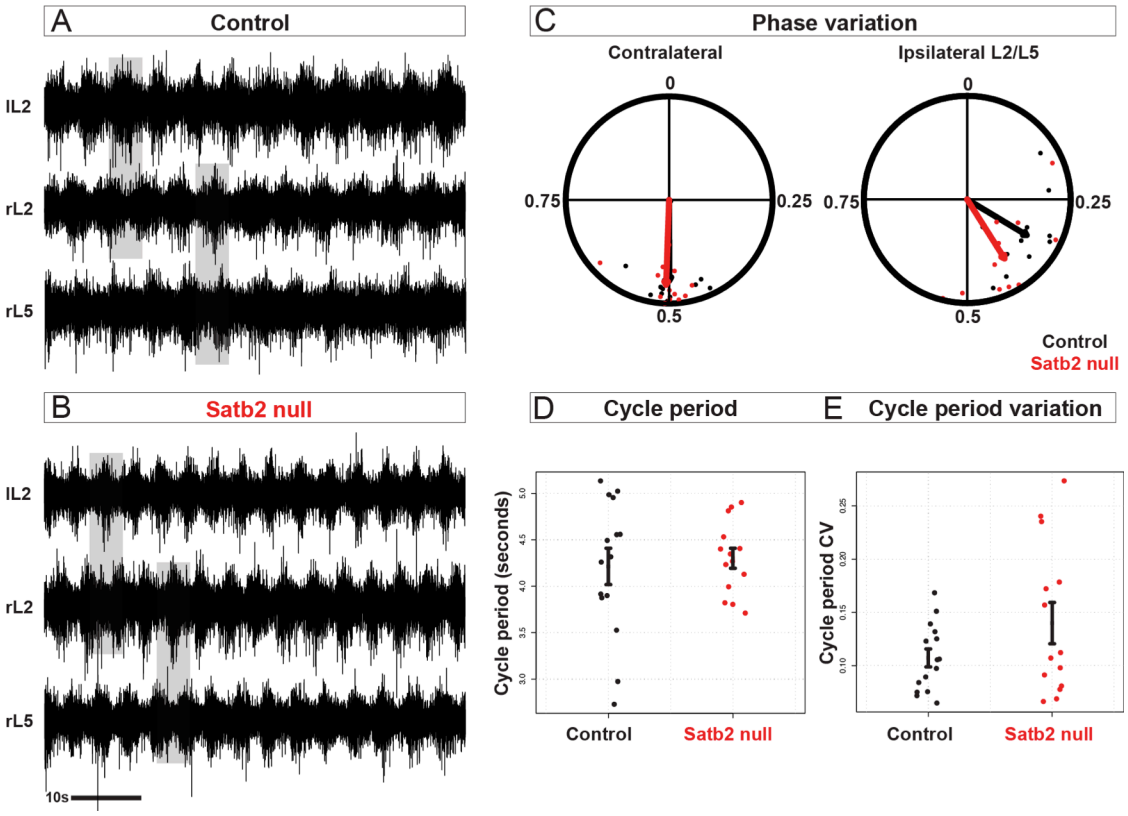

Figure 3.12: Satb2 is not required for normal fictive locomotor activity. (A, B) Example traces for left L2 (lL2), right L2 (rL2), and right L5 (rL5) ventral root recordings in wild type (A) or Satb2 null (B) spinal cords at e18.5. Neurochemically induced fictive locomotor activity in wild type spinal cords is characterized by alternating rhythmic bursts of motor neuron activity between contralateral L2 ventral roots and ipsilateral L2-L5 ventral roots. Neurochemical induction of fictive locomotor activity in Satb2 null spinal cords evokes rhythmic alternating bursts of motoneuron activity indistinguishable from wild type littermates. **C.** Quantification of phase analysis from contralateral and ipsilateral ventral root pairs reveals that fictive locomotor activity is normally coordinated in Satb2 null (red points) relative to wild type littermates (black points). Points near 0.5 represent alternating activity. **(D, E)** Loss of Satb2 does not alter the cycle period or regularity of fictive locomotor activity. Cycle period (D) of control (black) and Satb2 null (red) recordings. Cycle period for individuals are shown as dots. Mean +/- SEM is reported for each genotype. Cycle period variation (E) of control (black) and Satb2 null (red) recordings. Cycle period variation (cycle period CV) for individuals is shown as dots. Mean +/- SEM is reported for each genotype.

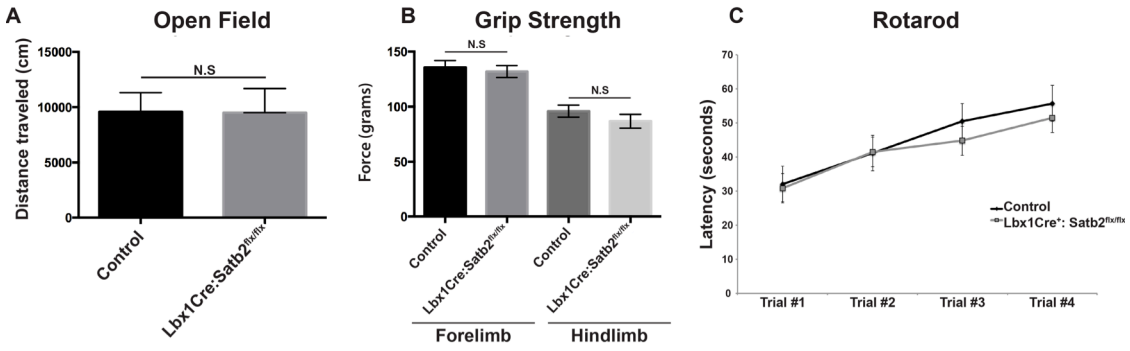

Figure 3.13: Motor coordination is normal in the absence of Satb2 in spinal interneurons. **(A)** Open field test measured the total distance traveled for Control and Lbx1Cre+/Satb2$^{flx/flx}$ animals. Mean +/- S.E.M is reported. Mann-Whitney test did not reach statistical significance (N.S). (**B)** Grip Strength test measuring muscle strength in force (grams). Mean +/- S.E.M is reported. Mann Whitney test to compare Control and Lbx1Cre+/Satb2$^{flx/flx}$ animals did not reach statistical significance (N.S) at forelimb or hindlimb levels. (**C)** Rotarod test for overall motor coordination. Mean +/- S.E.M is reported. Mann Whitney test to compare latency to fall (seconds) for control and Lbx1Cre+/Satb2$^{flx/flx}$ animals did not reach statistical significance for any of the 4 trials performed.

indistinguishable from control littermates at birth, and at 8 and 20 weeks of age. Lbx1Cre^{+}/Satb2$^{flx/flx}$ animals are born in normal numbers and have a normal lifespan and body weight (data not shown).

We performed behavioral tests that broadly examined motor function, including open field to test baseline motor activity and grip strength to test muscle strength. Lbx1Cre^{+}/Satb2$^{flx/flx}$ animals performed normally in each of these behavioral tests (Figure 3.13). Lbx1Cre^{+}/Satb2$^{flx/flx}$ also performed normally on the rotarod test measuring general motor coordination. In spite of the anatomical changes in proprioceptive transmission via Satb2+ interneurons, these findings indicate that Satb2 is dispensable for the coordination of walking and running behaviors.

Conditional ablation of Satb2 in spinal interneurons results in altered sensorimotor behavior

To test whether changes we identified in cell position and connectivity impact sensorimotor integration in behavior, we performed a series of tests to measure the motor response to noxious stimuli.

The Von Frey test is used to measure the response to mechanical pain, and was performed to analyze key components of the behavioral response: the threshold required to produce the nociceptive withdrawal reflex, the dynamics of the withdrawal, and the replacement of the limb following withdrawal. The threshold for producing the nociceptive withdrawal behavior following Von Frey fiber stimulation was normal in Lbx1Cre^{+}/Satb2$^{flx/flx}$ animals when compared with control littermates (Figure 3.14A). However, we observed a maintained flexion posture in Lbx1Cre^{+}/Satb2$^{flx/flx}$ animals following Von Frey stimulation (Figure 3.14B; 11/13 animals in Lbx1Cre^{+}/Satb2$^{flx/flx}$; 2/11 animals in Cre- control littermates), indicating that in response to loss of Satb2 there is an aberrant motor response to mechanical stimulation.

To test whether the maintained flexion posture occurs via multiple pain modalities, we performed the Hargreaves thermal pain test. A high intensity light source was shined on the

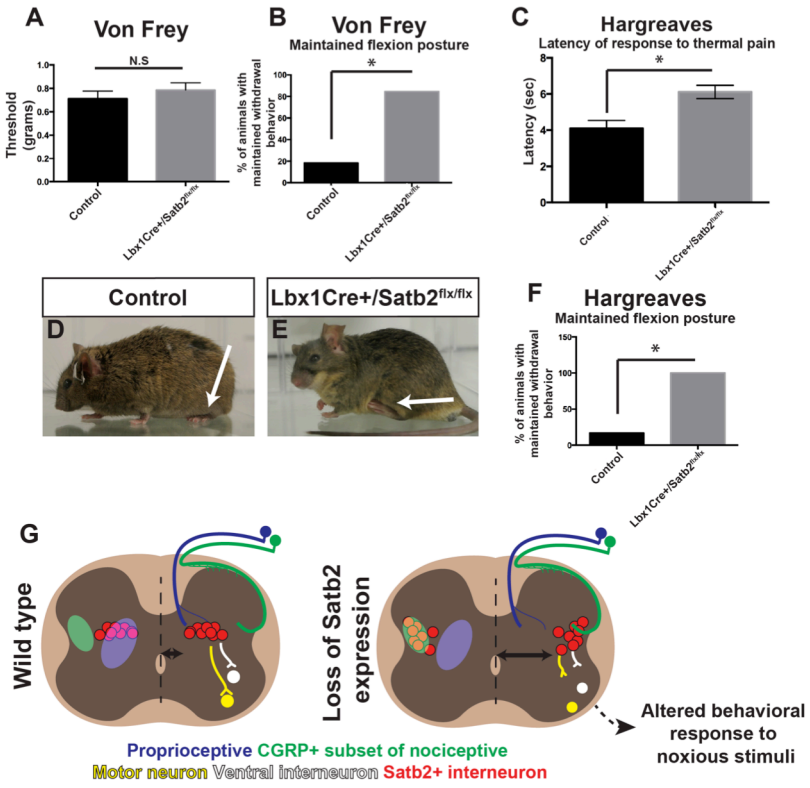

Figure 3.14: Loss of Satb2 in spinal interneurons perturbs the motor response to noxious stimuli. (A) Threshold to induce mechanical pain response in the Von Frey test was comparable between control and Lbx1Cre/Satb2$^{flx/flx}$ animals. Data is represented as mean threshold (grams of force) +/- S.E.M. N.S. indicates no significant difference ($p>0.05$; Mann Whitney). **(B)** Lbx1Cre/Satb2$^{flx/flx}$ animals display a prolonged withdrawal posture following Von Frey mechanical pain stimulation. Data is represented as mean (number of animals maintaining withdrawn posture) * indicates significant difference ($p=0.003$; Fischer's exact test). **(C)** Following the Hargreaves test for thermal pain, conditional loss of Satb2 in spinal interneurons in Lbx1Cre/Satb2$^{flx/flx}$ animals leads to an increase in the latency to withdrawal compared to control (Lbx1Cre-) animals. Data is represented as mean latency (seconds) +/- S.E.M. * indicates significant difference ($p<0.05$; Mann Whitney). **(D, E)** Representative images of Control (D) and Lbx1Cre/Satb2$^{flx/flx}$ (E) animals following withdrawal response to Hargreaves thermal pain test. Following the withdrawal response, control animals replace the limb to a resting position (arrow in D), while Lbx1Cre/Satb2$^{flx/flx}$ animals maintain the withdrawn posture (arrow in E). **(F)** Lbx1Cre/Satb2$^{flx/flx}$ animals display a prolonged withdrawal posture following Hargreaves stimulation, compared with control animals. Data is represented as mean (number of animals that maintain withdrawn posture) * indicates significant difference ($p=0.01$; Fischer's exact test). **(G)** Summary diagram of cell body position and circuitry changes that result from loss of Satb2. In control spinal cord, Satb2+ interneurons (red) are located at the intersection of proprioceptive (purple) and indirect nociceptive (black) modalities, commands that are directed toward motor circuitry in the ventral spinal cord (motor neurons, yellow; ventral interneurons, white). Following loss of Satb2, interneurons are shifted to a lateral position, overlapping with the termination domain of CGRP+ nociceptors (green). Synaptic input to the ventral spinal cord is significantly reduced. In addition there is an altered behavioral response to noxious stimulation. Arrows indicate cell body distance from the midline. Ovals indicate termination domains for proprioceptive (purple) and CGRP+ nociceptive (green) modalities.

footpad of test animals, eliciting an isolated, reproducible nociceptive withdrawal response of the foot [143,144].

We observed a small but significant increase in hindlimb response latency in Lbx1Cre^{+}/Satb2$^{flx/flx}$ animals when compared with control littermates (Figure 3.14C). Interestingly, Lbx1Cre^{+}/Satb2$^{flx/flx}$ animals maintained a flexed posture following thermal pain stimulation (Figure 3.14D-F; Videos 3.1 and 3.2; 6/6 animals in Lbx1Cre^{+}/Satb2$^{flx/flx}$; 1/6 animals in Cre- control littermates; p=0.015, Fischer's exact test), indicating that the motor response to both mechanical and thermal pain is perturbed following loss of Satb2 in spinal interneurons.

Taken together, these findings establish *Satb2* as a critical gene for sensory processing within the spinal cord, and reveal that in the absence of *Satb2* gene function in spinal interneurons, there is a defective transformation of sensory cues into the appropriate motor response.

Discussion

The mechanisms that are employed by the nervous system to integrate and translate multiple streams of information into meaningful behavior are not well understood. Within the spinal cord, commands from sensory pathways converge onto neurons in the deep dorsal horn, yet the molecular mechanisms that assemble spinal circuit components into functional networks remain elusive. Our studies demonstrate that Satb2 regulates the assembly of sensory-motor connections that comprise integrative circuitry important for the coordination of reflex behaviors. Loss of Satb2 leads to defects in cell body positioning, molecular profile, circuit integration and in the execution of sensorimotor behavior. This study establishes the *Satb2* gene as an essential component of spinal circuitry that integrates commands from multiple sensory pathways and regulates the behavioral response to noxious stimulation.

Satb2 as a regulator of circuit assembly programs

We report an altered molecular profile in response to loss of the *Satb2* gene (Figure 3.8, 3.9). Transcription factors such as Lbx1 and Ptf1a that specify progenitor domains within dorsal interneurons were unchanged in Satb2 null interneurons. We instead observed changes in the expression of genes that regulate subsequent phases of neural development. For instance, Bhlhb5, a gene that is involved in neuronal circuit assembly [145], is upregulated in a subset of Satb2 null interneurons that are positioned along the ventral midline. Pax2 is a downstream target of Lbx1 and Ptf1a, and is known to regulate glycinergic cell fate as well as the expression of neuropeptides used for inhibitory neurotransmission [127,134,135,146]. Although Satb2 null interneurons retain their inhibitory neurotransmitter identity, Pax2 expression is significantly upregulated, suggesting there may be changes in the specific composition of neurotransmitter and peptide signaling employed by these neurons.

In contrast to the role of Satb2 as a strict repressor of Ctip2 that has been reported in the cortex, we observe coexpression of these genes in a subset of Satb2+ spinal interneurons (Figure 3.4, 3.5). In response to loss of Satb2, Ctip2 expression is almost completely abolished. These findings reveal two critical aspects of gene regulatory networks in the spinal cord. First, in wild type spinal cords a subset of Satb2+ interneurons escapes the antagonistic gene interaction that separates cortical Satb2 and Ctip2 expression. Second, the molecular profile of Satb2 and Ctip2 expression subdivides Satb2+ interneurons along the mediolateral axis, and loss of Satb2 abolishes this genetic heterogeneity. Given the established topopgraphical organization of cell and fiber types in the deep dorsal horn, mediolateral segregation of Satb2+ interneurons may be a determinant of connectivity and function.

Spatial organization of integrative nodes implicated in motor control

The spinal cord integrates and processes multiple motor commands that originate in

peripheral sensory systems as well as descending pathways from brain centers. Despite the well established topography of these diverse inputs, the circuit logic that links somatotopic and action-based commands to muscle-based motor action has remained obscure .

Neurons in the superficial and deep dorsal horn have been described electrophysiologically and are known to receive convergent sensory information from nociceptive, mechanoreceptive, and proprioceptive modalities [147]. Yet the lack of molecular markers for sensory relay neurons has precluded genetic manipulations to understand how populations that receive convergent input are important in the behaving animal.

Our studies describe a population of inhibitory spinal neurons in lamina V that receives multimodal sensory input and are incorporated into feedforward circuitry that distributes these diverse cues to the ventral motor network. Perturbation of Satb2+ cells disrupts the dynamics of the withdrawal response following noxious stimulation, leading to a maintained flexion response of the hindlimb.

Recently, RORβ neurons in lamina II/III of the dorsal horn were identified as critical components of sensory-motor circuitry that mediate light touch and corrective motor behaviors. These neurons integrate information from corticospinal and cerebellar descending pathways, as well as mechanosensory neurons [148]. Additionally, somatostatin+ neurons in lamina II were identified as recipients of sensory input from multiple nociceptive fiber types, and are mediators of mechanical pain transmission [149]

These findings, together with our study, suggest that laminar location in the dorsal spinal cord is a determinant of the assortment of convergent input from motor control pathways and consequently, the behavioral context in which these cells are recruited. This integrative type of sensory processing at the level of spinal interneurons may provide a mechanism for transforming diverse cues into coherent commands for motor actions. Genetic isolation of spinal interneurons

has broadened our understanding of the convergent organization of circuit components, an arrangement that underlies the diverse behavioral repertoire of animals.

Cell body position and circuit miswiring

The wild type Satb2+ interneuron population spans the mediolateral axis and receives multimodal sensory input, suggesting that they participate in behaviors that integrate proprioceptive and nociceptive information. In response to loss of Satb2 function, cells reposition to the lateral spinal cord and lose their wild type pattern of convergent synaptic inputs and divergent synaptic outputs in the ventral spinal cord (Figure 3.14).

Monosynaptic connections to motor neurons have a well established role in controlling motor output, though the function of polysynaptic connections via spinal interneurons in the deep dorsal horn has not been described. Proprioceptive fibers have a major synaptic representation in the deep dorsal horn of the spinal cord, and Satb2+ interneurons are direct recipients of these connections (Figure 3.4). Surprisingly, although proprioceptive fibers have been disconnected from a subset of their synaptic targets in response to loss of Satb2 expression, animals with spinal interneuron-specific deletion of Satb2 had comparable performance in rotarod testing for overall motor coordination (Figure 3.13). Instead, Satb2 expression in spinal interneurons is required for an appropriate limb response following noxious stimulation.

Given the multimodal input onto Satb2+ interneurons, a defect in the integration of proprioceptive and nociceptive information may manifest as an inability for the spinal cord to instruct ongoing movement following pain stimulation. For instance, replacement of the hindlimb following nociceptive withdrawal likely requires proprioceptive feedback that senses that the injured limb is positioned in a flexed posture. This may account for the maintained withdrawal posture we observed in Satb2 mutant animals in response to pain, and support the idea that Satb2+ interneurons function as an integrative circuit hub that mediates the withdrawal behavior

following both thermal- and mechanical- stimulation.

Satb2+ interneurons are predominantly inhibitory, suggesting that genetic perturbation of the Satb2 population may result in loss of inhibitory control over excitatory commands from sensory systems. Similarly, changes we observed in the synaptic outputs from Satb2 null interneurons may lead to loss of inhibition onto ventral spinal circuitry. Although it is unclear whether defects in the transmission of sensory commands onto or from inhibitory Satb2+ interneurons could account for the maintained flexion response following nociceptive stimulation, these findings suggest that the transformation of sensory cues to motor output via Satb2+ interneurons is a critical pathway for mediating sensorimotor behavior.

Acknowledgements

Chapter 3 is an adaptation of a paper that was submitted for publication. The working citation is: Kathryn L Hilde, Ariel J. Levine, Christopher A. Hinckley, Marito Hayashi, Jessica M. Montgomery, Rudolf Grosschedl, Yoshinori Kohwi, Terumi Kohwi-Shigematsu, Samuel L. Pfaff. Satb2 controls spinal circuit assembly and sensorimotor reflex behavior. The authors of this manuscript would like to acknowledge the generosity and advice of Martyn Goulding, Catherine Farrokhi, Steeve Bourane, and Lidia Garcia-Campmany; Shawn Driscoll for guidance in statistical analyses, Qiufu Ma, Randy Johnson, and Carmen Birchmeier for providing reagents, Yelena Dayn for help with generation of the Satb2-Cre^{ERT2} transgenic mouse line. Karen Lettieri, Miriam Gullo and Colleen Heller provided support and advice. I was supported as a National Science Foundation Graduate Research Fellow and the Chapman Foundation. Ariel Levine was supported by George E. Hewitt Foundation for Medical Research and Christopher and Dana Reeve Foundation. Chris Hinckley was supported by a US National research Service Award Fellowship from US National Institutes of Health NINDS. Marito Hayashi was supported by the Timken-Sturgis Foundation and the Japanese Ministry of Education, Culture, Sports, Science, and

Technology Long-Term Student Support Program. Samuel Pfaff is supported as a Howard Hughes Medical Institute Investigator and as a Benjamin H. Lewis chair in neuroscience. This research was supported by funding from the Howard Hughes Medical Institute, the Marshall Foundation and the Sol Goldman Charitable Trust.

Methods

Chapter 1 Methods

Chapter 1 does not contain experimental data.

Chapter 2 Methods

Animals

The following strains of mice (male and female) were used: wild-type, *Emx1*$^{tm1(cre)Krj}$/*J* (Jax 005628), *Pvalb*$^{tm1(cre)Arbr}$/*J* (Jax 008069), *Gt(ROSA)26Sor*$^{tm34.1(CAG-Syp/tdTomato)Hze}$/*J* (Jax 012570), and a transgenic *Hb9:B19G* line that we generated. This last line was made using a DNA fragment with the *Hb9* promoter driving expression of the rabies B19G strain glycoprotein. We found that transgenic expression of B19G was inadequate for transsynaptic rabies spread, so this line was used in a limited number of experiments, and AAV:G was used together with this line. All experiments were done in accordance with Institutional Animal Care and Use Committee animal protocols and BSL2+ safety protocols, on animals housed in groups on a 12-h light-dark cycle.

Virus preparation and injections

AAV2/6 containing a general promoter and the rabies B19G strain glycoprotein was produced by Applied Viromics at a titer of 1×10^{12}–3×10^{13} genome copies/ml. Rabies virus was produced as described[150], with the following modifications. Rabies virus culture was performed in 2% serum at 35 °C with 3% CO_2 and two concentrating ultracentrifugation spins through sucrose were performed instead of one. Rabies starter viruses that contained either GFP, mCherry or ChR2 fused to mCherry (ChR2) were obtained from members of the Callaway lab[80,90]. AAV:G and rabies virus were mixed 4:1 immediately before injection. Injections were performed at P0 or

P7 by anesthetizing pups on ice, then performing single injections of 0.3–1.5 μl (depending on the muscle) of virus into the muscle with a Hamilton syringe. Injections were performed through the skin, except for quadriceps injections that were performed using a small incision above the knee to reveal the muscle, and with a direct intramuscular injection. Small muscles (such as the TA and wrist flexors and extensors) were injected with low volumes (0.3–0.75 μl) using a needle with a small tip and a 30° bevel, whereas larger muscles were injected with 0.5–1.5 μl using a needle with a larger tip. Intraspinal injections of RabΔG:ChR2 were performed on P3 or P4 mice, anesthetized on ice, following a small unilateral laminectomy, and using a fine glass needle and a picospritzer to deliver 0.25 ml of virus into L4/L5. Animals were analyzed at P6–P8. Cortical injections of AAV2/1 containing *CAG:Cre-iRES-EGFP* (at a titer of 5×10^{13} genome copies/ml) were performed using a fine glass needle and a picospritzer to deliver 0.25 ml of virus 0.6 mm lateral to bregma at a depth of 0.4–0.45 mm from the surface of the caudal motor cortex[101,151].

Capsaicin treatment

P8 animals were given two small injections in the right heel of 0.1% capsaicin in ethanol, and killed and perfused after a 1.5 h survival time.

Tissue processing, in situ hybridization, immunohistochemistry and cell quantification

Perfused spinal cords were isolated and immersion-fixed for an additional 1 h, washed in PBS, washed in 30% sucrose and embedded in O.C.T. compound. Cryosections were cut at 30 mm for *in situ* hybridization and at 50 mm for immunohistochemistry. *In situ* probes (vGlut2, Gad65 and Gad67) were provided by Q. Ma (Department of Neurobiology, Harvard Medical School)[146]. The following primary antibodies were used: rabbit anti-parvalbumin (Swant PV25,

1:1,000), rabbit anti-PSD95 (Invitrogen 51-6900, 1:500), guinea pig anti-vGlut1 (Millipore AB5905, 1:5,000), rabbit anti–c-fos (Santa Cruz sc-52, 1:2,000), rabbit anti-Pax2 (Invitrogen 716000, 1:1,000), rabbit anti-Tlx3 (provided by C. Birchmeier, Max Delbruck Center for Molecular Medicine), rabbit anti-Tcfap2β (Santa Cruz sc-8976, 1:500) and mouse anti-Satb1/2 (Abcam 51502, 1:500). In some cases, directly conjugated rabbit anti-Tcfap2b antibody was used, prepared with Apex antibody labeling kit (Invitrogen). Images were taken on a confocal microscope and are presented as *z*-projections unless otherwise noted. To count cells for location and marker positivity, all spinal cords were included that had at least 15 neurons in at least one 50 mm section, a minimum criteria for sufficient efficiency of transsynaptic spread. High magnification images of synaptic contacts were taken with a 60× SC objective (Olympus) and spatially oversampled ³ twofold. To confirm synaptic contacts, double or triple co-localized pixels were analyzed with the ImageJ colocalization plugin. Only 8-bit pixel intensities ³50 were considered for analysis. All averages were calculated with a s.d. Whole-cord reconstructions of transynaptic labeling were performed in ScaleA2 optically cleared intact spinal cords with a two-photon microscope and a 20× objective (Olympus). Individual *z*-stacks covering ~500 mm × 500 mm were combined using the pairwise stitching plugin for ImageJ. Three-dimenstionally rendered versions of confocal/two-photon *z*-stacks were generated with FluoRender.

Optical stimulation and electrophysiology

Animals were injected at P0 with ChR2-mCherry rabies virus, together with AAV:G. At P8, spinal cords were isolated in cold oxygenated dissection ACSF (128 mM NaCl; 4 mM KCl; 21 mM $NaHCO_3$; 0.5 mM NaH_2PO_4; 3 mM $MgSO_4$; 30 mM D-glucose; and 1 mM $CaCl_2$), hemisected, and transferred to oxygenated room temperature recording ACSF (128 mM NaCl; 4 mM KCl; 21 mM $NaHCO_3$; 0.5 mM NaH_2PO_4; 1 mM $MgSO_4$; 30 mM D-glucose; and 2 mM

$CaCl_2$) with the medial surface of the cord facing up and examined for trans-synaptic labeling (only cords with trans-synaptic labeling were analyzed). Suction electrodes were attached to the L2 and L4 or L5 ventral roots, and cords were then allowed to recover and equilibrate to room temperature for ~20 min. A 20× 1.0 numerical aperture (NA) objective was used to visualize cells and to deliver light to small groups of 2–10 cells. 50-ms light pulses were generated by a 200-W light source and high speed shutter controlled by TTL signals from pclamp software. Latencies to motorneuron responses were measured from the onset of the stimulation, and the shutter opened completely within 5 ms of the stimulation window. Motorneuron responses were recorded with a multiclamp 700B amplifier and filtered at 300 Hz to 1 kHz. Stimulations proceeded from the caudal end of the lumbar cord, at ~500-mm intervals to the lower thoracic cord, usually covering ~3 mm. In intracord-injected nonspecific interneuron experiments, stimulations were also performed at three different dorsal-ventral locations, and the analysis presented here was performed on the ventral stimulation sites. Data were analyzed offline with clampfit and igor pro software. After recording, cords were immersion-fixed and sectioned to analyze the extent and pattern of neuron labeling and the morphology of labeled cells. Extracellular recordings from the MSE white matter were conducted with ~1-MW glass pipettes filled with ACSF placed in the vicinity of directly visualized *RabΔG:ChR2-Cherry*–labeled MSE axons in the cornu-commisuralis of Marie. We found that optical stimulation first evoked local action potentials within the cornu-commisuralis of Marie 11.7 ± 0.8 ms after the onset of light exposure over MSE and that the conduction velocity was 0.95 ± 0.3 ms/mm, or ~2.9 ms between L2 and L5 spinal segments (n = 4 spinal cords, Supplementary Fig. 10).

Statistical analysis

No statistical methods were used to predetermine sample sizes, but our sample sizes are

similar to those generally used in the field. Data collection and analysis were not performed blind to the conditions of the experiments. A normal q-q plot was used to test for normal distribution of the ChR2-evoked motor response data. All cell and synaptic contact counts are presented as means and s.d. Statistical analysis of reliability of dual L2/L5 responses: Reliable dual-root response was defined as the percentage of locations in a given sample in which all trials produced L2 and L5 responses. Sample means were compared between MSE and nonspecific groups with a *t*-test.

Chapter 3 Methods

Animals

Satb2$^{flx/flx}$ (provided by R. Grosschedl, Max Planck Institute of Immunobiology and Epigenetics), Satb2$^{lacz/lacz}$[128], Lbx1-Cre[152], Lmx1b-Cre (provided by R. Johnson, University of Texas), Ptf1a-Cre [153], Parvalbumin-Cre (Jax Strain B6;129P2-Pvalb$^{tm1(cre)Arbr}$/J, Stock#008069), Rosa-LSL-TdTomato (Jax Strain B6;129S6-Gt(ROSA)26Sor$^{tm9(CAG-tdTomato)Hze}$/J, Stock#007905), Rosa-CAG-LSL-Syp-tdTomato-deltaNeo (Jax Strain B6;129S-Gt(ROSA)26Sort$^{tm34.1(CAG-Syp/tdTomato)Hze}$/J, Stock #012570), Actb-FLPe (Jax Strain B6N.Cg-Tg(ACTFLPe)9205Dym/CjDswJ, Stock #019100)[154]. All mouse work was conducted in accordance with IACUC guidelines.

Generation of Satb2:Cre^{ERT2}

A Cre^{ERT2}/WPRE/polyA/FRT-neo-FRT cassette was inserted into the ATG of the Satb2 locus. ES cells were electroporated and selected with neomycin. Positive clones were identified using PCR and Southern blot analysis with internal probes for Cre. Embryos were genotyped using primer sequences for Cre, as well as primers spanning the region upstream and downstream

from the ATG. Founder animals were crossed with Actb-FLPe mice in order to excise the Neo cassette from the targeted Satb2 genomic locus.

Tamoxifen was administered intraperitoneally. Stock tamoxifen (50mg/ml in 100% ethanol) was diluted 1:10 in Sunflower Seed Oil from *Helianthus Annuus* (Sigma S5007). For embryonic labeling, two doses (200-300ul of 1:10 dilution per dose) were administered to pregnant females between e9 and e14. For postnatal labeling, two doses were administered to neonatal pups between P0 and P3 (10-40ul of 1:10 dilution per dose).

Tissue processing, immunohistochemistry, and in situ hybridization

Spinal cords were dissected in PBS and fixed in 4% PFA in PBS for 1-3 hours, washed in PBS, then washed in 30% sucrose. Spinal cords were then embedded in OCT and cryosectioned at 30um for immunohistochemistry and in situ hybridization, and 50um for quantification of synaptic contacts.

The following primary antibodies were used: rabbit β-gal (Cappel; 1:5000), guinea pig anti-Brn3a [155], goat anti-Bhlhb5 (Santa Cruz Biotechnology, sc-6045, 1:300), rabbit anti-Calbindin (Swant, CB38, 1:100), rabbit anti c-fos (Santa Cruz Biotechnology sc-52, 1:2000), sheep anti-CGRP (Abcam ab22560, 1:1000), guinea pig anti-Chx10 [156], rat anti-Ctip2 (Abcam ab18465, 1:1000), rabbit anti-Evx1 [157], goat anti-Foxp2 (Santa Cruz Biotechnology, sc-21069, 1:200), guinea pig anti-Hb9 [156], rabbit anti-Isl1/2 [158], rabbit anti-Satb2 (provided by T. Kohwi-Shigematsu and Y. Kohwi, Lawrence Berkeley National Laboratory), rabbit anti-Lbx1 [159], rabbit anti-Lim1/2 [158], rabbit anti-parvalbumin (Swant PV25, 1:1000), rabbit anti-Pax2 (Invitrogen 716000, 1:1000), rabbit anti-RFP (MBL International, PM005, 1:2000), guinea pig anti-Tlx3 [160], guinea pig anti-vGlut1 (Millipore AB5905, 1:5000). For identification of cell bodies when examining synaptic contacts, we used neurotrace staining (Invitrogen N-21483).

In situ probes (GAD65, GAD67, and vGlut2) were provided by Q. Ma (Harvard Medical School)[146]. To generate the *in situ* probe for GlyT2, the following PCR primer sequences were used to amplify a 545bp fragment: Forward- GTAGTGTTGGGAACCGATGG; Reverse- AGTCCAAGCGTGAGAAGCAT.

For double labeling experiments in which we examined Pax2 marker expression in Satb2+ interneurons, directly conjugated Pax2 antibody was used (Apex Antibody Labeling Kit, Invitrogen). For double labeling experiments in which we examined lineage marker expression in the absence of Satb2 expression, we compared $Satb2^{OFF}$:TdTomato and $Satb2^{ON}$:TdTomato spinal cords for all experiments except those involving Ptf1a. In this case, Ptf1a-Cre was used in combination with Rosa-CAG-LSL-TdTomato animals. These mice were crossed into a $Satb2^{lacZ/lacZ}$ background, and the number of cell colabeled with TdTomato and bGal were quantified. Comparisons between $Satb2^{OFF}$ and $Satb2^{ON}$ were performed at e18.5, unless specified otherwise.

For double labeling experiments in which we identified co-labeling of TdTomato and in situ hybridization probes, immunohistochemistry with anti-RFP primary antibody was performed prior to in situ hybridization. After in situ hybridization, secondary antibody to detect RFP signal was applied, and sections were imaged using bright field and fluorescence microscopy. Unless otherwise noted, n=3-6 spinal cords for quantification of co-expression in double labeling experiments.

Rabies Virus Preparation and Labeling

Rabies virus preparation was performed as described in Chapter 2 Methods with the following modifications. Rabies starter viruses containing either mCherry or GFP were obtained from the Callaway lab [80,90]. For visualization of premotor neurons in Figure 3.6E, F, rabies virus (RabΔG) and AAV:G were mixed 4:1 prior to injections. For visualization of motor neurons

processes and soma in Figure 3.6D, rabies virus (RabΔG) and PBS were mixed 4:1 prior to injections.

Small volume injections (0.3-1.5ul) were performed in various hindlimb muscles at P0 using a Hamilton syringe. Spinal cords were analyzed at P7.

C-fos induction

Capsaicin (0.1% in Ethanol) or Formalin (5% formalin in PBS) was injected subcutaneously into the plantar surface of the foot in adult animals (<8 weeks). Animals were perfused after 90 minutes and spinal cords were taken for immunohistochemistry. Sections were selected for analysis based on the peak labeling of c-fos in caudal lumbar levels of the spinal cord.

Behavioral Testing

All behavioral testing was conducted according to procedures approved by the Salk Institute IACUC. For all behavioral testing animals were habituated in the testing room for 1 hour prior to the start of the test. Adult animals were used (<8 weeks of age; male and female) for all behavioral analysis.

Open Field Test

The open field test was performed by observing animals in clear chambers (40.6 x 40.6 x 38.1cm) containing infrared beams to measure horizontal movement. The overall locomotor activity was measured over a 60 minute time period. The distance traveled was analyzed and the mean+/-SEM is reported. n=14 for control, n=12 for $Lbx1Cre^{+}/Satb2^{flx/flx}$.

Rotarod

Animals were trained on a rotarod for 1 minute at 3rpm, then performed 4 trials in which the rotarod was accelerating from 0-50rpm over 5 minutes. Trials were separated by 10 minutes. The latency to fall was recorded for each individual for 4 trials, and the mean+/-SEM for each trial is reported. n=17 for Lbx1Cre^{+}/Satb2$^{flx/flx}$, n=20 for control (Cre-) littermates.

Hindlimb Grip Strength

A digital grip strength meter (San Diego Instruments) was used to measure force (grams) of mouse forelimb and hindlimb grip response. For hindlimb measurements, animals were positioned to avoid contact of the forelimbs with the meter and to maximize grip reflex of the hindlimb. 5 trials were performed for each animal and the 3 maximum trials were averaged. n=11 for Lbx1Cre^{+}/Satb2$^{flx/flx}$, n=11 for control (Cre-) littermates.

Hargreaves Thermal Pain Test

Animals were habituated in a plastic container on a glass surface. Thermal pain was induced using a radiant heat beam (IITC). Intensity of the heat beam was adjusted so that the withdrawal response occurred within a range of ~3-8 seconds. A maximum of 20 seconds was applied to prevent tissue damage. 2 trials were performed on each hindlimb, and an average of left and right hindlimb (4 trials total) was used for each individual. Latency measurements, n=9 for Lbx1Cre^{+}/Satb2$^{flx/flx}$, n=7 for control (Cre-) littermates. Examination of the withdrawal response revealed the normal withdrawal behavior in which animals replaced the limb following painful stimulation. Identification of the aberrant withdrawal behavior was assigned as a binary response (maintained flexion or normal response).

Von Frey

The threshold for mechanical pain was measured using Von Frey filaments (0.008-2.0g). 5 trials were performed on each hindlimb. Threshold was assigned based on whether the animal responded greater than 50% of the time (3/5 trials or greater). The average of left and right hindlimb was used for each individual. n=7 for Lbx1Cre^{+}/Satb2$^{flx/flx}$, n=9 for control (Cre-) littermates. Examination of the withdrawal response revealed the normal withdrawal behavior in which animals replaced the limb following painful stimulation. Identification of the aberrant withdrawal behavior was assigned as a binary response (maintained flexion or normal response).

Fictive Locomotion Experiments

Fictive locomotion experiments were performed as described previously[161] with the following modifications. Lumbar spinal cords of e18.5 embryos were dissected in cold dissecting ACSF (128 mM NaCl; 4 mM KCl; 21 mM $NaHCO_3$; 0.5 mM NaH_2PO_4; 3 mM $MgSO_4$; 30 mM d-glucose; and 1 mM $CaCl_2$) oxygenated with 90% O_2/ 5% CO_2. Dissected spinal cords were transferred to room tempereature oxygenated recording solution (128 mM NaCl; 4 mM KCl; 21 mM $NaHCO_3$; 0.5 mM NaH_2PO_4; 1 mM $MgSO_4$; 30 mM d-glucose; and 2 mM $CaCl_2$). Locomotor activity was induced by bath application of 20uM serotonin (5-HT), 10um N-methyl-D, L-aspartate (NMA). Motoneuron activity was recorded from the ventral roots with suction electrodes, amplified 1000x and filtered from 100Hz-3kHz The activity of left and right L2 ventral roots were recorded for contralateral phase comparisons, and ipsilateral L2 and L5 ventral roots for ipsilateral flexor extensor phase comparisons. Analysis of fictive locomotor activity phase and cycle period was conducted offline with custom written scripts in R. Satb2 null (Satb2$^{lacZ/lacZ}$) and control littermates were used. n=7 for Satb2 null, n=4 for control.

Pixel Intensity Quantification

Spinal cords from Satb2^{ON}:Syn-Tom and Satb2^{OFF}:Syn-Tom animals were sectioned and immunohistochemistry for RFP was performed simultaneously. Pixel intensities were mapped along the dorso-ventral axis using the plot profile function of ImageJ software to correspond pixel intensity to distance along the dorsoventral axis. Hemicords were used for region of interest (ROI) for plot profiles. The dorsoventral distance of the spinal cord was normalized to the average of the population in order to correct for variability of section size. n=5 for Satb2^{OFF} n=6 for Satb2^{ON}.

Identification of synaptic contacts and quantification of proprioceptive input

Individual synaptic contacts were identified based on colocalization between TdTomato+ presynaptic terminals and neurotrace+ cell bodies by examining images of high magnification single focal planes.

To visualize proprioceptive contacts, spinal cords from Parvalbumin:Syn-Tom animals were sectioned and immunohistochemistry for Satb2 and neurotrace was performed. Thick (50um) sections were imaged at high resolution. Cells for quantification of proprioceptive input were selected based on whether the entire cell body was captured in the image stack. Individual synaptic contacts were identified based on colocalization between presynaptic terminals and neurotrace+ cell bodies of Satb2+ interneurons by examining serial image slices. The number of synaptic contacts were then binned and correlated to mediolateral position. n=34 cells in three spinal cords. In some cases, parvalbumin and vGlut1 colocalization was used to identify proprioceptive contacts on cell soma and processes of Satb2:TdTomato interneurons.

References

References

1 Alaynick, W. A., Jessell, T. M. & Pfaff, S. L. SnapShot: spinal cord development. *Cell* **146**, 178-178 e171, doi:10.1016/j.cell.2011.06.038 (2011).

2 Stepien, A. E., Tripodi, M. & Arber, S. Monosynaptic rabies virus reveals premotor network organization and synaptic specificity of cholinergic partition cells. *Neuron* **68**, 456-472, doi:S0896-6273(10)00869-X [pii] 10.1016/j.neuron.2010.10.019 (2010).

3 Kandel, E. R., Schwartz, J. H. & Jessell, T. M. *Principles of neural science*. 4th edn, (McGraw-Hill, Health Professions Division, 2000).

4 McHanwell, S. & Biscoe, T. J. The localization of motoneurons supplying the hindlimb muscles of the mouse. *Philosophical transactions of the Royal Society of London. Series B, Biological sciences* **293**, 477-508 (1981).

5 Nicolopoulos-Stournaras, S. & Iles, J. F. Motor neuron columns in the lumbar spinal cord of the rat. *The Journal of comparative neurology* **217**, 75-85, doi:10.1002/cne.902170107 (1983).

6 Romanes, G. J. The motor cell columns of the lumbo-sacral spinal cord of the cat. *The Journal of comparative neurology* **94**, 313-363 (1951).

7 Romanes, G. J. The Motor Pools of the Spinal Cord. *Progress in brain research* **11**, 93-119 (1964).

8 Vanderhorst, V. G. & Holstege, G. Organization of lumbosacral motoneuronal cell groups innervating hindlimb, pelvic floor, and axial muscles in the cat. *The Journal of comparative neurology* **382**, 46-76 (1997).

9 Shirasaki, R. & Pfaff, S. L. Transcriptional codes and the control of neuronal identity. *Annual review of neuroscience* **25**, 251-281, doi:10.1146/annurev.neuro.25.112701.142916 112701.142916 [pii] (2002).

10 Demireva, E. Y., Shapiro, L. S., Jessell, T. M. & Zampieri, N. Motor neuron position and topographic order imposed by beta- and gamma-catenin activities. *Cell* **147**, 641-652, doi:S0092-8674(11)01148-2 [pii] 10.1016/j.cell.2011.09.037.

11 Phillips, C. G. & Porter, R. Corticospinal neurones. Their role in movement. *Monographs of the Physiological Society*, v-xii, 1-450 (1977).

12 Ferrier, D. Experimental Researches in Cerebral Physiology and Pathology. *Journal of anatomy and physiology* **8**, 152-155 (1873).

13 Akintunde, A. & Buxton, D. F. Differential sites of origin and collateralization of corticospinal neurons in the rat: a multiple fluorescent retrograde tracer study. *Brain research* **575**, 86-92 (1992).

14 Tennant, K. A., Adkins, D. L., Donlan, N. A., Asay, A. L., Thomas, N., Kleim, J. A. & Jones, T. A. The organization of the forelimb representation of the C57BL/6 mouse motor cortex as defined by intracortical microstimulation and cytoarchitecture. *Cereb Cortex* **21**, 865-876, doi:10.1093/cercor/bhq159 (2011).

15 Phillips, C. G. & Porter, R. *Corticospinal Neurones: Their Role in Movement*. 5-52 (Academic Press, 1977).

16 Leyton, S. S. F. & Sherrington, C. S. Observations on the excitable cortex of the chipanzee, orang-utan and gorilla. *Experimental Physiology* **11**, 135-222 (1917).

17 Schieber, M. H. & Hibbard, L. S. How somatotopic is the motor cortex hand area? *Science* **261**, 489-492 (1993).

18 Monfils, M. H., Plautz, E. J. & Kleim, J. A. In search of the motor engram: motor map plasticity as a mechanism for encoding motor experience. *Neuroscientist* **11**, 471-483, doi:11/5/471 [pii]
10.1177/1073858405278015 (2005).

19 Aflalo, T. N. & Graziano, M. S. Relationship between unconstrained arm movements and single-neuron firing in the macaque motor cortex. *The Journal of neuroscience : the official journal of the Society for Neuroscience* **27**, 2760-2780, doi:10.1523/JNEUROSCI.3147-06.2007 (2007).

20 Georgopoulos, A. P., Kettner, R. E. & Schwartz, A. B. Primate motor cortex and free arm movements to visual targets in three-dimensional space. II. Coding of the direction of movement by a neuronal population. *J Neurosci* **8**, 2928-2937 (1988).

21 Georgopoulos, A. P., Kalaska, J. F., Caminiti, R. & Massey, J. T. On the relations between the direction of two-dimensional arm movements and cell discharge in primate motor cortex. *J Neurosci* **2**, 1527-1537 (1982).

22 Evarts, E. V. Relation of pyramidal tract activity to force exerted during voluntary movement. *J Neurophysiol* **31**, 14-27 (1968).

23 Graziano, M. S. & Aflalo, T. N. Mapping behavioral repertoire onto the cortex. *Neuron* **56**, 239-251, doi:10.1016/j.neuron.2007.09.013 (2007).

24 Dombeck, D. A., Graziano, M. S. & Tank, D. W. Functional clustering of neurons in motor cortex determined by cellular resolution imaging in awake behaving mice. *The Journal of neuroscience : the official journal of the Society for Neuroscience* **29**, 13751-13760, doi:10.1523/JNEUROSCI.2985-09.2009 (2009).

25 Graziano, M. S., Taylor, C. S. & Moore, T. Complex movements evoked by microstimulation of precentral cortex. *Neuron* **34**, 841-851 (2002).

26 Ramanathan, D., Conner, J. M. & Tuszynski, M. H. A form of motor cortical plasticity that correlates with recovery of function after brain injury. *Proceedings of the National Academy of Sciences of the United States of America* **103**, 11370-11375, doi:10.1073/pnas.0601065103 (2006).

27 Harrison, T. C., Ayling, O. G. & Murphy, T. H. Distinct cortical circuit mechanisms for complex forelimb movement and motor map topography. *Neuron* **74**, 397-409, doi:10.1016/j.neuron.2012.02.028 (2012).

28 Capaday, C., Ethier, C., Brizzi, L., Sik, A., van Vreeswijk, C. & Gingras, D. On the nature of the intrinsic connectivity of the cat motor cortex: evidence for a recurrent neural network topology. *Journal of neurophysiology* **102**, 2131-2141, doi:10.1152/jn.91319.2008 (2009).

29 Capaday, C., van Vreeswijk, C., Ethier, C., Ferkinghoff-Borg, J. & Weber, D. Neural mechanism of activity spread in the cat motor cortex and its relation to the intrinsic connectivity. *The Journal of physiology* **589**, 2515-2528, doi:10.1113/jphysiol.2011.206938 (2011).

30 Ethier, C., Brizzi, L., Darling, W. G. & Capaday, C. Linear summation of cat motor cortex outputs. *The Journal of neuroscience : the official journal of the Society for Neuroscience* **26**, 5574-5581, doi:10.1523/JNEUROSCI.5332-05.2006 (2006).

31 Lemon, R. N. Descending pathways in motor control. *Annual review of neuroscience* **31**, 195-218, doi:10.1146/annurev.neuro.31.060407.125547 (2008).

32 Bortoff, G. A. & Strick, P. L. Corticospinal terminations in two new-world primates: further evidence that corticomotoneuronal connections provide part of the neural substrate for manual dexterity. *J Neurosci* **13**, 5105-5118 (1993).

33 Rathelot, J. A. & Strick, P. L. Subdivisions of primary motor cortex based on cortico-motoneuronal cells. *Proceedings of the National Academy of Sciences of the United States of America* **106**, 918-923, doi:10.1073/pnas.0808362106 (2009).

34 Shalit, U., Zinger, N., Joshua, M. & Prut, Y. Descending Systems Translate Transient Cortical Commands into a Sustained Muscle Activation Signal. *Cereb Cortex*, doi:10.1093/cercor/bhr267 (2011).

35 Granmo, M., Petersson, P. & Schouenborg, J. Action-based body maps in the spinal cord emerge from a transitory floating organization. *The Journal of neuroscience : the official journal of the Society for Neuroscience* **28**, 5494-5503, doi:10.1523/JNEUROSCI.0651-08.2008 (2008).

36 Swett, J. E. & Woolf, C. J. The somatotopic organization of primary afferent terminals in the superficial laminae of the dorsal horn of the rat spinal cord. *The Journal of comparative neurology* **231**, 66-77, doi:10.1002/cne.902310106 (1985).

37 Nyberg, G. & Blomqvist, A. The somatotopic organization of forelimb cutaneous nerves in the brachial dorsal horn: an anatomical study in the cat. *The Journal of comparative neurology* **242**, 28-39, doi:10.1002/cne.902420103 (1985).

38 Willis, W. D. & Coggeshall, R. E. *Sensory Mechanisms of the Spinal Cord*. Vol. 2 789-876 (Kluwer Academic, 2004).

39 Eccles, J. C., Fatt, P. & Landgren, S. Central pathway for direct inhibitory action of impulses in largest afferent nerve fibres to muscle. *Journal of neurophysiology* **19**, 75-98 (1956).

40 Jankowska, E. & Lindstrom, S. Morphology of interneurones mediating Ia reciprocal inhibition of motoneurones in the spinal cord of the cat. *The Journal of physiology* **226**, 805-823 (1972).

41 Jankowska, E. & Roberts, W. J. Synaptic actions of single interneurones mediating reciprocal Ia inhibition of motoneurones. *The Journal of physiology* **222**, 623-642 (1972).

42 Koo, S. J. & Pfaff, S. L. Fine-tuning motor neuron properties: signaling from the periphery. *Neuron* **35**, 823-826, doi:S089662730200870X [pii] (2002).

43 Marmigere, F. & Ernfors, P. Specification and connectivity of neuronal subtypes in the sensory lineage. *Nature reviews. Neuroscience* **8**, 114-127, doi:10.1038/nrn2057 (2007).

44 Chen, H. H., Hippenmeyer, S., Arber, S. & Frank, E. Development of the monosynaptic stretch reflex circuit. *Current opinion in neurobiology* **13**, 96-102, doi:S0959438803000060 [pii] (2003).

45 Surmeli, G., Akay, T., Ippolito, G. C., Tucker, P. W. & Jessell, T. M. Patterns of spinal sensory-motor connectivity prescribed by a dorsoventral positional template. *Cell* **147**, 653-665, doi:S0092-8674(11)01210-4 [pii] 10.1016/j.cell.2011.10.012.

46 Levinsson, A., Holmberg, H., Broman, J., Zhang, M. & Schouenborg, J. Spinal sensorimotor transformation: relation between cutaneous somatotopy and a reflex network. *The Journal of neuroscience : the official journal of the Society for Neuroscience* **22**, 8170-8182 (2002).

47 Schouenborg, J., Weng, H. R., Kalliomaki, J. & Holmberg, H. A survey of spinal dorsal horn neurones encoding the spatial organization of withdrawal reflexes in the rat. *Experimental brain research. Experimentelle Hirnforschung. Experimentation cerebrale* **106**, 19-27 (1995).

48 Schouenborg, J. Action-based sensory encoding in spinal sensorimotor circuits. *Brain research reviews* **57**, 111-117, doi:10.1016/j.brainresrev.2007.08.007 (2008).

49 Li, L., Rutlin, M., Abraira, V. E., Cassidy, C., Kus, L., Gong, S., Jankowski, M. P., Luo, W., Heintz, N., Koerber, H. R., Woodbury, C. J. & Ginty, D. D. The functional organization of cutaneous low-threshold mechanosensory neurons. *Cell* **147**, 1615-1627, doi:10.1016/j.cell.2011.11.027 (2011).

50 Goulding, M. Circuits controlling vertebrate locomotion: moving in a new direction. *Nature reviews. Neuroscience* **10**, 507-518, doi:nrn2608 [pii] 10.1038/nrn2608 (2009).

51 Grillner, S. & Jessell, T. M. Measured motion: searching for simplicity in spinal locomotor networks. *Current opinion in neurobiology* **19**, 572-586, doi:S0959-4388(09)00148-2 [pii]
10.1016/j.conb.2009.10.011 (2009).

52 Stepien, A. E. & Arber, S. Probing the locomotor conundrum: descending the 'V' interneuron ladder. *Neuron* **60**, 1-4, doi:S0896-6273(08)00809-X [pii]
10.1016/j.neuron.2008.09.030 (2008).

53 Goulding, M. & Pfaff, S. L. Development of circuits that generate simple rhythmic behaviors in vertebrates. *Current opinion in neurobiology* **15**, 14-20, doi:S0959-4388(05)00018-8 [pii]
10.1016/j.conb.2005.01.017 (2005).

54 Alvarez, F. J., Jonas, P. C., Sapir, T., Hartley, R., Berrocal, M. C., Geiman, E. J., Todd, A. J. & Goulding, M. Postnatal phenotype and localization of spinal cord V1 derived interneurons. *The Journal of comparative neurology* **493**, 177-192, doi:10.1002/cne.20711 (2005).

55 Zagoraiou, L., Akay, T., Martin, J. F., Brownstone, R. M., Jessell, T. M. & Miles, G. B. A cluster of cholinergic premotor interneurons modulates mouse locomotor activity. *Neuron* **64**, 645-662, doi:10.1016/j.neuron.2009.10.017 (2009).

56 Wilson, J. M., Hartley, R., Maxwell, D. J., Todd, A. J., Lieberam, I., Kaltschmidt, J. A., Yoshida, Y., Jessell, T. M. & Brownstone, R. M. Conditional rhythmicity of ventral spinal interneurons defined by expression of the Hb9 homeodomain protein. *The Journal of neuroscience : the official journal of the Society for Neuroscience* **25**, 5710-5719, doi:25/24/5710 [pii]
10.1523/JNEUROSCI.0274-05.2005 (2005).

57 Hinckley, C. A., Hartley, R., Wu, L., Todd, A. & Ziskind-Conhaim, L. Locomotor-like rhythms in a genetically distinct cluster of interneurons in the mammalian spinal cord. *Journal of neurophysiology* **93**, 1439-1449, doi:00647.2004 [pii]
10.1152/jn.00647.2004 [doi] (2005).

58 Butt, S. J., Lebret, J. M. & Kiehn, O. Organization of left-right coordination in the mammalian locomotor network. *Brain research. Brain research reviews* **40**, 107-117, doi:S0165017302001947 [pii] (2002).

59 Harrison, P. J., Jankowska, E. & Zytnicki, D. Lamina VIII interneurones interposed in crossed reflex pathways in the cat. *The Journal of physiology* **371**, 147-166 (1986).

60 Jankowska, E. & Skoog, B. Labelling of midlumbar neurones projecting to cat hindlimb motoneurones by transneuronal transport of a horseradish peroxidase conjugate. *Neuroscience letters* **71**, 163-168, doi:0304-3940(86)90552-5 [pii] (1986).

61 Ruigrok, T. J., Pijpers, A., Goedknegt-Sabel, E. & Coulon, P. Multiple cerebellar zones are involved in the control of individual muscles: a retrograde transneuronal tracing study with rabies virus in the rat. *The European journal of neuroscience* **28**, 181-200, doi:10.1111/j.1460-9568.2008.06294.x (2008).

62 Jankowska, E. Further indications for enhancement of retrograde transneuronal transport of WGA-HRP by synaptic activity. *Brain research* **341**, 403-408, doi:0006-8993(85)91084-4 [pii] (1985).

63 Wickersham, I. R., Lyon, D. C., Barnard, R. J., Mori, T., Finke, S., Conzelmann, K. K., Young, J. A. & Callaway, E. M. Monosynaptic restriction of transsynaptic tracing from single, genetically targeted neurons. *Neuron* **53**, 639-647, doi:S0896-6273(07)00078-5 [pii]
10.1016/j.neuron.2007.01.033 (2007).

64 Tripodi, M., Stepien, A. E. & Arber, S. Motor antagonism exposed by spatial segregation and timing of neurogenesis. *Nature* **479**, 61-66, doi:10.1038/nature10538 (2011).

65 Coffman, K. A., Dum, R. P. & Strick, P. L. Cerebellar vermis is a target of projections from the motor areas in the cerebral cortex. *Proceedings of the National Academy of Sciences of the United States of America* **108**, 16068-16073, doi:10.1073/pnas.1107904108 (2011).

66 Chklovskii, D. B., Schikorski, T. & Stevens, C. F. Wiring optimization in cortical circuits. *Neuron* **34**, 341-347, doi:S0896627302006797 [pii] (2002).

67 Mitchison, G. Axonal trees and cortical architecture. *Trends Neurosci* **15**, 122-126, doi:0166-2236(92)90352-9 [pii] (1992).

68 Cherniak, C. Neural component placement. *Trends Neurosci* **18**, 522-527, doi:0166223695983737 [pii] (1995).

69 Ivanenko, Y. P., Poppele, R. E. & Lacquaniti, F. Spinal cord maps of spatiotemporal alpha-motoneuron activation in humans walking at different speeds. *Journal of neurophysiology* **95**, 602-618, doi:10.1152/jn.00767.2005 (2006).

70 Yakovenko, S., Mushahwar, V., VanderHorst, V., Holstege, G. & Prochazka, A. Spatiotemporal activation of lumbosacral motoneurons in the locomotor step cycle. *Journal of neurophysiology* **87**, 1542-1553 (2002).

71 Combes, D., Merrywest, S. D., Simmers, J. & Sillar, K. T. Developmental segregation of spinal networks driving axial- and hindlimb-based locomotion in metamorphosing Xenopus laevis. *The Journal of physiology* **559**, 17-24, doi:10.1113/jphysiol.2004.069542 (2004).

72 Wallen, P. & Williams, T. L. Fictive locomotion in the lamprey spinal cord in vitro compared with swimming in the intact and spinal animal. *The Journal of physiology* **347**, 225-239 (1984).

73 Bizzi, E., Cheung, V. C., d'Avella, A., Saltiel, P. & Tresch, M. Combining modules for movement. *Brain research reviews* **57**, 125-133, doi:10.1016/j.brainresrev.2007.08.004 (2008).

74 Duysens, J., De Groote, F. & Jonkers, I. The flexion synergy, mother of all synergies and father of new models of gait. *Frontiers in computational neuroscience* **7**, 14, doi:10.3389/fncom.2013.00014 (2013).

75 Tresch, M. C., Saltiel, P., d'Avella, A. & Bizzi, E. Coordination and localization in spinal motor systems. *Brain research. Brain research reviews* **40**, 66-79 (2002).

76 Leyton, S. & Sherrington, C. S. Observations on the excitable cortex of the chimpanzee, orang-utan and gorilla. *QJ Experimental Physiology* **11**, 135-222 (1917).

77 Lundberg, A. Supraspinal Control of Transmission in Reflex Paths to Motoneurones and Primary Afferents. *Progress in brain research* **12**, 197-221 (1964).

78 Sherrington, C. S. *The integrative action of the nervous system*. (C. Scribner's sons, 1906).

79 de Leon, R., Hodgson, J. A., Roy, R. R. & Edgerton, V. R. Extensor- and flexor-like modulation within motor pools of the rat hindlimb during treadmill locomotion and swimming. *Brain research* **654**, 241-250 (1994).

80 Wickersham, I. R., Finke, S., Conzelmann, K. K. & Callaway, E. M. Retrograde neuronal tracing with a deletion-mutant rabies virus. *Nature methods* **4**, 47-49, doi:10.1038/nmeth999 (2007).

81 Coulon, P., Bras, H. & Vinay, L. Characterization of last-order premotor interneurons by transneuronal tracing with rabies virus in the neonatal mouse spinal cord. *The Journal of comparative neurology* **519**, 3470-3487, doi:10.1002/cne.22717 (2011).

82 Scheibel, M. E. & Scheibel, A. B. Terminal axonal patterns in cat spinal cord. II. The dorsal horn. *Brain research* **9**, 32-58 (1968).

83 Sherrington, C. S. & Laslett, E. E. Observations on some spinal reflexes and the interconnection of spinal segments. *The Journal of physiology* **29**, 58-96 (1903).

84 Sengul, G., Puchalski, R. B. & Watson, C. Cytoarchitecture of the spinal cord of the postnatal (P4) mouse. *Anat Rec (Hoboken)* **295**, 837-845, doi:10.1002/ar.22450 (2012).

85 Asante, C. O. & Martin, J. H. Differential Joint-Specific Corticospinal Tract Projections within the Cervical Enlargement. *PloS one* **8**, e74454, doi:10.1371/journal.pone.0074454 (2013).

86 Hongo, T., Kitazawa, S., Ohki, Y., Sasaki, M. & Xi, M. C. A physiological and morphological study of premotor interneurones in the cutaneous reflex pathways in cats. *Brain research* **505**, 163-166 (1989).

87 Hongo, T., Kitazawa, S., Ohki, Y. & Xi, M. C. Functional identification of last-order interneurones of skin reflex pathways in the cat forelimb segments. *Brain research* **505**, 167-170 (1989).

88 Puskar, Z. & Antal, M. Localization of last-order premotor interneurons in the lumbar spinal cord of rats. *The Journal of comparative neurology* **389**, 377-389 (1997).

89 Tresch, M. C. & Bizzi, E. Responses to spinal microstimulation in the chronically spinalized rat and their relationship to spinal systems activated by low threshold cutaneous stimulation. *Experimental brain research. Experimentelle Hirnforschung. Experimentation cerebrale* **129**, 401-416 (1999).

90 Osakada, F., Mori, T., Cetin, A. H., Marshel, J. H., Virgen, B. & Callaway, E. M. New rabies virus variants for monitoring and manipulating activity and gene expression in defined neural circuits. *Neuron* **71**, 617-631, doi:10.1016/j.neuron.2011.07.005 (2011).

91 Clarke, R. W. & Harris, J. The organization of motor responses to noxious stimuli. *Brain research. Brain research reviews* **46**, 163-172, doi:10.1016/j.brainresrev.2004.07.005 (2004).

92 Pierrot-Deseilligny, E. & Burke, D. *The Circuitry of the Human Spinal Cord*. p350-352 (Cambridge University Press, 2012).

93 Schouenborg, J. & Kalliomaki, J. Functional organization of the nociceptive withdrawal reflexes. I. Activation of hindlimb muscles in the rat. *Experimental brain research. Experimentelle Hirnforschung. Experimentation cerebrale* **83**, 67-78 (1990).

94 Gong, S., Zheng, C., Doughty, M. L., Losos, K., Didkovsky, N., Schambra, U. B., Nowak, N. J., Joyner, A., Leblanc, G., Hatten, M. E. & Heintz, N. A gene expression atlas of the central nervous system based on bacterial artificial chromosomes. *Nature* **425**, 917-925, doi:10.1038/nature02033 (2003).

95 Henry, A. M. & Hohmann, J. G. High-resolution gene expression atlases for adult and developing mouse brain and spinal cord. *Mammalian genome : official journal of the International Mammalian Genome Society* **23**, 539-549, doi:10.1007/s00335-012-9406-2 (2012).

96 Britanova, O., Akopov, S., Lukyanov, S., Gruss, P. & Tarabykin, V. Novel transcription factor Satb2 interacts with matrix attachment region DNA elements in a tissue-specific manner and demonstrates cell-type-dependent expression in the developing mouse CNS. *The European journal of neuroscience* **21**, 658-668, doi:10.1111/j.1460-9568.2005.03897.x (2005).

97 Wildner, H., Das Gupta, R., Brohl, D., Heppenstall, P. A., Zeilhofer, H. U. & Birchmeier, C. Genome-wide expression analysis of Ptf1a- and Ascl1-deficient mice reveals new markers for distinct dorsal horn interneuron populations contributing to nociceptive reflex plasticity. *The Journal of neuroscience : the official journal of the Society for Neuroscience* **33**, 7299-7307, doi:10.1523/JNEUROSCI.0491-13.2013 (2013).

98 Ishizuka, N., Mannen, H., Hongo, T. & Sasaki, S. Trajectory of group Ia afferent fibers stained with horseradish peroxidase in the lumbosacral spinal cord of the cat: three dimensional reconstructions from serial sections. *The Journal of comparative neurology* **186**, 189-211, doi:10.1002/cne.901860206 (1979).

99 Scheibel, M. E. & Scheibel, A. B. Terminal patterns in cat spinal cord. 3. Primary afferent collaterals. *Brain research* **13**, 417-443 (1969).

100 Curfs, M. H., Gribnau, A. A. & Dederen, P. J. Selective elimination of transient corticospinal projections in the rat cervical spinal cord gray matter. *Brain research. Developmental brain research* **78**, 182-190 (1994).

101 Gianino, S., Stein, S. A., Li, H., Lu, X., Biesiada, E., Ulas, J. & Xu, X. M. Postnatal growth of corticospinal axons in the spinal cord of developing mice. *Brain research. Developmental brain research* **112**, 189-204 (1999).

102 Martin, J. H. Differential spinal projections from the forelimb areas of the rostral and caudal subregions of primary motor cortex in the cat. *Experimental brain research. Experimentelle Hirnforschung. Experimentation cerebrale* **108**, 191-205 (1996).

103 Saltiel, P., Tresch, M. C. & Bizzi, E. Spinal cord modular organization and rhythm generation: an NMDA iontophoretic study in the frog. *Journal of neurophysiology* **80**, 2323-2339 (1998).

104 Bareyre, F. M., Kerschensteiner, M., Misgeld, T. & Sanes, J. R. Transgenic labeling of the corticospinal tract for monitoring axonal responses to spinal cord injury. *Nature medicine* **11**, 1355-1360, doi:10.1038/nm1331 (2005).

105 Antal, M., Sholomenko, G. N., Moschovakis, A. K., Storm-Mathisen, J., Heizmann, C. W. & Hunziker, W. The termination pattern and postsynaptic targets of rubrospinal fibers in the rat spinal cord: a light and electron microscopic study. *The Journal of comparative neurology* **325**, 22-37, doi:10.1002/cne.903250103 (1992).

106 Brown, L. T. Rubrospinal projections in the rat. *The Journal of comparative neurology* **154**, 169-187, doi:10.1002/cne.901540205 (1974).

107 Liang, H., Paxinos, G. & Watson, C. The red nucleus and the rubrospinal projection in the mouse. *Brain structure & function* **217**, 221-232, doi:10.1007/s00429-011-0348-3 (2012).

108 Lundberg, A. Multisensory control of spinal reflex pathways. *Progress in brain research* **50**, 11-28, doi:10.1016/S0079-6123(08)60803-1 (1979).

109 Schomburg, E. D. Spinal sensorimotor systems and their supraspinal control. *Neuroscience research* **7**, 265-340 (1990).

110 Andersen, O. K., Sonnenborg, F., Matjacic, Z. & Arendt-Nielsen, L. Foot-sole reflex receptive fields for human withdrawal reflexes in symmetrical standing position. *Experimental brain research. Experimentelle Hirnforschung. Experimentation cerebrale* **152**, 434-443, doi:10.1007/s00221-003-1550-1 (2003).

111 Burke, R. E. The use of state-dependent modulation of spinal reflexes as a tool to investigate the organization of spinal interneurons. *Experimental brain research. Experimentelle Hirnforschung. Experimentation cerebrale* **128**, 263-277 (1999).

112 Duysens, J., Tax, A. A., Trippel, M. & Dietz, V. Phase-dependent reversal of reflexly induced movements during human gait. *Experimental brain research. Experimentelle Hirnforschung. Experimentation cerebrale* **90**, 404-414 (1992).

113 Serrao, M., Pierelli, F., Don, R., Ranavolo, A., Cacchio, A., Curra, A., Sandrini, G., Frascarelli, M. & Santilli, V. Kinematic and electromyographic study of the nociceptive withdrawal reflex in the upper limbs during rest and movement. *The Journal of neuroscience : the official journal of the Society for Neuroscience* **26**, 3505-3513, doi:10.1523/JNEUROSCI.5160-05.2006 (2006).

114 Sonnenborg, F. A., Andersen, O. K., Arendt-Nielsen, L. & Treede, R. D. Withdrawal reflex organisation to electrical stimulation of the dorsal foot in humans. *Experimental brain research. Experimentelle Hirnforschung. Experimentation cerebrale* **136**, 303-312 (2001).

115 Spaich, E. G., Andersen, O. K. & Arendt-Nielsen, L. Tibialis Anterior and Soleus Withdrawal Reflexes Elicited by Electrical Stimulation of the Sole of the Foot during Gait. *Neuromodulation : journal of the International Neuromodulation Society* **7**, 126-132, doi:10.1111/j.1094-7159.2004.04016.x (2004).

116 Spaich, E. G., Arendt-Nielsen, L. & Andersen, O. K. Modulation of lower limb withdrawal reflexes during gait: a topographical study. *Journal of neurophysiology* **91**, 258-266, doi:10.1152/jn.00360.2003 (2004).

117 Hunt, S. P., Pini, A. & Evan, G. Induction of c-fos-like protein in spinal cord neurons following sensory stimulation. *Nature* **328**, 632-634, doi:10.1038/328632a0 (1987).

118 Ritz, L. A. & Greenspan, J. D. Morphological features of lamina V neurons receiving nociceptive input in cat sacrocaudal spinal cord. *The Journal of comparative neurology* **238**, 440-452, doi:10.1002/cne.902380408 (1985).

119 Surmeier, D. J., Honda, C. N. & Willis, W. D., Jr. Natural groupings of primate spinothalamic neurons based on cutaneous stimulation. Physiological and anatomical features. *Journal of neurophysiology* **59**, 833-860 (1988).

120 Levine, A. J., Hinckley, C. A., Hilde, K. L., Driscoll, S. P., Poon, T. H., Montgomery, J. M. & Pfaff, S. L. Identification of a cellular node for motor control pathways. *Nature neuroscience* **17**, 586-593, doi:10.1038/nn.3675 (2014).

121 Levine, A. J., Lewallen, K. A. & Pfaff, S. L. Spatial organization of cortical and spinal neurons controlling motor behavior. *Current opinion in neurobiology* **22**, 812-821, doi:10.1016/j.conb.2012.07.002 (2012).

122 Balasubramanian, M., Smith, K., Basel-Vanagaite, L., Feingold, M. F., Brock, P., Gowans, G. C., Vasudevan, P. C., Cresswell, L., Taylor, E. J., Harris, C. J., Friedman, N., Moran, R., Feret, H., Zackai, E. H., Theisen, A., Rosenfeld, J. A. & Parker, M. J. Case series: 2q33.1 microdeletion syndrome--further delineation of the phenotype. *Journal of medical genetics* **48**, 290-298, doi:10.1136/jmg.2010.084491 (2011).

123 FitzPatrick, D. R., Carr, I. M., McLaren, L., Leek, J. P., Wightman, P., Williamson, K., Gautier, P., McGill, N., Hayward, C., Firth, H., Markham, A. F., Fantes, J. A. & Bonthron, D. T. Identification of SATB2 as the cleft palate gene on 2q32-q33. *Human molecular genetics* **12**, 2491-2501, doi:10.1093/hmg/ddg248 (2003).

124 Van Buggenhout, G., Van Ravenswaaij-Arts, C., Mc Maas, N., Thoelen, R., Vogels, A., Smeets, D., Salden, I., Matthijs, G., Fryns, J. P. & Vermeesch, J. R. The del(2)(q32.2q33) deletion syndrome defined by clinical and molecular characterization of four patients. *European journal of medical genetics* **48**, 276-289, doi:10.1016/j.ejmg.2005.05.005 (2005).

125 Alcamo, E. A., Chirivella, L., Dautzenberg, M., Dobreva, G., Farinas, I., Grosschedl, R. & McConnell, S. K. Satb2 regulates callosal projection neuron identity in the developing cerebral cortex. *Neuron* **57**, 364-377, doi:10.1016/j.neuron.2007.12.012 (2008).

126 Britanova, O., de Juan Romero, C., Cheung, A., Kwan, K. Y., Schwark, M., Gyorgy, A., Vogel, T., Akopov, S., Mitkovski, M., Agoston, D., Sestan, N., Molnar, Z. & Tarabykin, V. Satb2 is a postmitotic determinant for upper-layer neuron specification in the neocortex. *Neuron* **57**, 378-392, doi:10.1016/j.neuron.2007.12.028 (2008).

127 Gross, M. K., Dottori, M. & Goulding, M. Lbx1 specifies somatosensory association interneurons in the dorsal spinal cord. *Neuron* **34**, 535-549, doi:S0896627302006906 [pii] (2002).

128 Dobreva, G., Chahrour, M., Dautzenberg, M., Chirivella, L., Kanzler, B., Farinas, I., Karsenty, G. & Grosschedl, R. SATB2 is a multifunctional determinant of craniofacial patterning and osteoblast differentiation. *Cell* **125**, 971-986, doi:10.1016/j.cell.2006.05.012 (2006).

129 Szemes, M., Gyorgy, A., Paweletz, C., Dobi, A. & Agoston, D. V. Isolation and characterization of SATB2, a novel AT-rich DNA binding protein expressed in development- and cell-specific manner in the rat brain. *Neurochemical research* **31**, 237-246, doi:10.1007/s11064-005-9012-8 (2006).

130 Schubert, F. R., Dietrich, S., Mootoosamy, R. C., Chapman, S. C. & Lumsden, A. Lbx1 marks a subset of interneurons in chick hindbrain and spinal cord. *Mechanisms of development* **101**, 181-185 (2001).

131 Muller, T., Brohmann, H., Pierani, A., Heppenstall, P. A., Lewin, G. R., Jessell, T. M. & Birchmeier, C. The homeodomain factor lbx1 distinguishes two major programs of neuronal differentiation in the dorsal spinal cord. *Neuron* **34**, 551-562, doi:S089662730200689X [pii] (2002).

132 Dubuisson, D. & Dennis, S. G. The formalin test: a quantitative study of the analgesic effects of morphine, meperidine, and brain stem stimulation in rats and cats. *Pain* **4**, 161-174 (1977).

133 Arber, S. Motor circuits in action: specification, connectivity, and function. *Neuron* **74**, 975-989, doi:10.1016/j.neuron.2012.05.011 (2012).

134 Brohl, D., Strehle, M., Wende, H., Hori, K., Bormuth, I., Nave, K. A., Muller, T. & Birchmeier, C. A transcriptional network coordinately determines transmitter and peptidergic fate in the dorsal spinal cord. *Developmental biology* **322**, 381-393, doi:10.1016/j.ydbio.2008.08.002 (2008).

135 Huang, M., Huang, T., Xiang, Y., Xie, Z., Chen, Y., Yan, R., Xu, J. & Cheng, L. Ptf1a, Lbx1 and Pax2 coordinate glycinergic and peptidergic transmitter phenotypes in dorsal spinal inhibitory neurons. *Developmental biology* **322**, 394-405, doi:10.1016/j.ydbio.2008.06.031 (2008).

136 Guo, T., Mandai, K., Condie, B. G., Wickramasinghe, S. R., Capecchi, M. R. & Ginty, D. D. An evolving NGF-Hoxd1 signaling pathway mediates development of divergent neural circuits in vertebrates. *Nature neuroscience* **14**, 31-36, doi:10.1038/nn.2710 (2011).

137 Crone, S. A., Zhong, G., Harris-Warrick, R. & Sharma, K. In mice lacking V2a interneurons, gait depends on speed of locomotion. *The Journal of neuroscience : the official journal of the Society for Neuroscience* **29**, 7098-7109, doi:29/21/7098 [pii] 10.1523/JNEUROSCI.1206-09.2009 (2009).

138 Gosgnach, S., Lanuza, G. M., Butt, S. J., Saueressig, H., Zhang, Y., Velasquez, T., Riethmacher, D., Callaway, E. M., Kiehn, O. & Goulding, M. V1 spinal neurons regulate the speed of vertebrate locomotor outputs. *Nature* **440**, 215-219, doi:nature04545 [pii] 10.1038/nature04545 (2006).

139 Zhang, J., Lanuza, G. M., Britz, O., Wang, Z., Siembab, V. C., Zhang, Y., Velasquez, T., Alvarez, F. J., Frank, E. & Goulding, M. V1 and v2b interneurons secure the alternating flexor-extensor motor activity mice require for limbed locomotion. *Neuron* **82**, 138-150, doi:10.1016/j.neuron.2014.02.013 (2014).

140 Lanuza, G. M., Gosgnach, S., Pierani, A., Jessell, T. M. & Goulding, M. Genetic identification of spinal interneurons that coordinate left-right locomotor activity necessary for walking movements. *Neuron* **42**, 375-386, doi:S0896627304002491 [pii] (2004).

141 Zhang, Y., Narayan, S., Geiman, E., Lanuza, G. M., Velasquez, T., Shanks, B., Akay, T., Dyck, J., Pearson, K., Gosgnach, S., Fan, C. M. & Goulding, M. V3 spinal neurons establish a robust and balanced locomotor rhythm during walking. *Neuron* **60**, 84-96, doi:10.1016/j.neuron.2008.09.027 (2008).

142 Kjaerulff, O. & Kiehn, O. Distribution of networks generating and coordinating locomotor activity in the neonatal rat spinal cord in vitro: a lesion study. *The Journal of neuroscience : the official journal of the Society for Neuroscience* **16**, 5777-5794 (1996).

143 Allen, J. W. & Yaksh, T. L. Assessment of acute thermal nociception in laboratory animals. *Methods in molecular medicine* **99**, 11-23, doi:10.1385/1-59259-770-X:011 (2004).

144 Hargreaves, K., Dubner, R., Brown, F., Flores, C. & Joris, J. A new and sensitive method for measuring thermal nociception in cutaneous hyperalgesia. *Pain* **32**, 77-88 (1988).

145 Ross, S. E., McCord, A. E., Jung, C., Atan, D., Mok, S. I., Hemberg, M., Kim, T. K., Salogiannis, J., Hu, L., Cohen, S., Lin, Y., Harrar, D., McInnes, R. R. & Greenberg, M. E. Bhlhb5 and Prdm8 form a repressor complex involved in neuronal circuit assembly. *Neuron* **73**, 292-303, doi:10.1016/j.neuron.2011.09.035 (2012).

146 Cheng, L., Arata, A., Mizuguchi, R., Qian, Y., Karunaratne, A., Gray, P. A., Arata, S., Shirasawa, S., Bouchard, M., Luo, P., Chen, C. L., Busslinger, M., Goulding, M., Onimaru, H. & Ma, Q. Tlx3 and Tlx1 are post-mitotic selector genes determining glutamatergic over GABAergic cell fates. *Nature neuroscience* **7**, 510-517, doi:10.1038/nn1221
nn1221 [pii] (2004).

147 Craig, A. D. Pain mechanisms: labeled lines versus convergence in central processing. *Annual review of neuroscience* **26**, 1-30, doi:10.1146/annurev.neuro.26.041002.131022 (2003).

148 Bourane, S., Grossmann, K. S., Britz, O., Dalet, A., Del Barrio, M. G., Stam, F. J., Garcia-Campmany, L., Koch, S. & Goulding, M. Identification of a spinal circuit for light touch and fine motor control. *Cell* **160**, 503-515, doi:10.1016/j.cell.2015.01.011 (2015).

149 Duan, B., Cheng, L., Bourane, S., Britz, O., Padilla, C., Garcia-Campmany, L., Krashes, M., Knowlton, W., Velasquez, T., Ren, X., Ross, S. E., Lowell, B. B., Wang, Y., Goulding, M. & Ma, Q. Identification of spinal circuits transmitting and gating mechanical pain. *Cell* **159**, 1417-1432, doi:10.1016/j.cell.2014.11.003 (2014).

150 Wickersham, I. R., Sullivan, H. A. & Seung, H. S. Production of glycoprotein-deleted rabies viruses for monosynaptic tracing and high-level gene expression in neurons. *Nature protocols* **5**, 595-606, doi:10.1038/nprot.2009.248 (2010).

151 Joshi, P. S., Molyneaux, B. J., Feng, L., Xie, X., Macklis, J. D. & Gan, L. Bhlhb5 regulates the postmitotic acquisition of area identities in layers II-V of the developing neocortex. *Neuron* **60**, 258-272, doi:10.1016/j.neuron.2008.08.006 (2008).

152 Sieber, M. A., Storm, R., Martinez-de-la-Torre, M., Muller, T., Wende, H., Reuter, K., Vasyutina, E. & Birchmeier, C. Lbx1 acts as a selector gene in the fate determination of somatosensory and viscerosensory relay neurons in the hindbrain. *The Journal of neuroscience : the official journal of the Society for Neuroscience* **27**, 4902-4909, doi:10.1523/JNEUROSCI.0717-07.2007 (2007).

153 Kawaguchi, Y., Cooper, B., Gannon, M., Ray, M., MacDonald, R. J. & Wright, C. V. The role of the transcriptional regulator Ptf1a in converting intestinal to pancreatic progenitors. *Nature genetics* **32**, 128-134, doi:10.1038/ng959 (2002).

154 Rodriguez, C. I., Buchholz, F., Galloway, J., Sequerra, R., Kasper, J., Ayala, R., Stewart, A. F. & Dymecki, S. M. High-efficiency deleter mice show that FLPe is an alternative to Cre-loxP. *Nature genetics* **25**, 139-140, doi:10.1038/75973 (2000).

155 Fedtsova, N. G. & Turner, E. E. Brn-3.0 expression identifies early post-mitotic CNS neurons and sensory neural precursors. *Mechanisms of development* **53**, 291-304 (1995).

156 Thaler, J., Harrison, K., Sharma, K., Lettieri, K., Kehrl, J. & Pfaff, S. L. Active suppression of interneuron programs within developing motor neurons revealed by analysis of homeodomain factor HB9. *Neuron* **23**, 675-687, doi:S0896-6273(01)80027-1 [pii] (1999).

157 Moran-Rivard, L., Kagawa, T., Saueressig, H., Gross, M. K., Burrill, J. & Goulding, M. Evx1 is a postmitotic determinant of v0 interneuron identity in the spinal cord. *Neuron* **29**, 385-399, doi:S0896-6273(01)00213-6 [pii] (2001).

158 Tsuchida, T., Ensini, M., Morton, S. B., Baldassare, M., Edlund, T., Jessell, T. M. & Pfaff, S. L. Topographic organization of embryonic motor neurons defined by expression of LIM homeobox genes. *Cell* **79**, 957-970 (1994).

159 Gross, M. K., Moran-Rivard, L., Velasquez, T., Nakatsu, M. N., Jagla, K. & Goulding, M. Lbx1 is required for muscle precursor migration along a lateral pathway into the limb. *Development* **127**, 413-424 (2000).

160 Muller, T., Anlag, K., Wildner, H., Britsch, S., Treier, M. & Birchmeier, C. The bHLH factor Olig3 coordinates the specification of dorsal neurons in the spinal cord. *Genes & development* **19**, 733-743, doi:19/6/733 [pii] 10.1101/gad.326105 (2005).

161 Myers, C. P., Lewcock, J. W., Hanson, M. G., Gosgnach, S., Aimone, J. B., Gage, F. H., Lee, K. F., Landmesser, L. T. & Pfaff, S. L. Cholinergic input is required during embryonic development to mediate proper assembly of spinal locomotor circuits. *Neuron* **46**, 37-49, doi:S0896-6273(05)00165-0 [pii] 10.1016/j.neuron.2005.02.022 (2005).